UNH SEA GRANT PROGRAMS

UNH RAYTHEON SEA GRANT PROJECT

TECHNICAL REPORT

MEASUREMENTS AND CORRELATION FUNCTIONS

R. Carrier, H. Tugal, and
M. Yildiz
Mechanics Research Laboratory

UNH SEA GRANT PROGRAMS

UNH-RAYTHEON SEA GRANT PROJECT

TECHNICAL REPORT

Measurements and Correlation Functions

R. Carrier, H. Tugal, and M. Yildiz
Mechanics Research Laboratory

A Report of a
Cooperative University-Industry Research Project
between

University of New Hampshire
Durham, New Hampshire

Raytheon Company
Portsmouth, Rhode Island

UNIVERSITY of NEW HAMPSHIRE
DURHAM, NEW HAMPSHIRE 03824

Report No. UNH-SG-131

April 1974

A TECHNICAL REPORT TO

THE NATIONAL SEA GRANT PROGRAM

OF

THE NATIONAL OCEANIC AND ATMOSPHERIC ADMINISTRATION

U. S. DEPARTMENT OF COMMERCE

MEASUREMENTS AND CORRELATION FUNCTIONS

by

R. Carrier, H. Tugal, and M. Yildiz
Mechanics Research Laboratory

This work is a result of research sponsored by NOAA Office of Sea Grant, Department of Commerce, under Grant No. D of C -04-3-158-69. The U.S. Government is authorized to produce and distribute reprints for governmental purposes, notwithstanding any copyright notation that may appear hereon.

Approved:

m · yildiz

Musa Yildiz - Technical Director

COOPERATING INSTITUTIONS

University of New Hampshire
Durham, New Hampshire 03824

Submarine Signal Division
Raytheon Company
Portsmouth, Rhode Island 02871

TABLE OF CONTENTS

ABSTRACT

A typical set of acoustic signatures remotely acquired by Raytheon Company over ocean subbottom are analyzed. This data have been obtained from at-sea tests conducted in Massachusetts Bay to evaluate the concept of acquisition of ocean bottom sediment parameters. A multichannel array was designed and constructed to collect this data. It is noted that acoustic response is sensitive to changes in all structural parameters and, therefore, it is necessary to measure and compare relative changes in the input and output acoustic signals. By employing the fast Fourier transform and Hilbert transform techniques we do the following signal analysis:

Take measured input signal in the ocean which is in the form of time series, and

1) evaluate even part of time series;
2) evaluate odd part of time series;
3) evaluate even part of the Fourier transform of time series (frequency domain representation);
4) evaluate odd part of the Fourier transform of time series (frequency domain representation);
5) evaluate absolute value of the input signal in frequency domain obtained by fast Fourier transform technique. Thus, this way we are able to measure quality factor Q of input signal;
6) evaluate the spectral density of the input signal;
7) evaluate autocorrelation function of the input signal which is calculated from inverse Fourier transform of spectral density.

The acoustic data (output signal) was corrected for calibration and geometry factors and converted from analog to digital form in computer-compatible formats for signal processing at UNH and at the Raytheon Company. The calculations performed from (1) to (7) to output signals (received acoustical responses) is repeated. In this way we are able to measure and compare the changes between input and output signals.

INTRODUCTION

The raw acoustic data have been acquired from a series of at-sea tests conducted in Massachusetts Bay by the Raytheon Company to evaluate the concept of acquisition of ocean bottom sediment parameters. A multichannel array was designed and constructed by the company to collect data. The array concept was adopted for three main reasons. First, the angular dependence of the reflection coefficient was determined. Second, the towed array essentially fixes the individual source-receiver pair geometries in space rather than necessitating recomputation of a time varying geometry as required by either a two-ship or single-ship sonobuoy approach. The towed array additionally allows almost complete decoupling of the sensors, i.e., source and receivers from both ocean surface and ship motion. The third reason was one of economics in which neither a second vessel nor the sophisticated communications for data transfer and radio controlled timing link were required. Furthermore, the array approach allows more continuous data acquisition operations and simplified logistics.

The array consists of a series of discrete receiving elements which simultaneously sense the return echoes from ocean subbottom soil. To improve data quality, the array also incorporates specialized mechanical damping mechanisms and self-contained signal processing, the latter primarily directed toward signal to noise ratio improvement. The received echoes (signals) are further processed by the shipboard portion of the system employing a processor which substantially increases the effective dynamic range of the acoustic signals recorded for subsequent computer analysis.

The prototype systems have only been evaluated in relatively shallow water (50 meters), although there appears to be no technical limitation to increasing operational capability to include areas of higher water depths. Similarly, the subbottom penetration depths in excess of 20 meters now being achieved could also be extended. It should be noted, however,that

the total penetration depths achievable are not specifically predictable, and in common with all other acoustic systems, they are a function of sediment (subbottom soil) characteristics.

One of the main objectives in this project is to initiate soil mechanics studies of bottom soils, building both a theoretical and practical understanding of sediment parameters relating acoustics to load-bearing predictions. This includes the development of the constitutive equations as well as the design of instrumentation for parameter measurement and the collection of related data. To accomplish the above a mechanical model of the ocean and bottom sediment must be developed. A mechanical system can be understood by theory and by experiment. Here, as discussed in previous pages, the emphasis is on the experiment which is concerned with the determination of bottom soil parameters by analyzing the return echo signals from the ocean bottom acquired by towed array concept. It is in this spirit that we write this report.

From Figure - (1) we see that the subbottom soil as a mechanical system is vibrating since its parts fluctuate in time. In studying such time series records it is natural to look for some kind of regularity in order to characterize the vibration in a simple manner. When there is no obvious pattern in a vibration record it is sometimes called a random vibration. Randomness involves the notion that in addition to the given record one should consider the totality of possible records that might equally well have been produced under the same conditions. If the identical experiment is performed many times and the records obtained are always alike the process is said to be deterministic. However, if when all conditions under control of the experimenter are maintained the same, the records continually differ from each other, the process is said to be random. In this case a single record is not as meaningful as a statistical description of totality of possible records.

Entering the field of probability and statistics in order to obtain sediment parameters is a convenience which cannot be overlooked. The statistical analysis of the return echoes gives results which predicts the soil characteristics in a consistent manner.

For many purposes the statistical answers are adequate and easier to obtain. The vibration record as seen in Figure - (1) is characterized by its amplitude and frequency. For this time series the phase is unimportant. This vibration record, Figure - (2), can be sufficiently characterized by an average amplitude and by a decomposition in frequency. The average amplitude can be determined by the determinaiton of root-mean square value. The frequency decomposition is indicated by the mean-square spectral density. Another statistical parameter, the quality factor Q, can be obtained to provide a more complete picture of the record. It is the latter parameter Q obtained from the analysis of Figure (1) presented in this report. From Q we can easily determine the attenuation constant for the ocean sediment. An accurate determiantion of a (schotastic) process would require an analysis of the stationary random phenomena during an infinite time interval. In this case a significant problem is to estimate some of the characteristics of the sediment from measurements made with one or two samples. In the Appendix of this report the problem of estimating the spectral density and the autocorrelation function of a stationary random process response r(t) is presented and for simplicity, the availability of a single sample is assumed.

It should be noted that the determination of an accurate spectral density or autocorrelation is a difficult and expensive process requiring a high degree of engineering competence. There is a long chain of instrumentation and data processing between the transducer and the desired spectral statistical responses. Considering that all operations involved in the process of measurement are mathematically accurate, the result obtained is only an estimate of the true spectral density. The problem of spectral density is divided naturally into two tasks:

a) To refine the quality of the estimate, i.e. to assure that the resulting measurement is well within the desired assumption of the true power spectral density;

b) To increase the accuracy of the measurements, i.e., the reduction of the smallest degree of experimental error in the value of the estimate itself.

It seems unreasonable to expect high measurement accuracy under conditions which supply demonstrably poor estimates. Conversely, carefully designed experiments which would yield accurate estimates may be ruined by experimental processing errors. The balance between these two extremes is the characteristic

of valuable, well-designed spectral density measurements. Two methods of determining power spectral density are available:

1. "Spectral density" - filtering in the frequency domain.
2. "Autocorrelation" - filtering in the time domain.

Although the practical problems encountered in the computations are widely different from one method to another, both methods can be done through either analog or digital processing. Before discussing the procedures in detail the reasons why the spectral density, rather than the autocorrelation function, is usually considered as the useful end product of the analysis will be presented.

Most signal modifiers (transducers, transmission lines, modulation, amplifiers) are known or can be calibrated on the basis of their transfer functions (Green's functions). Transfer functions can easily be measured in steady state sinusoidol excitation. The justification of the emphasis to the spectral density formulation lies in the simplicity of handling transfer functions in the frequency domain the expression of relationships between input and response spectral densities. The figure below is a flow chart showing the effect of a transfer function on the spectral density.

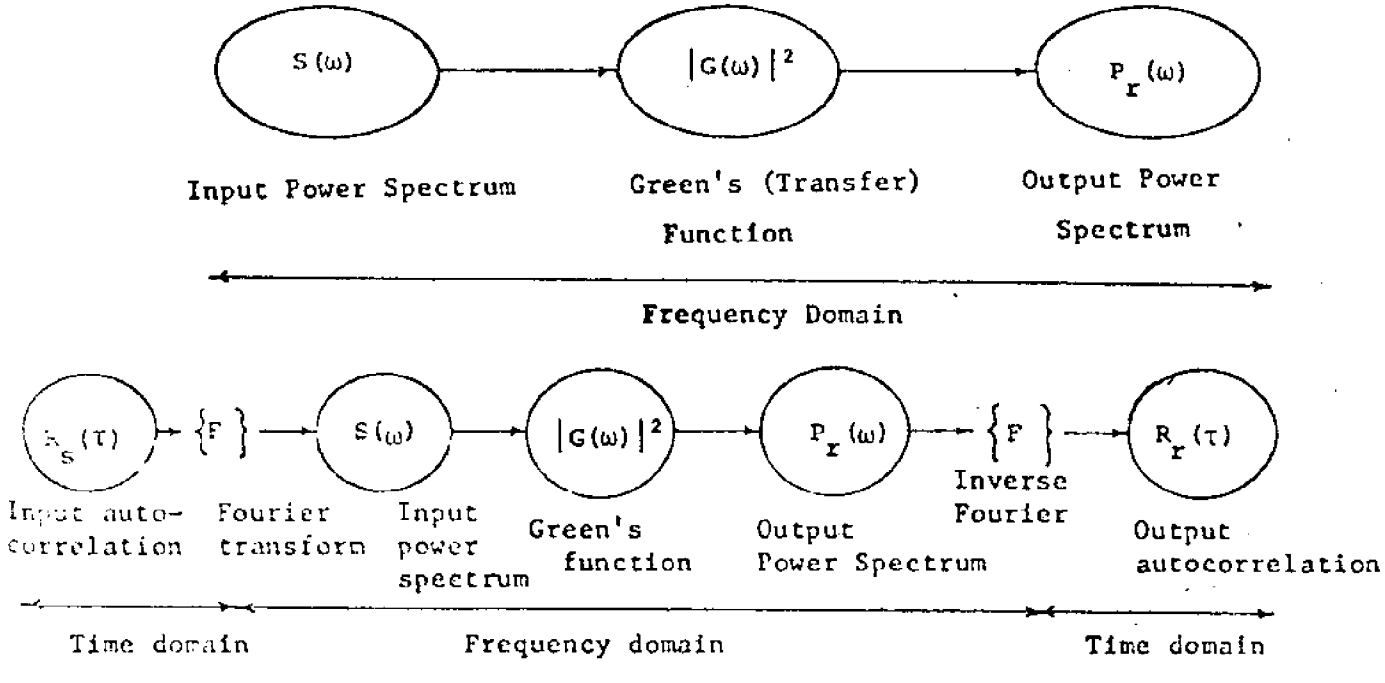

Most engineers are familiar with the concept of frequency response in steady state sinusoidol excitation, and therefore, the spectral analysis does weigh heavily as contrasted with autocorrelation analysis. Nevertheless, the complete theoretical equivalence of the two methods should be understood.

DISCUSSION OF THE GRAPHS

Figure (1): represents the raw acoustic data in a digitized raw time series.

The indicated separations of the data are interpreted as follows:

SECTION (1): The input signals.

SECTION (2): The first return echo from the ocean subbottom soil.

SECTION (3): The second return echo from the ocean subbottom soil.

SECTION (4): The third return echo from the ocean subbottom soil.

SECTION (1):

Figure (2): represents only the measured input signal in the ocean in time series

Figure (3): represents the even part in time series of the input signal

Figure (4): represents the odd part in time series of the input signal

Figure (5): represents the real part of the Fourier transform of the input signal. The fast Fourier transform technique enables us to compute from a digitized raw time series by a modified version of the Mertz program which employs the well-known Cooley and Tukey fast Fourier transform algorithm. To abate leakage into side slobes, a cosine taper window is applied to the data before it is transformed.

Figure (6): represents the imaginary part of the Fourier transform of the input signal obtained by the fast Fourier transform technique.

Figure (7): represents the magnified real part of the input signal in frequency domain obtained by fast Fourier transform technique.

Figure (8): represents the magnified imaginary part of the input signal in frequency domain obtained by fast Fourier transform technique.

Figure (9): represents the absolute value of the input signal in frequency domain obtained by the fast Fourier transform technique. The peak value frequency of the input is 5.12 KHz.

Figure (10): represents the spectral density of the input signal in frequency domain as shown by Equation (1) of the Appendix.

Figure (11): represents the autocorrelation function of the input signal in time series which is calculated from the inverse Fourier transform of the power spectrum of the real data, unmodified, except for the appending of at least as many zeros as there are time samplings.

SECTION (2):

Figure (12): represents only the first return echo from the ocean subbottom soil in time series.

Figure (13): represents the even part of the first return echo in time series.

Figure (14): represents the odd part of the first return echo in time series.

Figure (15): represents the real part of the first return echo in frequency domain obtained from the fast Fourier transform technique applied to the first return echo in time series.

Figure (16): represents the odd part of the first return echo in frequency domain obtained from the fast Fourier transform technique applied to the first return echo in time series.

Figure (17): represents the absolute value of the first return echo in frequency domain obtained from the fast Fourier transform technique applied to the first return echo in time series. The peak value frequency of the return is 5.20 KHz.

Figure (18): represents the spectral density of the first return echo in frequency domain.

Figure (19): represents the autocorrelation function of the first return echo in time series which is calculated from the inverse Fourier transform of the power spectrum.

SECTION (3):

Figure (20): represents only the second return echo from the ocean subbottom soil in time series.

Figure (21): represents the even part of the second return echo in time series.

Figure (22): represents the odd part of the second return echo in time series.

Figure (23): represents the real part of the second return echo in frequency domain obtained from the fast Fourier transform technique applied to the second return echo in time series.

Figure (24): represents the imaginary part of the second return echo in frequency domain obtained from the fast Fourier transform technique applied to the second return echo in time series.

Figure (25): represents the absolute value of the second return echo in frequency domain obtained from the fast Fourier transform technique applied to the second return echo in time series. The peak value frequency is 5.20 KHz.

Figure (26): represents the power spectral density of the second return echo in frequency domain.

Figure (27): represents the autocorrelation function of the first return echo in time series which is calculated from the inverse Fourier transform of the power spectrum.

SECTION (4):

Figure (28): represents only the third return echo from the ocean subbottom soil in time series.

Figure (29): represents the even part of the third return echo in time series.

Figure (30): represents the odd part of the third return echo in time series.

Figure (31): represents the real part of the third return echo in frequency domain obtained from the fast Fourier transform technique applied to the third return echo in time series.

Figure (32): represents the imaginary part of the third return echo in frequency domain obtained from the fast Fourier transform technique applied to the third return echo in time series.

Figure (33): represents the absolute value of the third return echo in frequency domain obtained from the fast Fourier transform technique applied to the third return echo in time series. The peak value frequency is 4.75 KHz.

Figure (34): represents the power spectral density of the third return echo in frequency domain.

Figure (35): represents the autocorrelation function of the third return echo in time series which is calculated from the inverse Fourier transform of the power spectrum.

Figure (36): represents the transfer function in time series defined as the ratio of the first three return echos, sections (1) through (4), and the input signal which is only section (1).

Figure (37): represents the real part of the transfer function in frequency domain obtained from the fast Fourier transform technique.

Figure (38): represents the imaginary part of the transfer function in frequency domain obtained from the fast Fourier transform technique.

Figure (39): represents the absolute value of the transfer function in frequency domain.

COMPARISON OF QUALITY FACTORS

The quality factor, Q, of a system is defined by the ratio $1/2\xi$ where ξ is the system damping constant. Graphically Q can be determined from the absolute value figures as sketched below.

Thus, the Q value for the ocean water medium from Figure (9) and for the first, second, and third return echoes from the ocean subbottom soil from Figures (17), (25) and (33), respectively, can be determined. Now, a comparison of the Q values of the first three return echos relative to the Q value of the input signal is presented by the ratio Q_{return}/Q_{input} where $Q_{input} = 1$ is taken for convenience.

$Q(\text{first return echo})/Q_{input}$	Frequency (KHz)
0.702	4.53
0.706	4.60
0.710	4.68
0.715	4.75
0.720	4.82
0.725	4.90
0.731	5.05
0.743	5.12
0.749	5.20
0.756	5.27
0.764	5.34
0.772	5.42
0.780	5.49

Average ratio: 0.736 Standard deviation: 0.025

Q(second return echo)/Q_{input}	Frequency (KHz)
0.290	4.53
0.271	4.60
0.263	4.68
0.264	4.75
0.271	4.82
0.283	4.90
0.296	4.97
0.308	5.05
0.317	5.12
0.323	5.20
0.325	5.27
0.323	5.34
0.316	5.42
0.305	5.49
Average ratio: 0.297	Standard deviation: 0.023

Q(third return echo)Q_{input}	Frequency (KHz)
0.260	4.53
0.254	4.60
0.247	4.68
0.240	4.75
0.232	4.82
0.223	4.90
0.215	4.97
0.206	5.05
0.198	5.12
0.189	5.20
0.181	5.27
0.173	5.34
0.164	5.42
0.157	5.49
Average ratio: 0.210	Standard deviation: 0.034

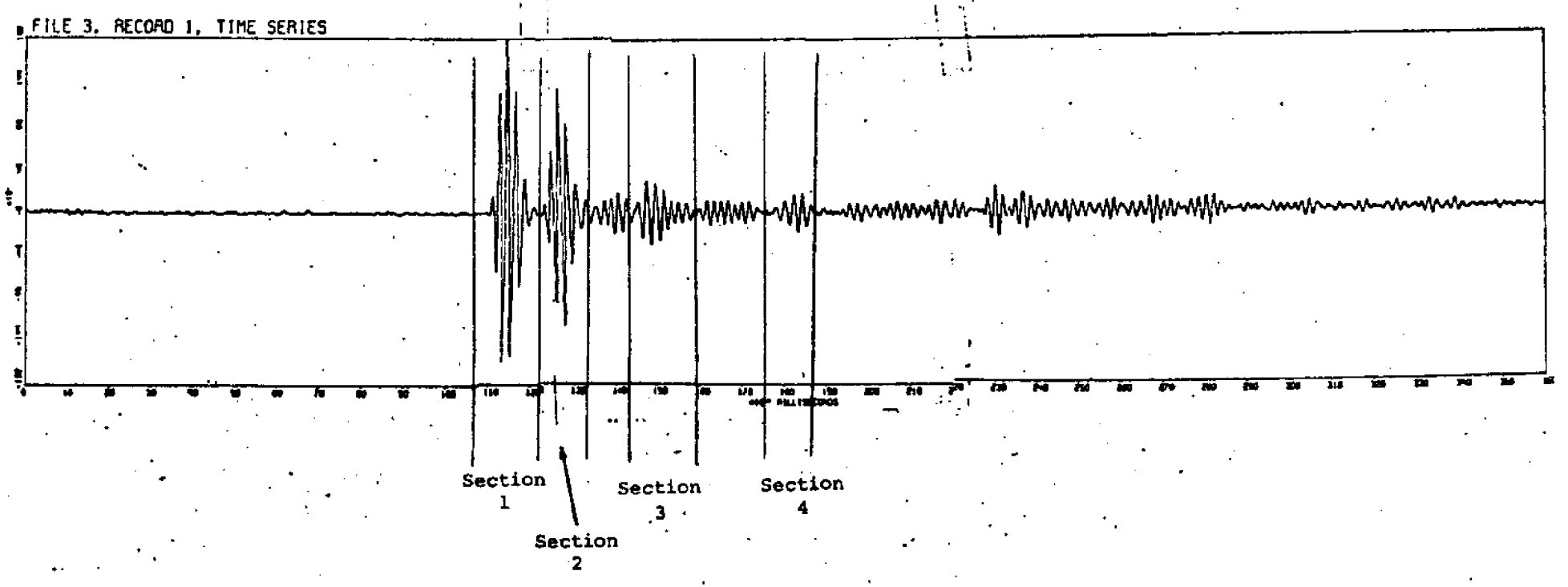
FILE 3. RECORD 1. TIME SERIES
Section 1
Section 2
Section 3
Section 4

FIGURE (1)

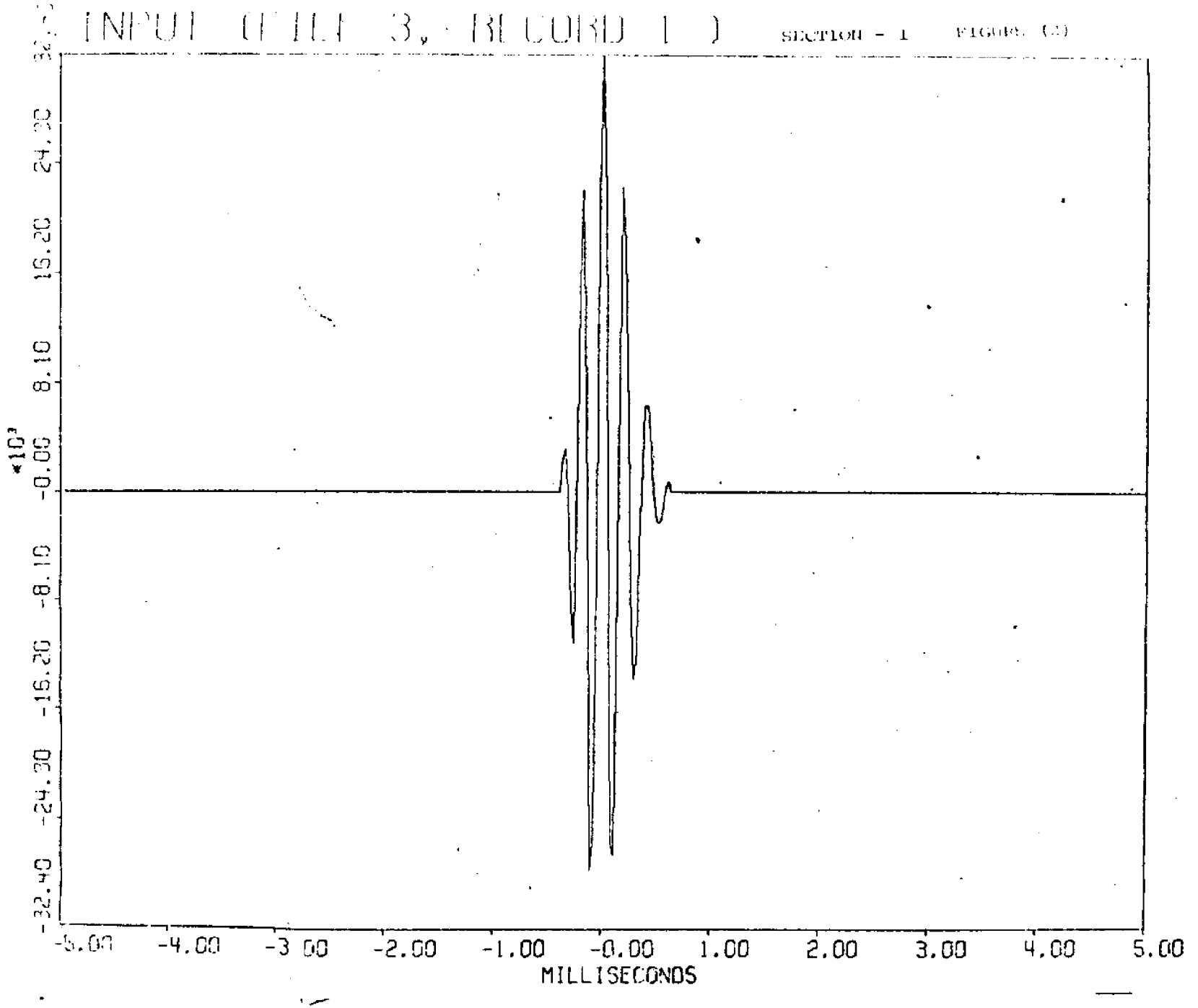
INPUT (FILE 3, RECORD 1)
SECTION - 1
FIGURE (3)
*10³
32.40
24.30
16.20
8.10
-0.00
-8.10
-16.20
-24.30
-32.40
-5.00
-4.00
-3.00
-2.00
-1.00
-0.00
1.00
2.00
3.00
4.00
5.00
MILLISECONDS

FIGURE (3)

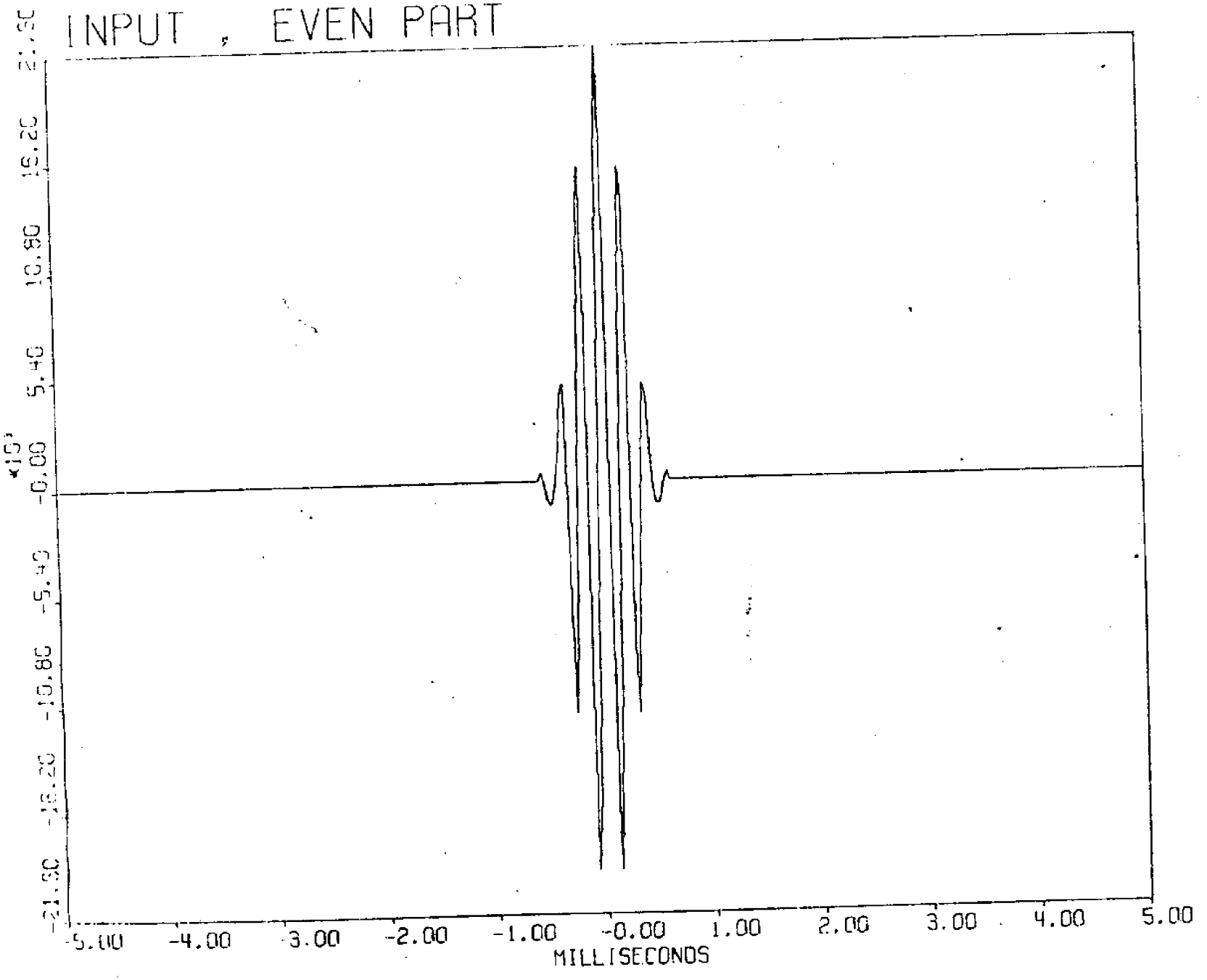
INPUT , EVEN PART
21.60
16.20
10.80
5.40
*10^3
-0.00
-5.40
-10.80
-16.20
-21.60
-5.00
-4.00
-3.00
-2.00
-1.00
-0.00
1.00
2.00
3.00
4.00
5.00
MILLISECONDS

FIGURE (4)

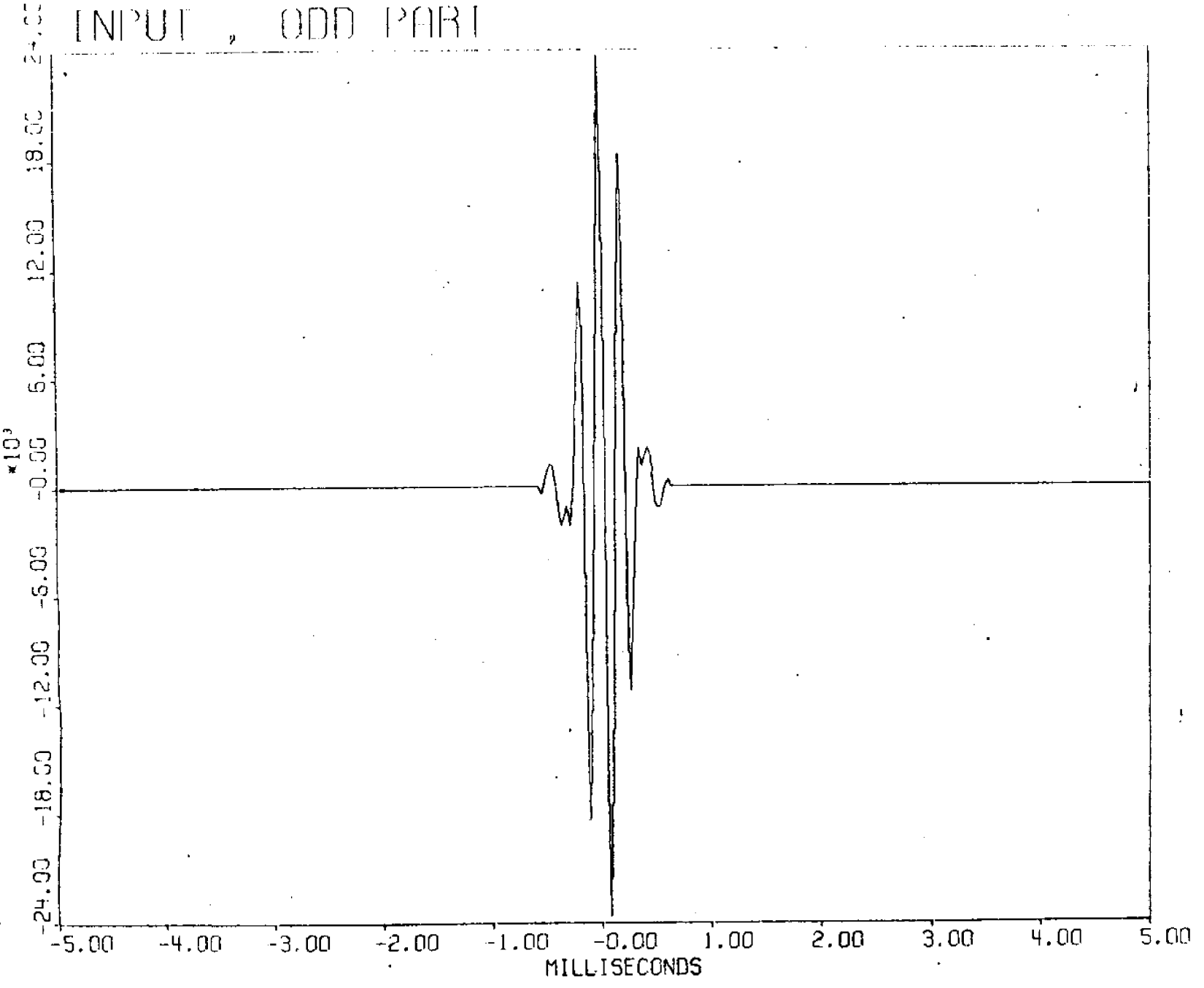
INPUT , ODD PART
*10³
24.00
18.00
12.00
6.00
-0.00
-6.00
-12.00
-18.00
-24.00
-5.00
-4.00
-3.00
-2.00
-1.00
-0.00
1.00
2.00
3.00
4.00
5.00
MILLISECONDS

FIGURE (5)

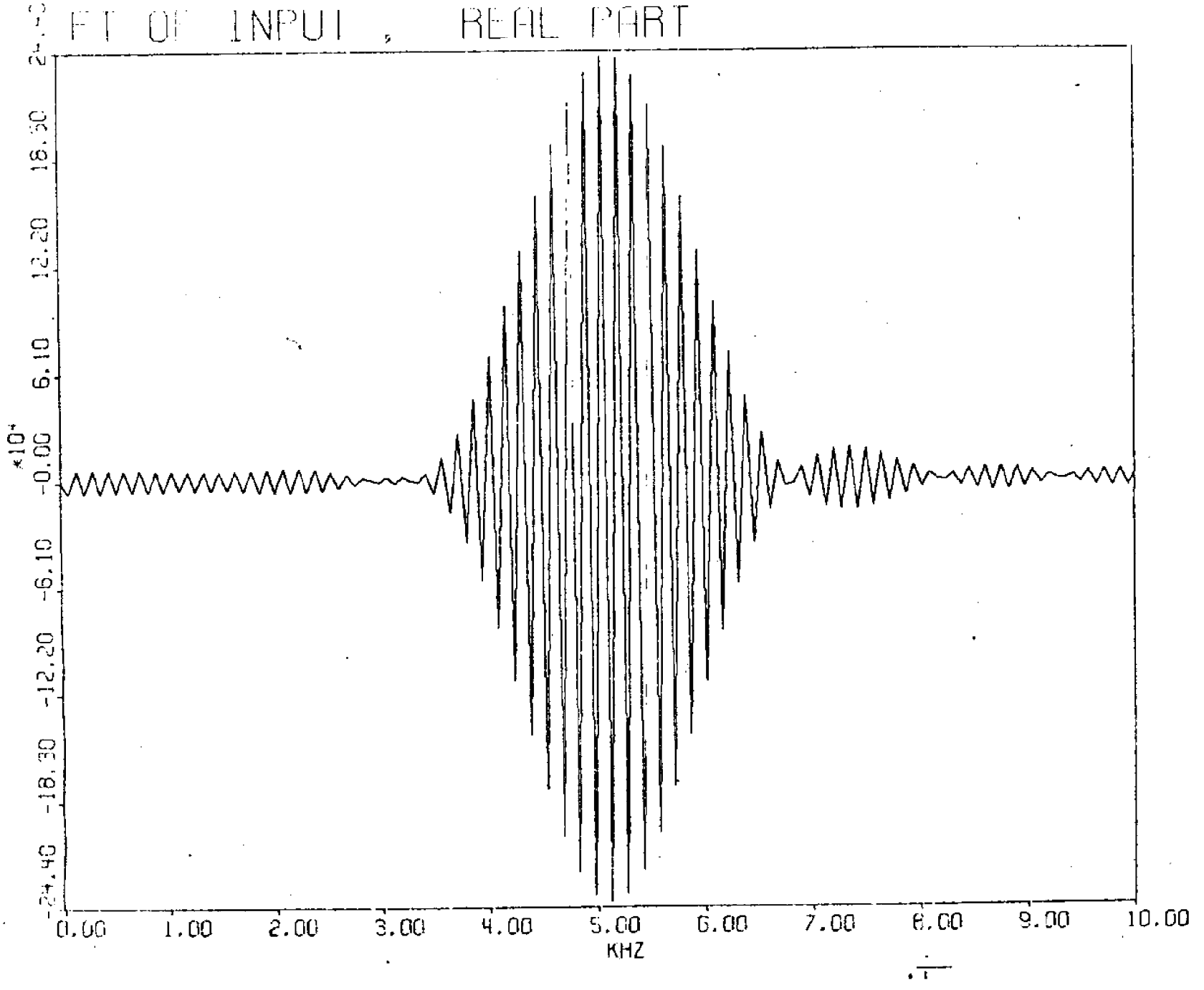
FT OF INPUT , REAL PART
*10⁴
6.10
-0.00
-6.10
-12.20
-18.30
0.00
1.00
2.00
3.00
4.00
5.00
6.00
7.00
8.00
9.00
10.00
KHZ

FIGURE (6)

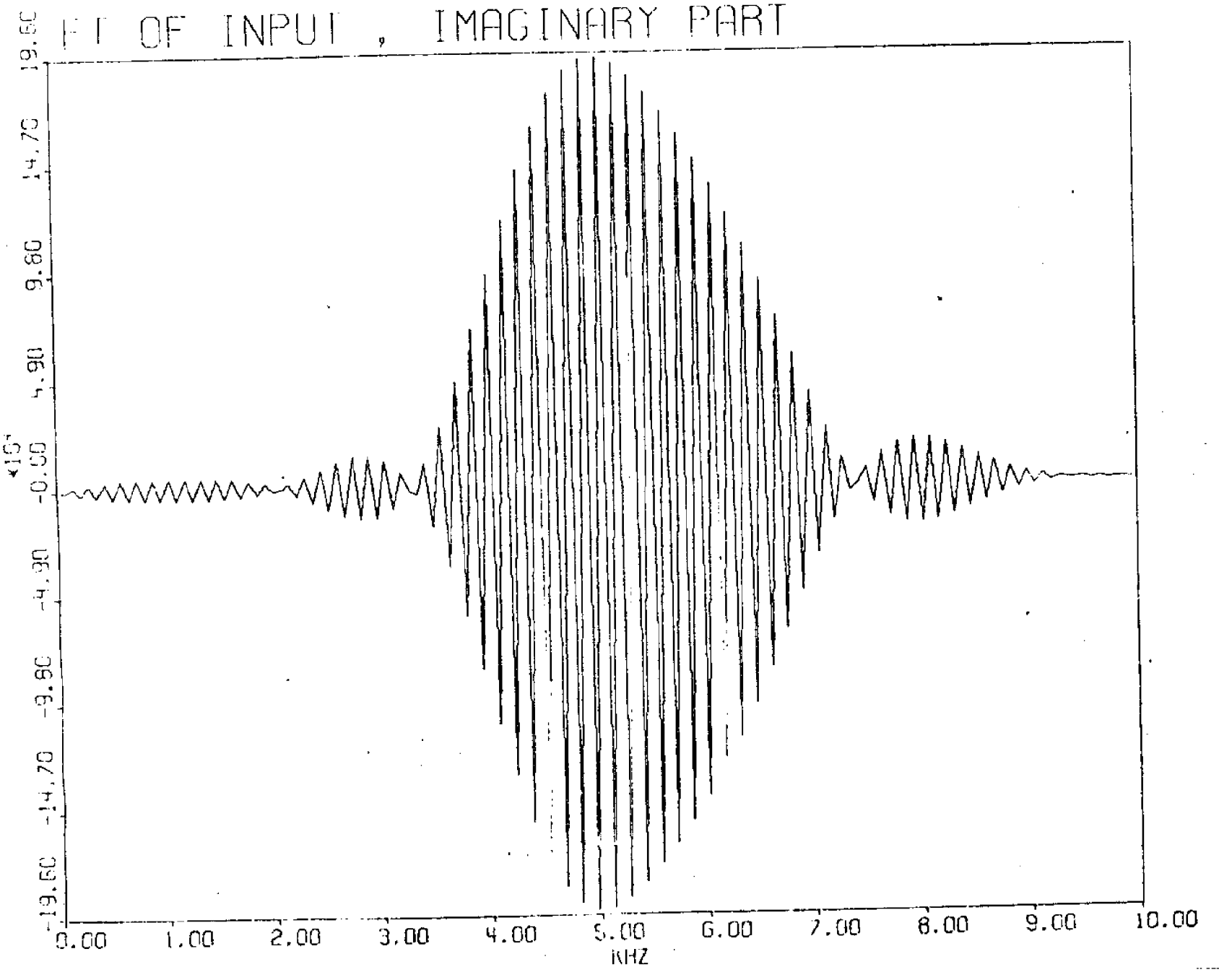
FT OF INPUT , IMAGINARY PART
19.60
14.70
9.80
4.90
-0.00
-4.90
-9.80
-14.70
-19.60
*10^
0.00
1.00
2.00
3.00
4.00
5.00
6.00
7.00
8.00
9.00
10.00
KHZ

FIGURE (7)

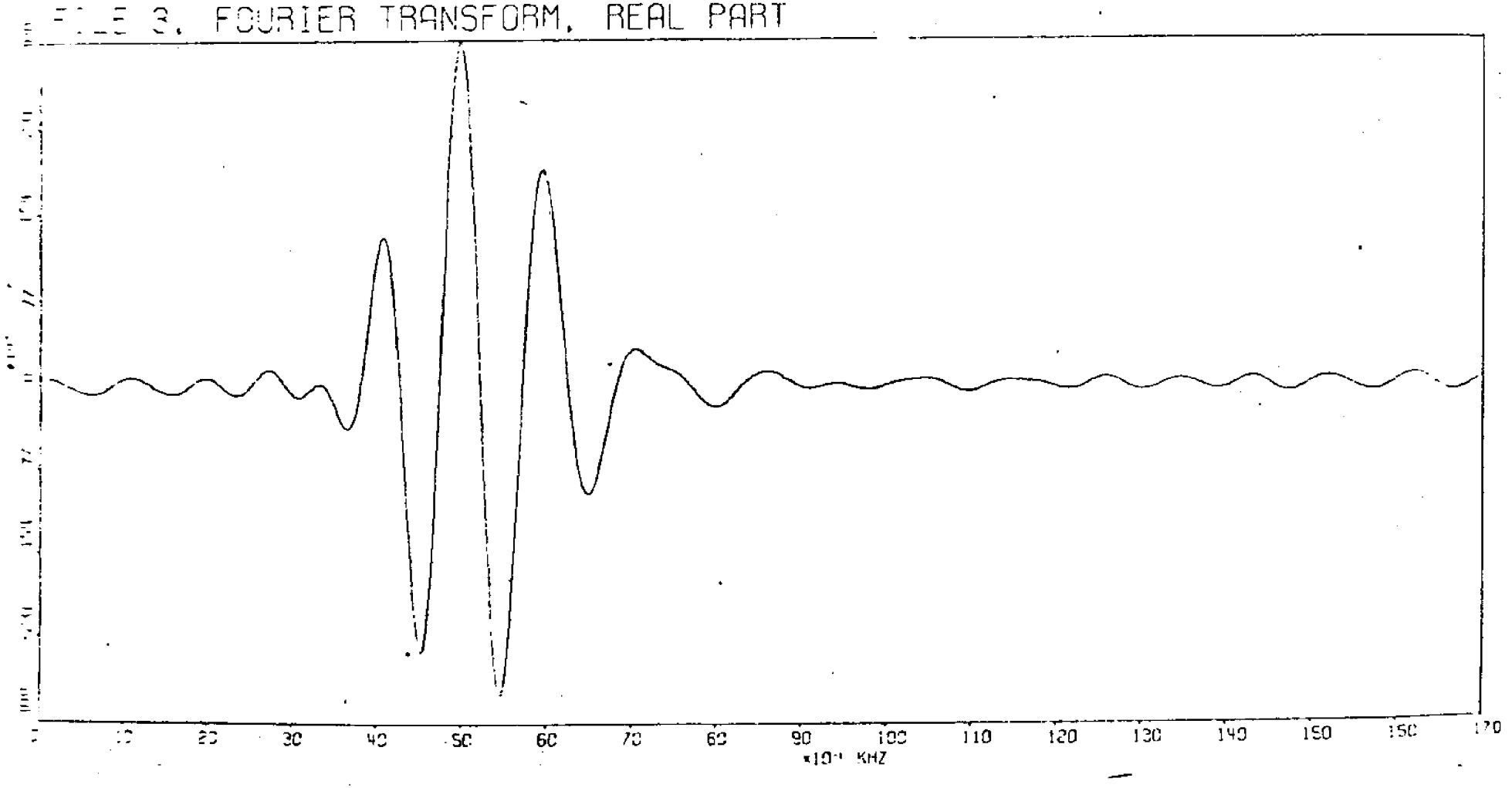
FILE 3. FOURIER TRANSFORM, REAL PART
10
20
30
40
50
60
70
80
90
100
110
120
130
140
150
160
170
KHZ

FIGURE (8)

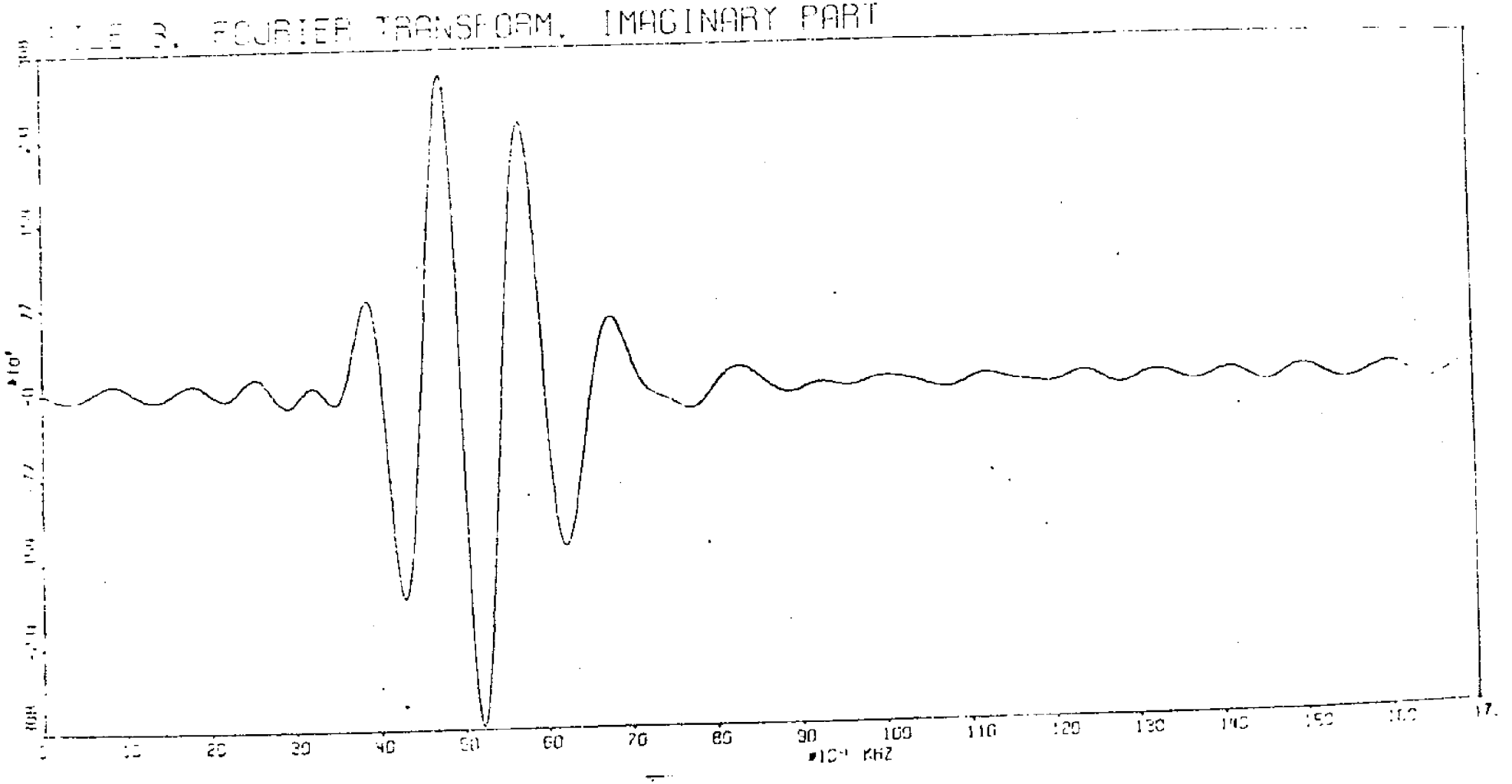
FOURIER TRANSFORM, IMAGINARY PART
0
10
20
30
40
50
60
70
80
90
100
110
120
130
140
150
160
170
KHZ

FIGURE (9)

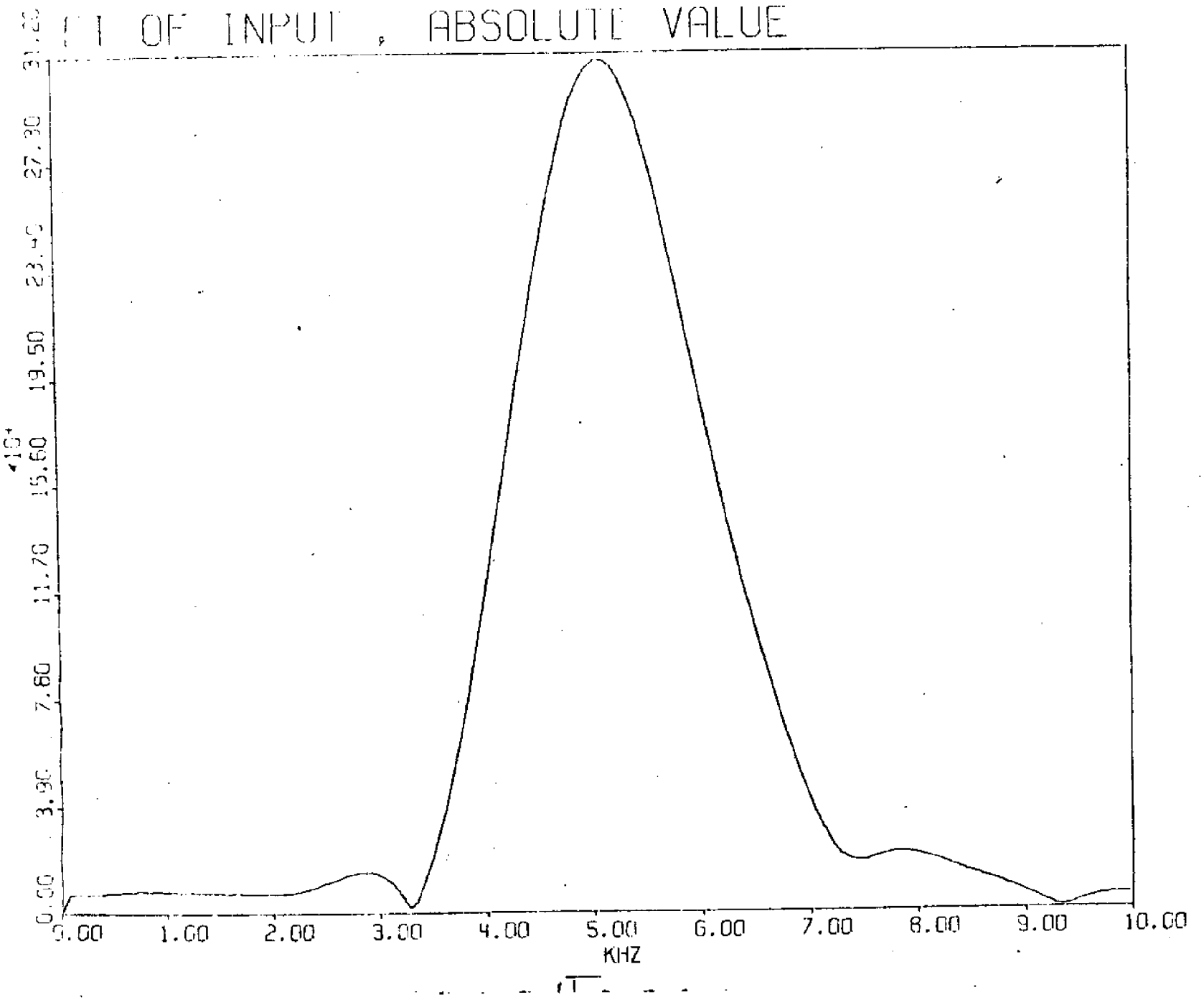
FT OF INPUT , ABSOLUTE VALUE
0.00
3.90
7.80
11.70
15.60
19.50
27.30
0.00
1.00
2.00
3.00
4.00
5.00
6.00
7.00
8.00
9.00
10.00
KHZ

FIGURE (19)

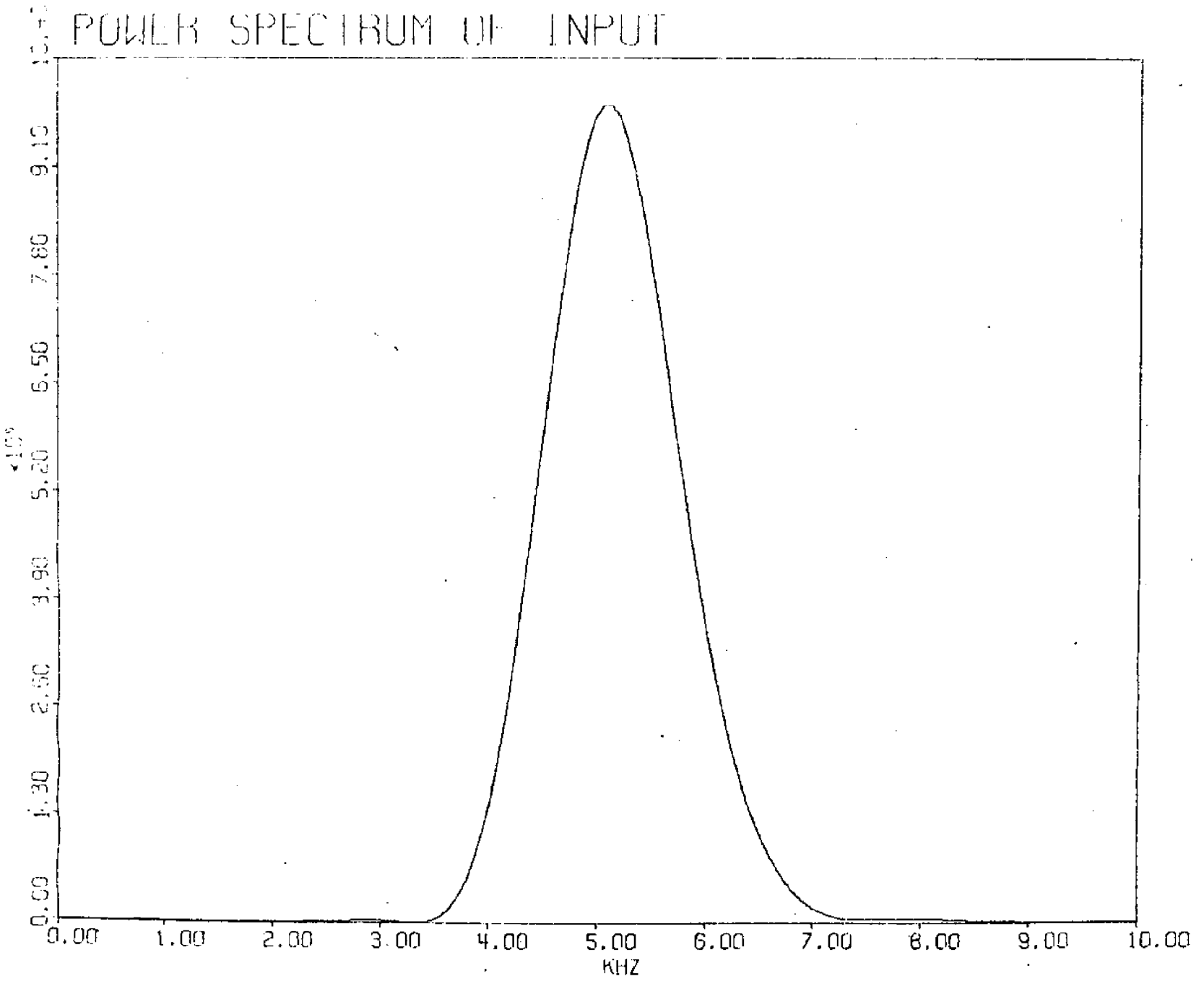
POWER SPECTRUM OF INPUT
0.00
1.30
2.60
3.90
5.20
6.50
7.80
9.10
0.00
1.00
2.00
3.00
4.00
5.00
6.00
7.00
8.00
9.00
10.00
KHZ

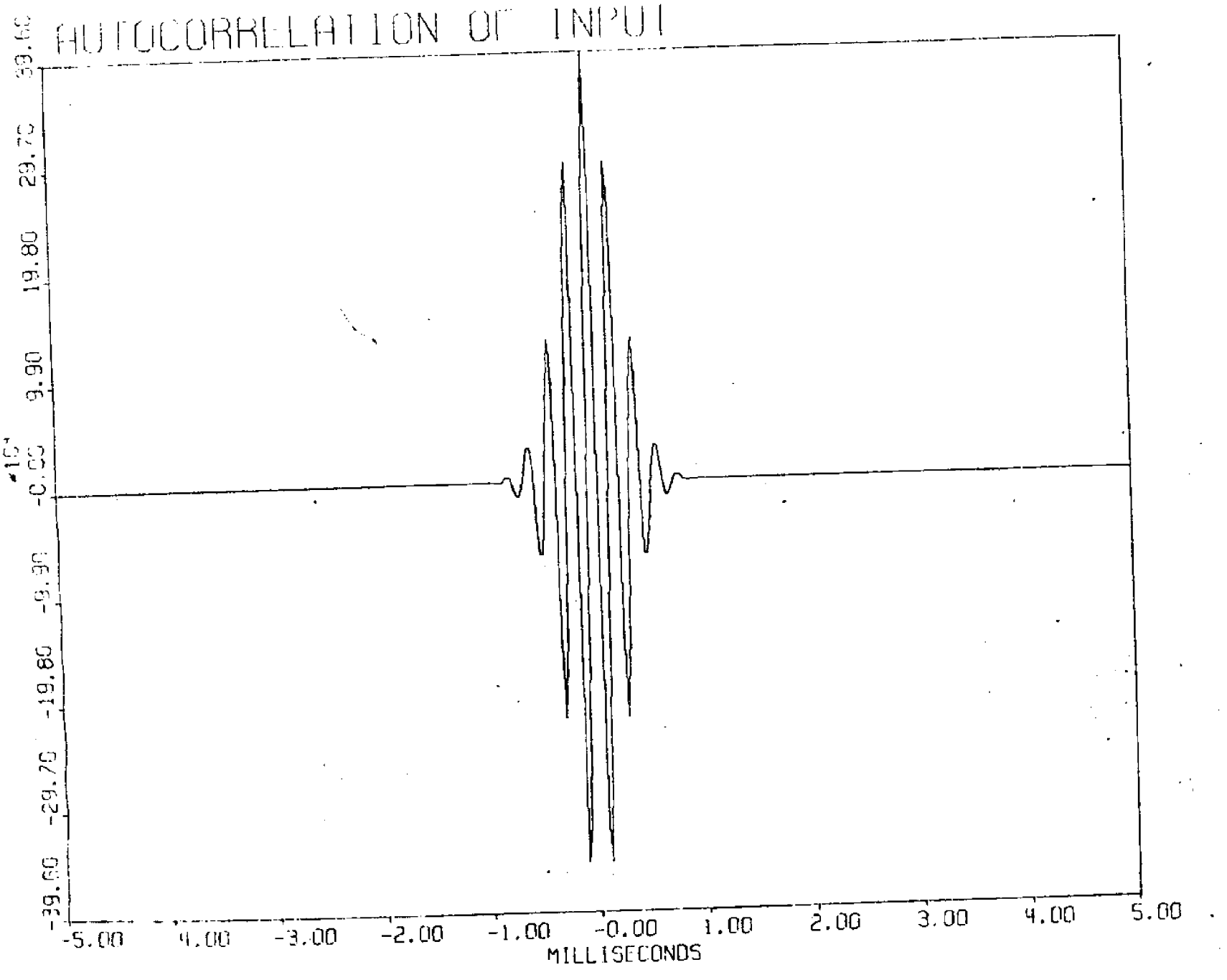
AUTOCORRELATION OF INPUT
MILLISECONDS
-5.00
-4.00
-3.00
-2.00
-1.00
-0.00
1.00
2.00
3.00
4.00
5.00

FIGURE (12)

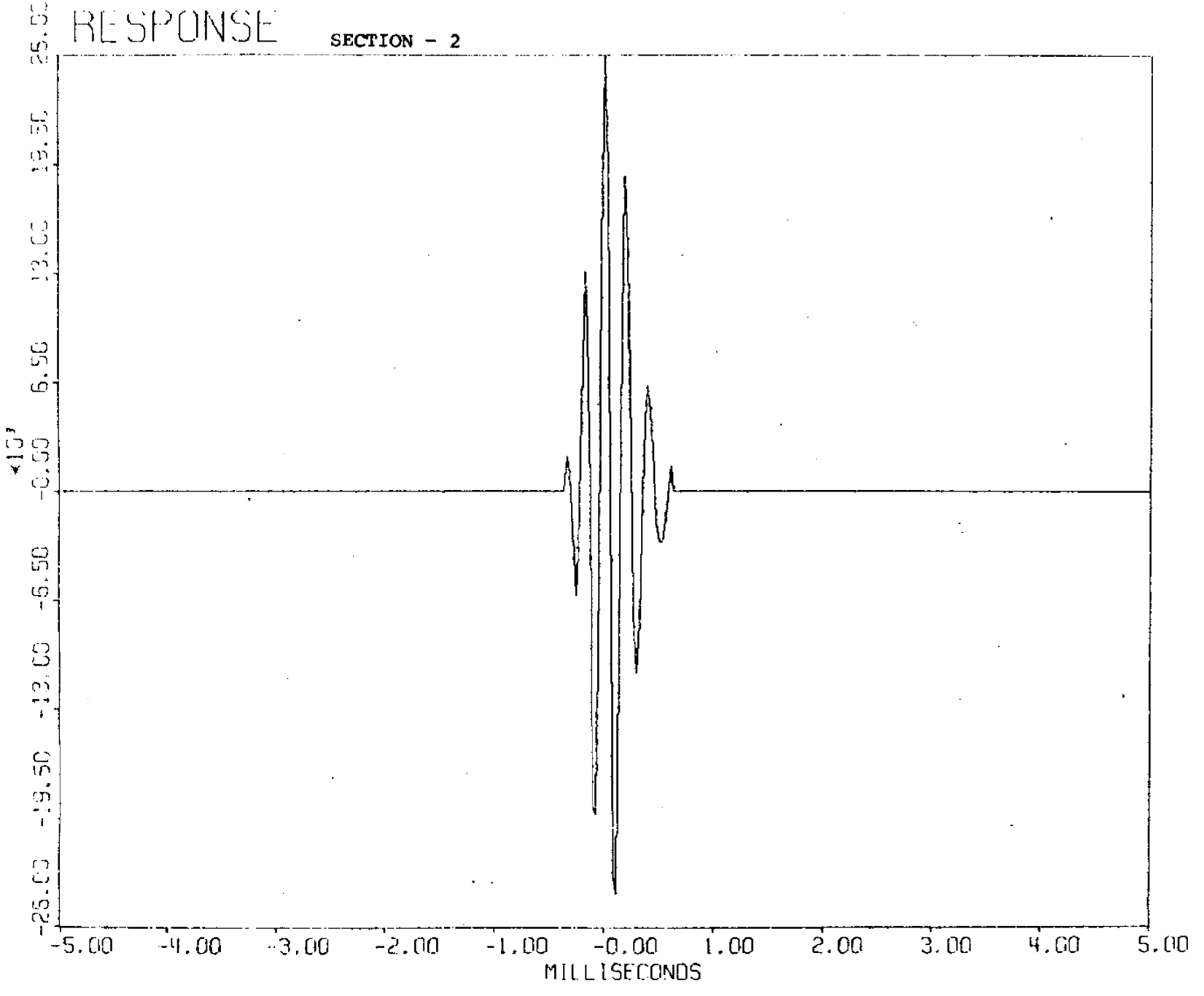
RESPONSE
SECTION - 2
25.50
13.50
6.50
-0.50
-6.50
-13.00
-19.50
-25.00
*10³
-5.00
-4.00
-3.00
-2.00
-1.00
-0.00
1.00
2.00
3.00
4.00
5.00
MILLISECONDS

FIGURE (13)

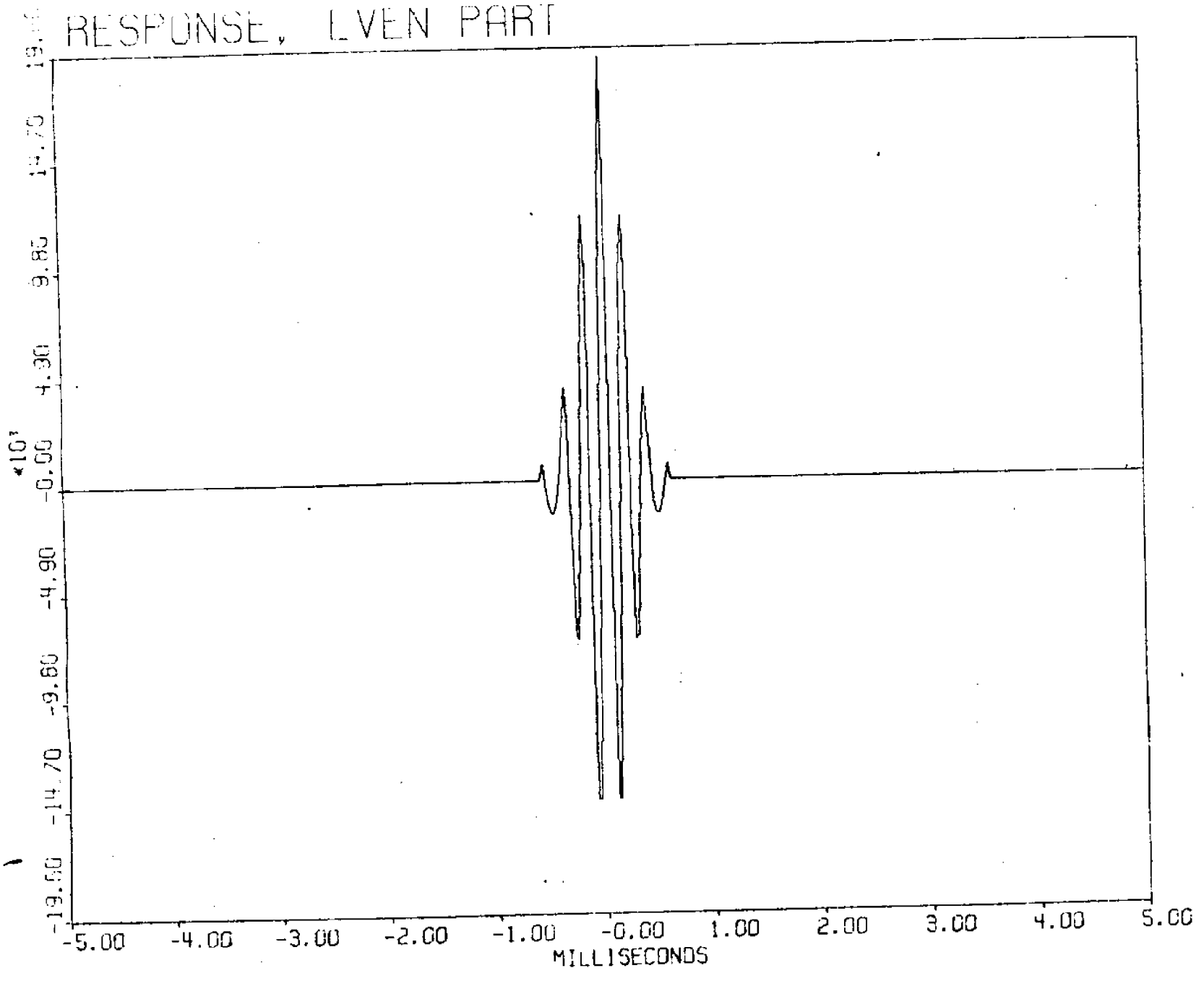
RESPONSE, EVEN PART
*10³
19.70
14.75
9.85
4.90
-0.00
-4.90
-9.80
-14.70
-19.60
-5.00
-4.00
-3.00
-2.00
-1.00
-0.00
1.00
2.00
3.00
4.00
5.00
MILLISECONDS

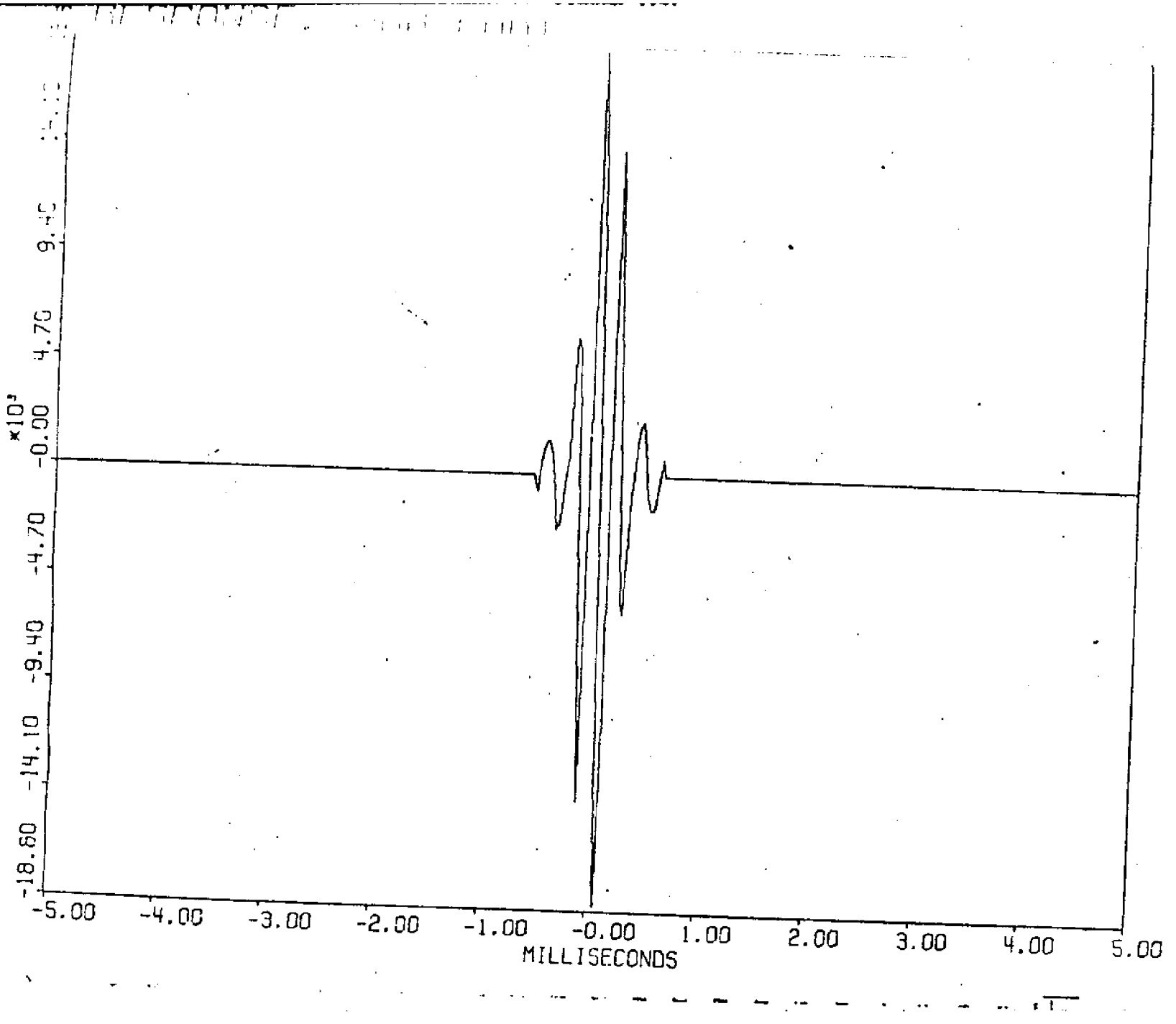
9.40
4.70
*10³
-0.00
-4.70
-9.40
-14.10
-18.80
-5.00
-4.00
-3.00
-2.00
-1.00
-0.00
1.00
2.00
3.00
4.00
5.00
MILLISECONDS

FIGURE (15)

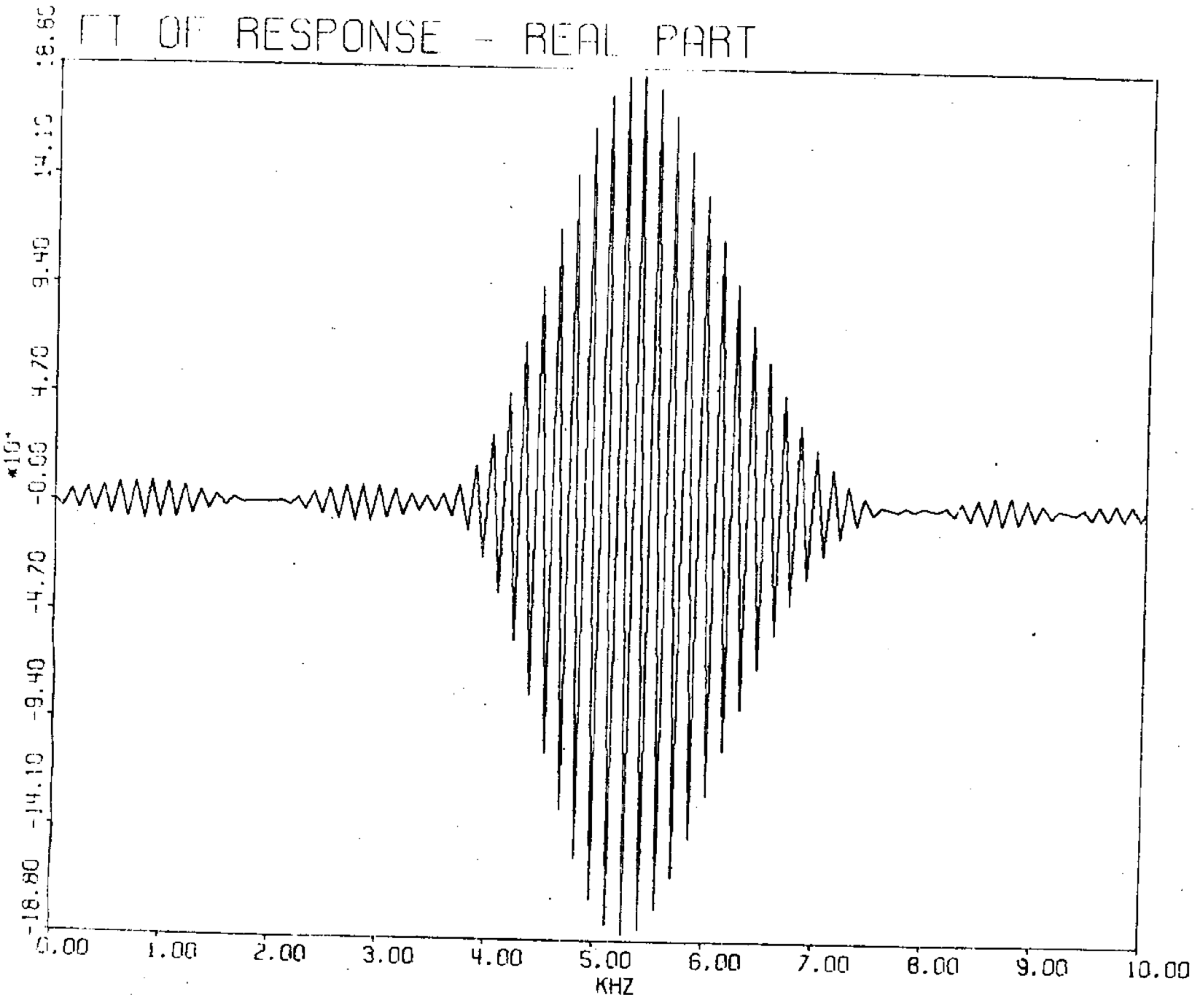
FT OF RESPONSE - REAL PART
*10^
-18.80
-14.10
-9.40
-4.70
0.00
4.70
9.40
14.10
18.80
0.00
1.00
2.00
3.00
4.00
5.00
6.00
7.00
8.00
9.00
10.00
KHZ

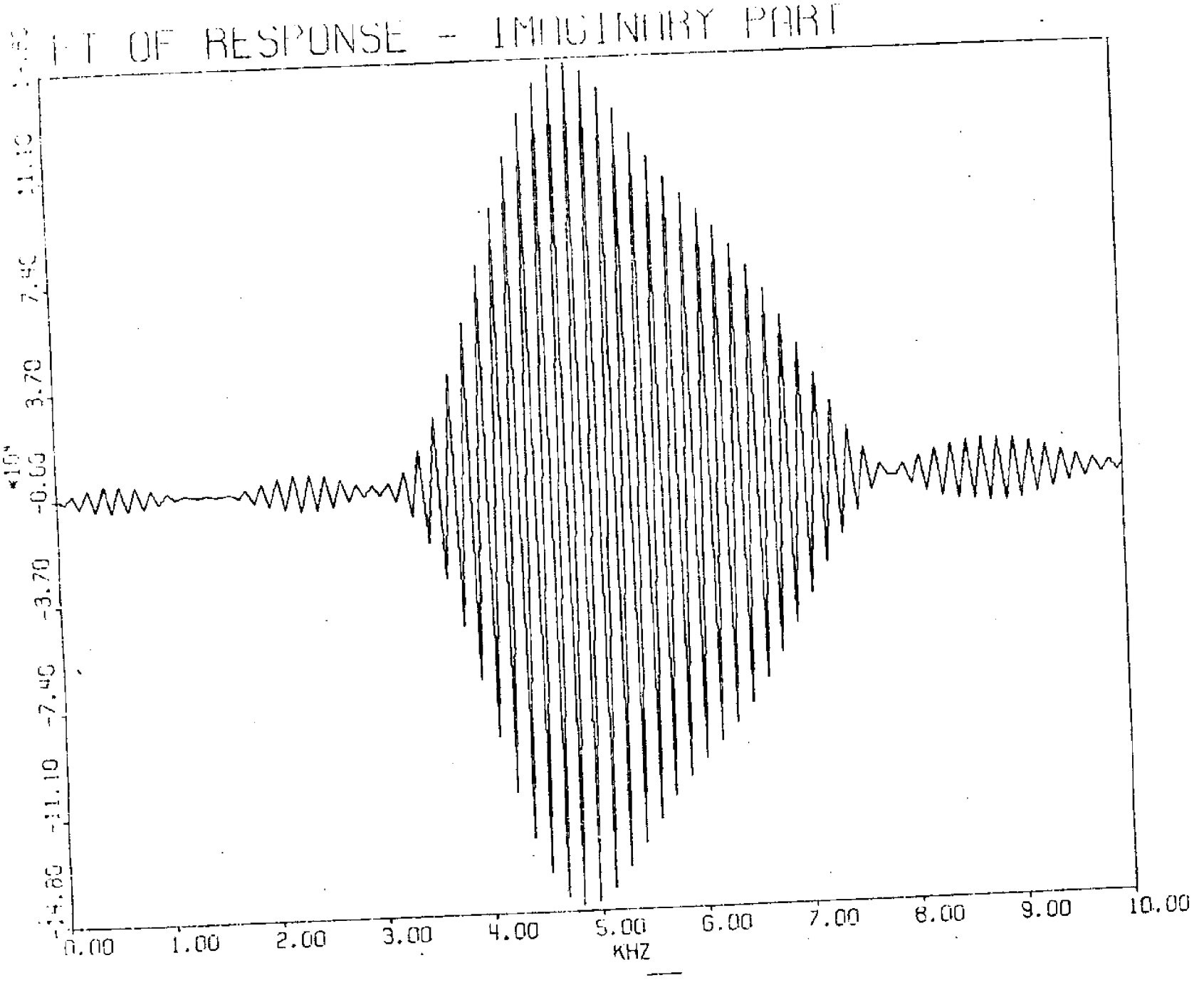
FT OF RESPONSE - IMAGINARY PART
*10^
3.70
-0.00
-3.70
-7.40
0.00
1.00
2.00
3.00
4.00
5.00
6.00
7.00
8.00
9.00
10.00
KHZ

FIGURE (17)

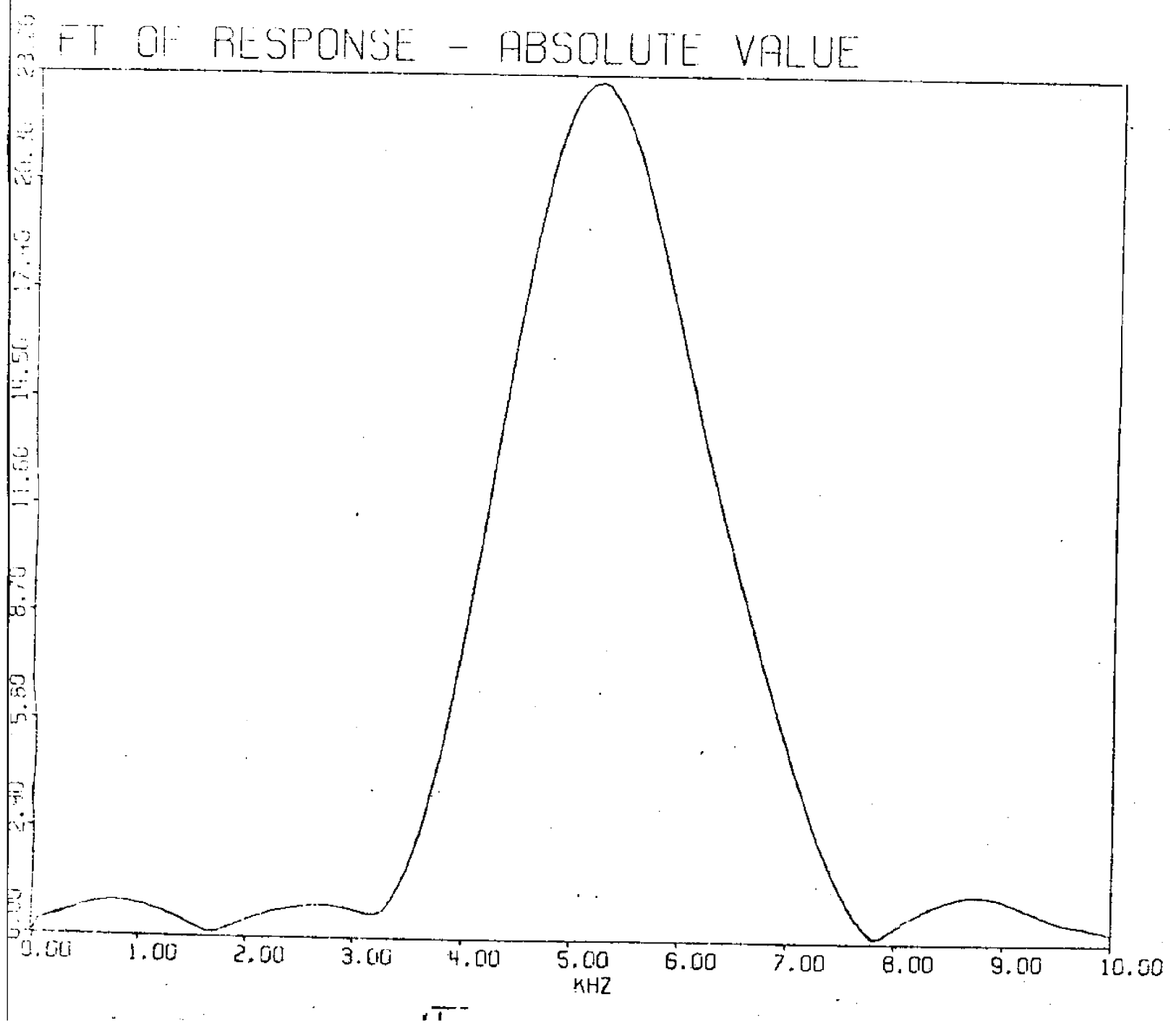
FT OF RESPONSE - ABSOLUTE VALUE
0.00
1.00
2.00
3.00
4.00
5.00
6.00
7.00
8.00
9.00
10.00
KHZ

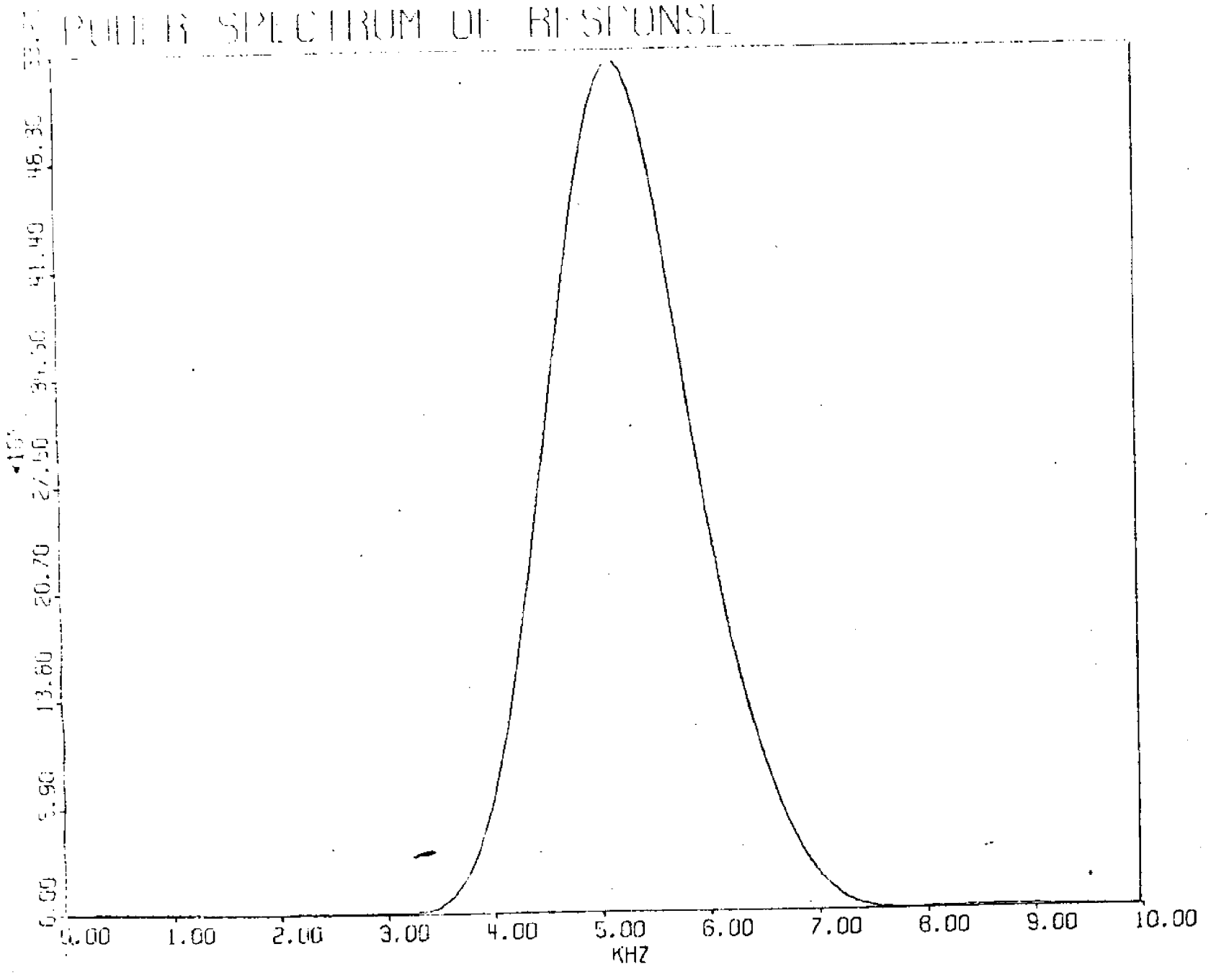
POWER SPECTRUM OF RESPONSE
6.90
13.80
20.70
27.50
34.30
41.40
48.30
0.00
1.00
2.00
3.00
4.00
5.00
6.00
7.00
8.00
9.00
10.00
KHZ

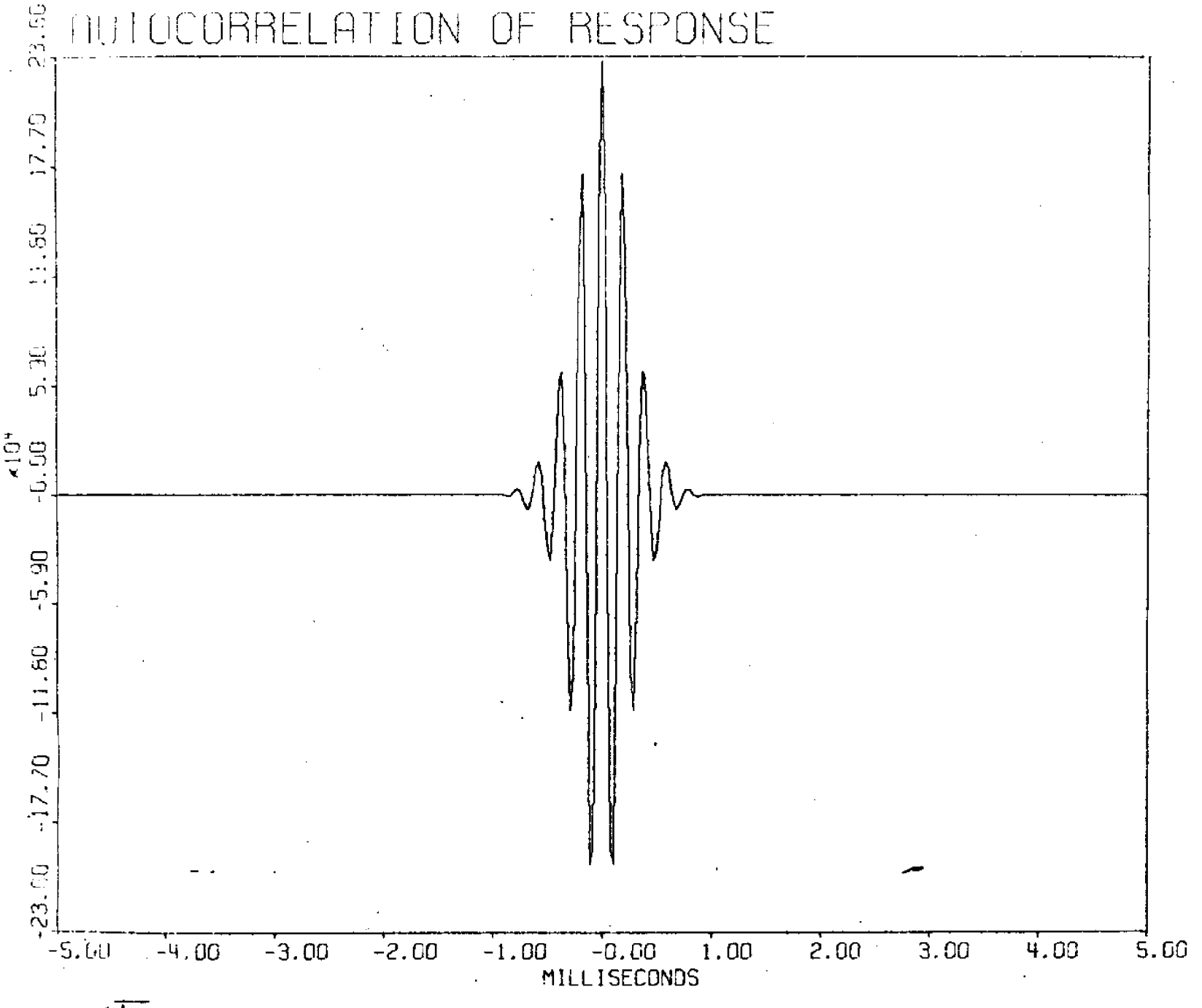
AUTOCORRELATION OF RESPONSE
23.50
17.70
11.80
5.90
-0.00
-5.90
-11.80
-17.70
-23.00
x10⁴
-5.00
-4.00
-3.00
-2.00
-1.00
-0.00
1.00
2.00
3.00
4.00
5.00
MILLISECONDS

FIGURE (20)

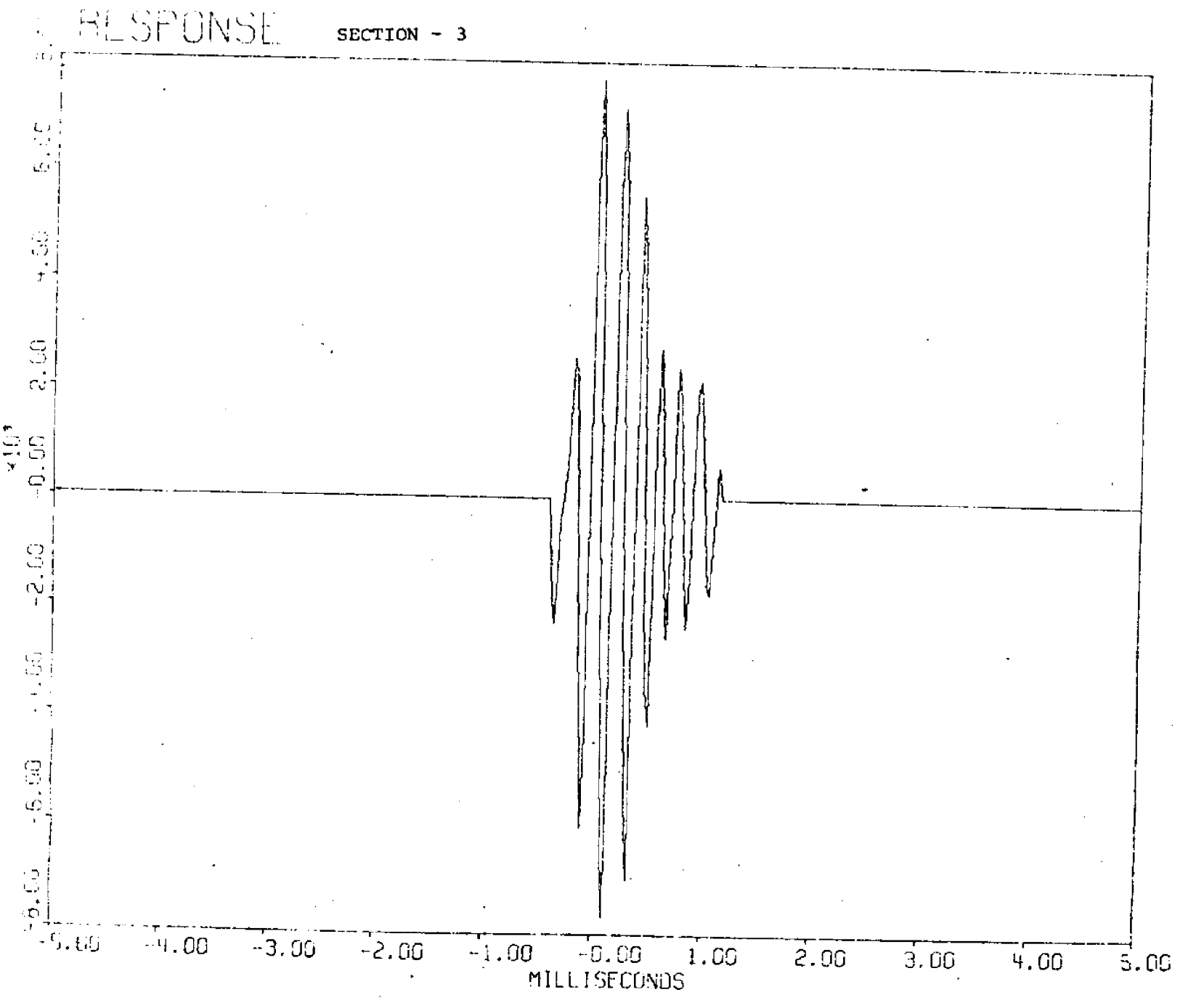
RESPONSE
SECTION - 3
-2.00
-0.00
-5.00
-4.00
-3.00
-2.00
-1.00
-0.00
1.00
2.00
3.00
4.00
5.00
MILLISECONDS

FIGURE (21)

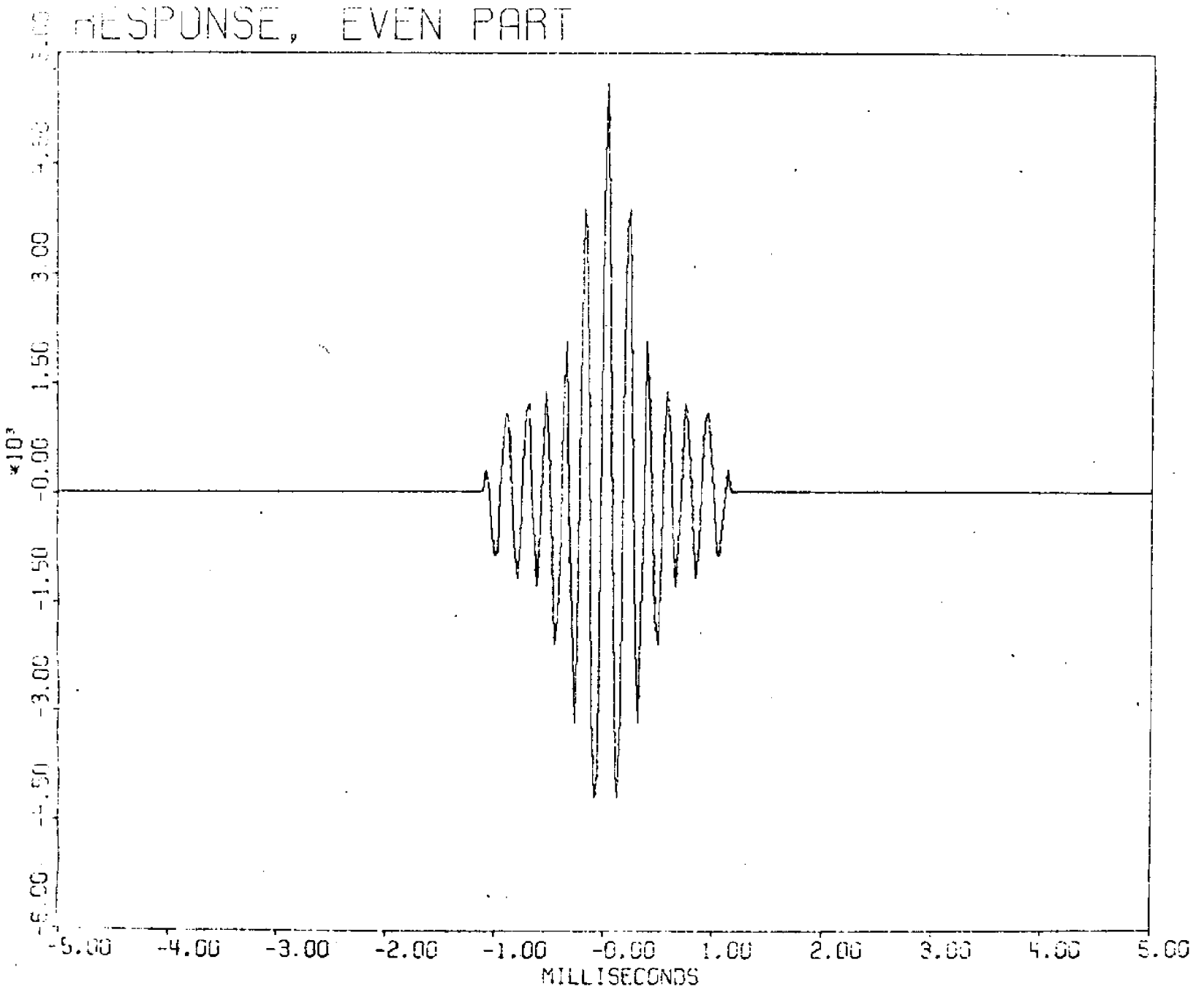
RESPONSE, EVEN PART
*10³
3.00
1.50
-0.00
-1.50
-3.00
-5.00
-5.00
-4.00
-3.00
-2.00
-1.00
-0.00
1.00
2.00
3.00
4.00
5.00
MILLISECONDS

FIGURE (12)

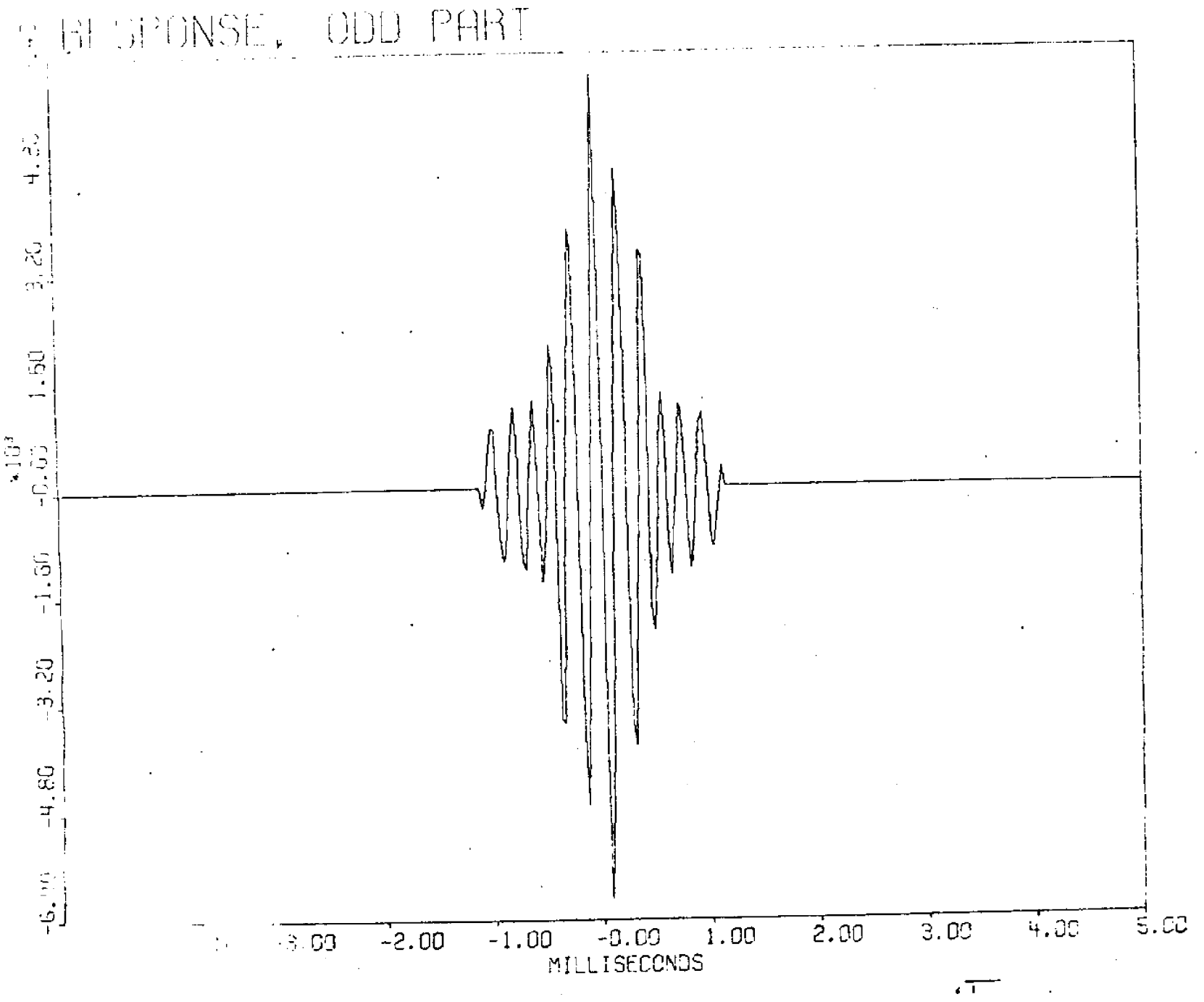
RESPONSE, ODD PART
*10³
4.80
3.20
1.60
-0.00
-1.60
-3.20
-4.80
-6.40
-3.00
-2.00
-1.00
-0.00
1.00
2.00
3.00
4.00
5.00
MILLISECONDS

FIGURE (23)

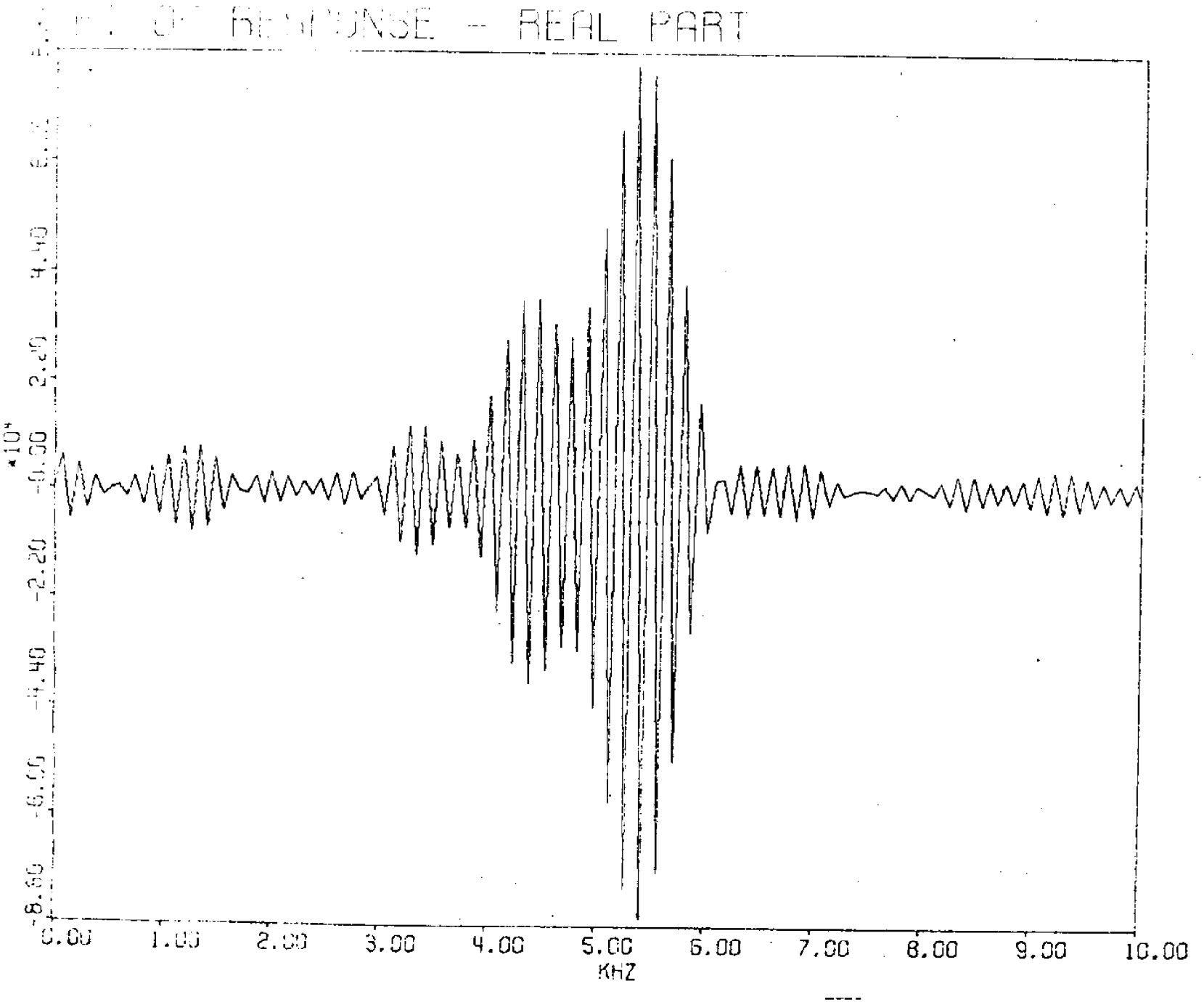
REAL PART
*10⁴
-8.80
-6.60
-4.40
-2.20
-0.00
2.20
4.40
0.00
1.00
2.00
3.00
4.00
5.00
6.00
7.00
8.00
9.00
10.00
KHZ

FIGURE (24)

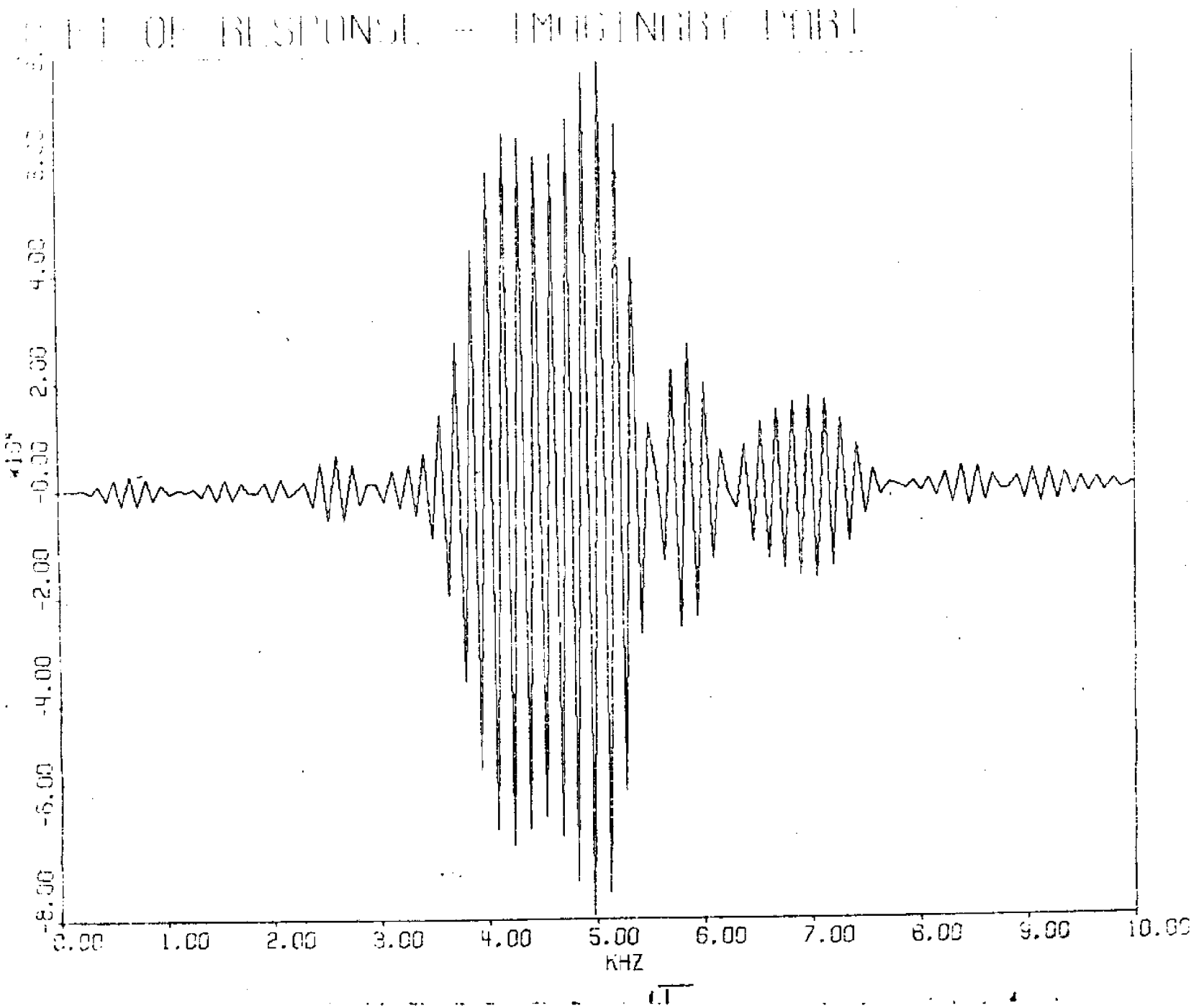
-8.00
-6.00
-4.00
-2.00
-0.00
2.00
4.00
0.00
1.00
2.00
3.00
4.00
5.00
6.00
7.00
8.00
9.00
10.00
KHZ

FIGURE (25)

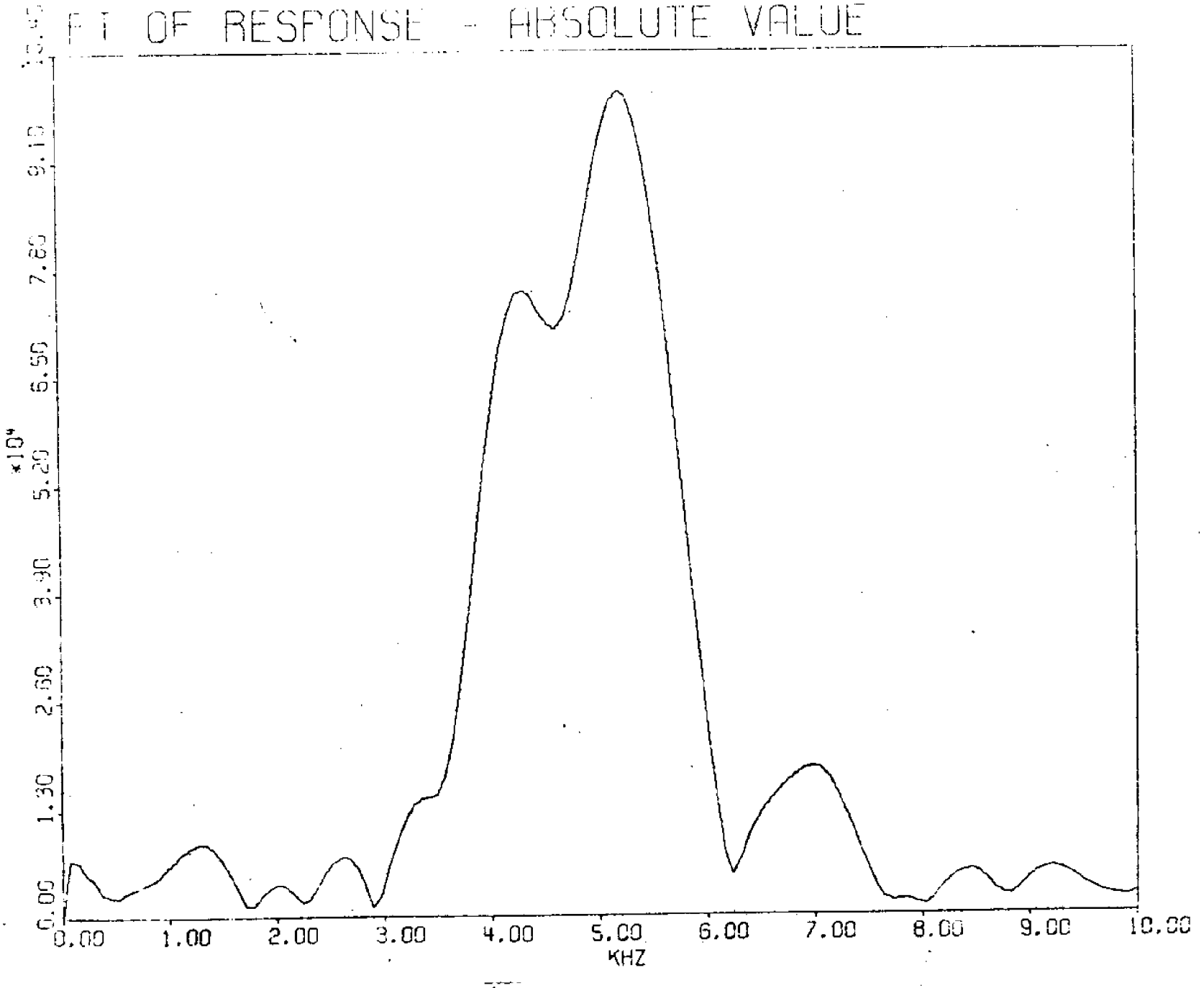
FT OF RESPONSE - ABSOLUTE VALUE
*10⁴
0.00
1.30
2.60
3.90
5.20
6.50
7.80
9.10
0.00
1.00
2.00
3.00
4.00
5.00
6.00
7.00
8.00
9.00
10.00
KHZ

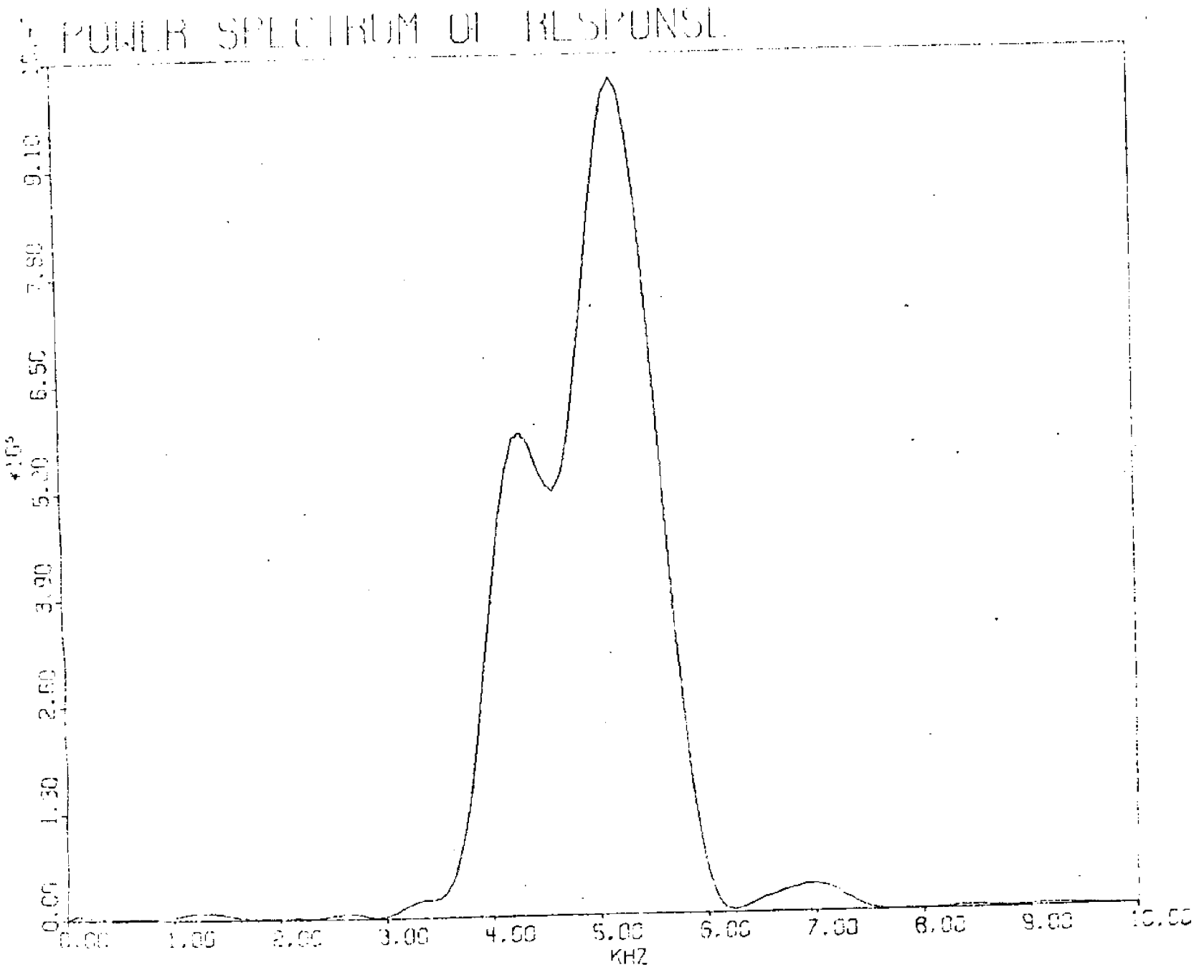
POWER SPECTRUM OF RESPONSE
9.10
7.80
6.50
5.20
3.90
2.60
1.30
0.00
*10³
0.00
1.00
2.00
3.00
4.00
5.00
6.00
7.00
8.00
9.00
10.00
KHZ

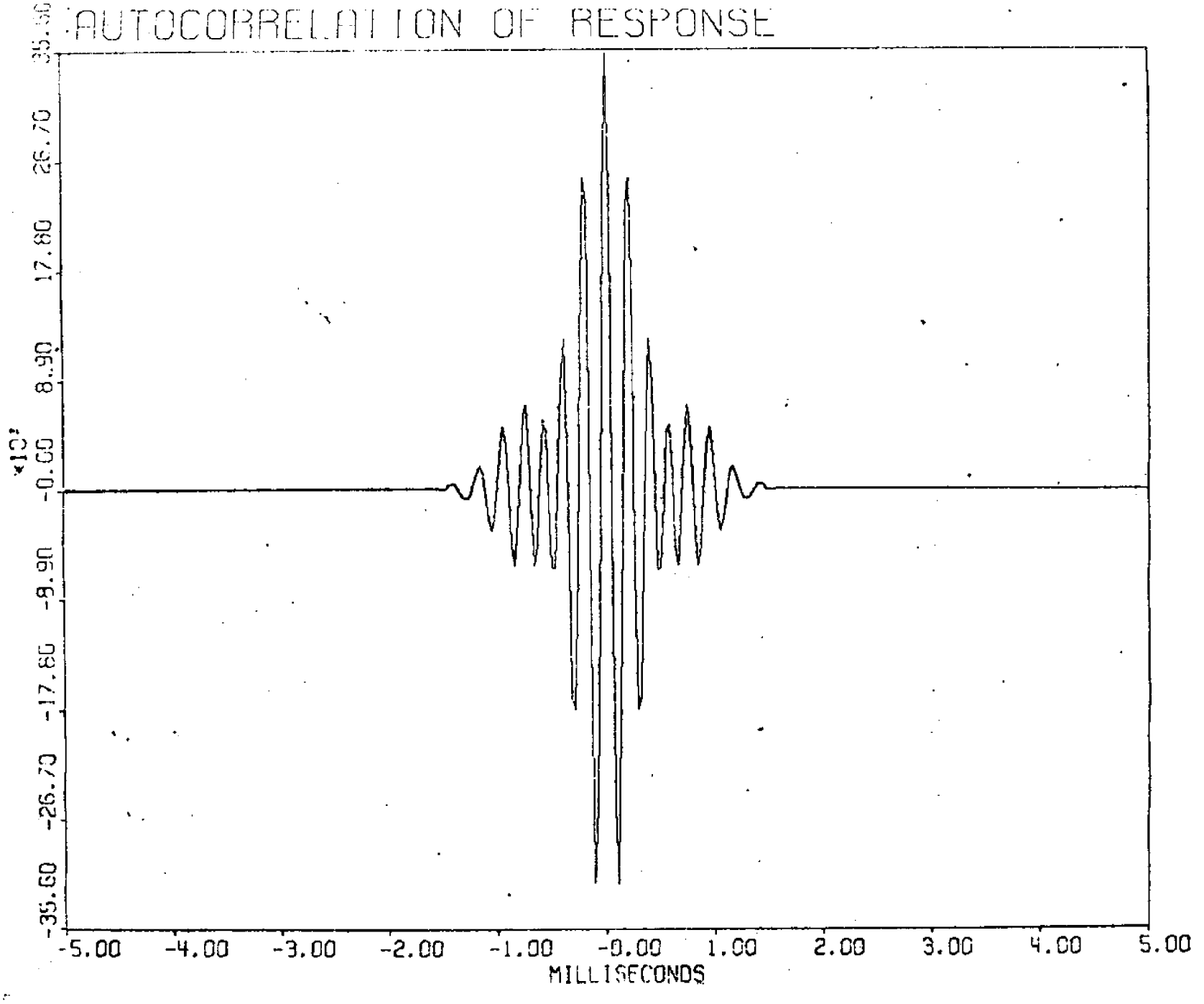
AUTOCORRELATION OF RESPONSE
35.60
26.70
17.80
8.90
-0.00
-8.90
-17.80
-26.70
-35.60
*10³
-5.00
-4.00
-3.00
-2.00
-1.00
-0.00
1.00
2.00
3.00
4.00
5.00
MILLISECONDS

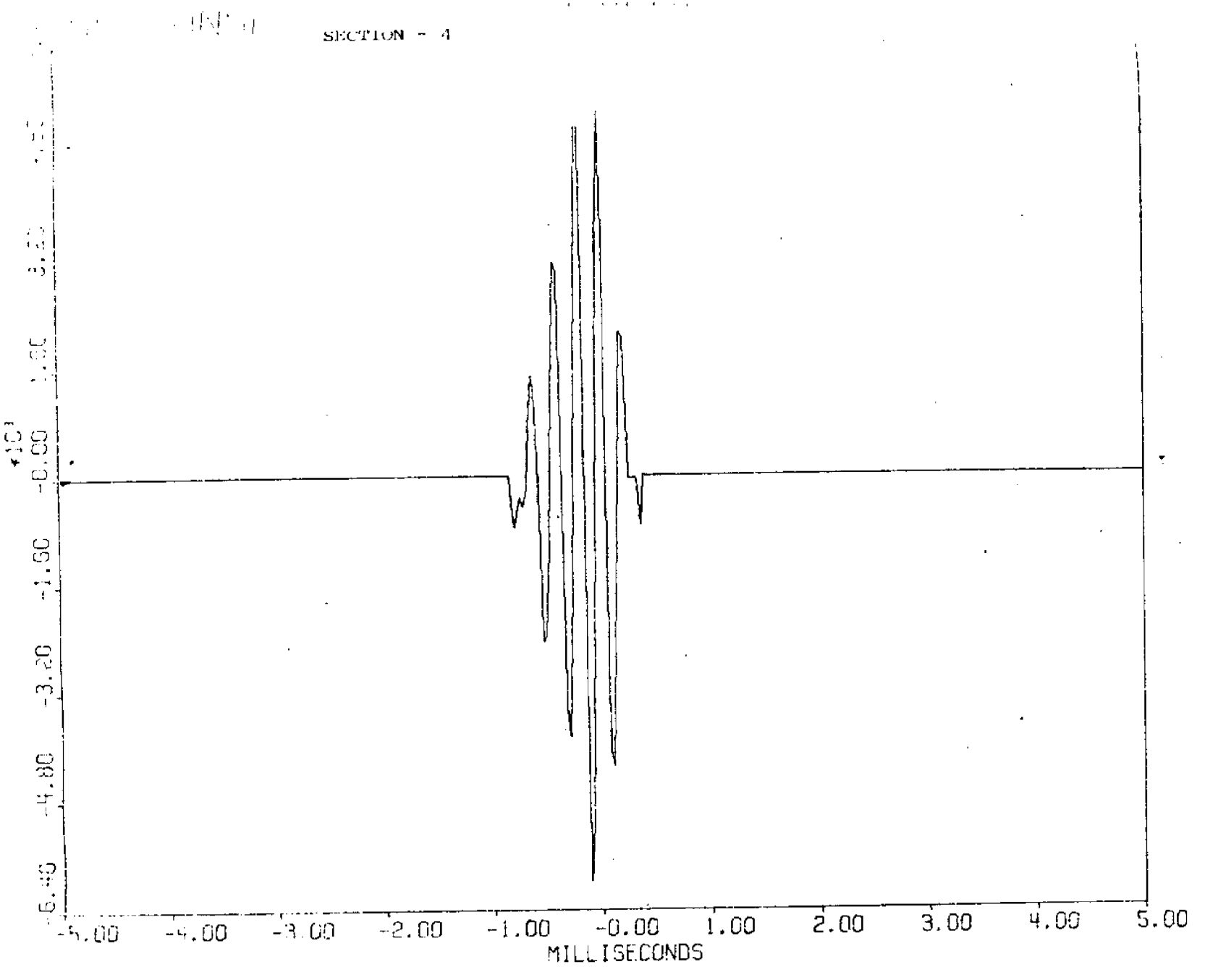
SECTION - 4
-0.00
-1.60
-3.20
-4.80
-5.00
-4.00
-3.00
-2.00
-1.00
-0.00
1.00
2.00
3.00
4.00
5.00
MILLISECONDS

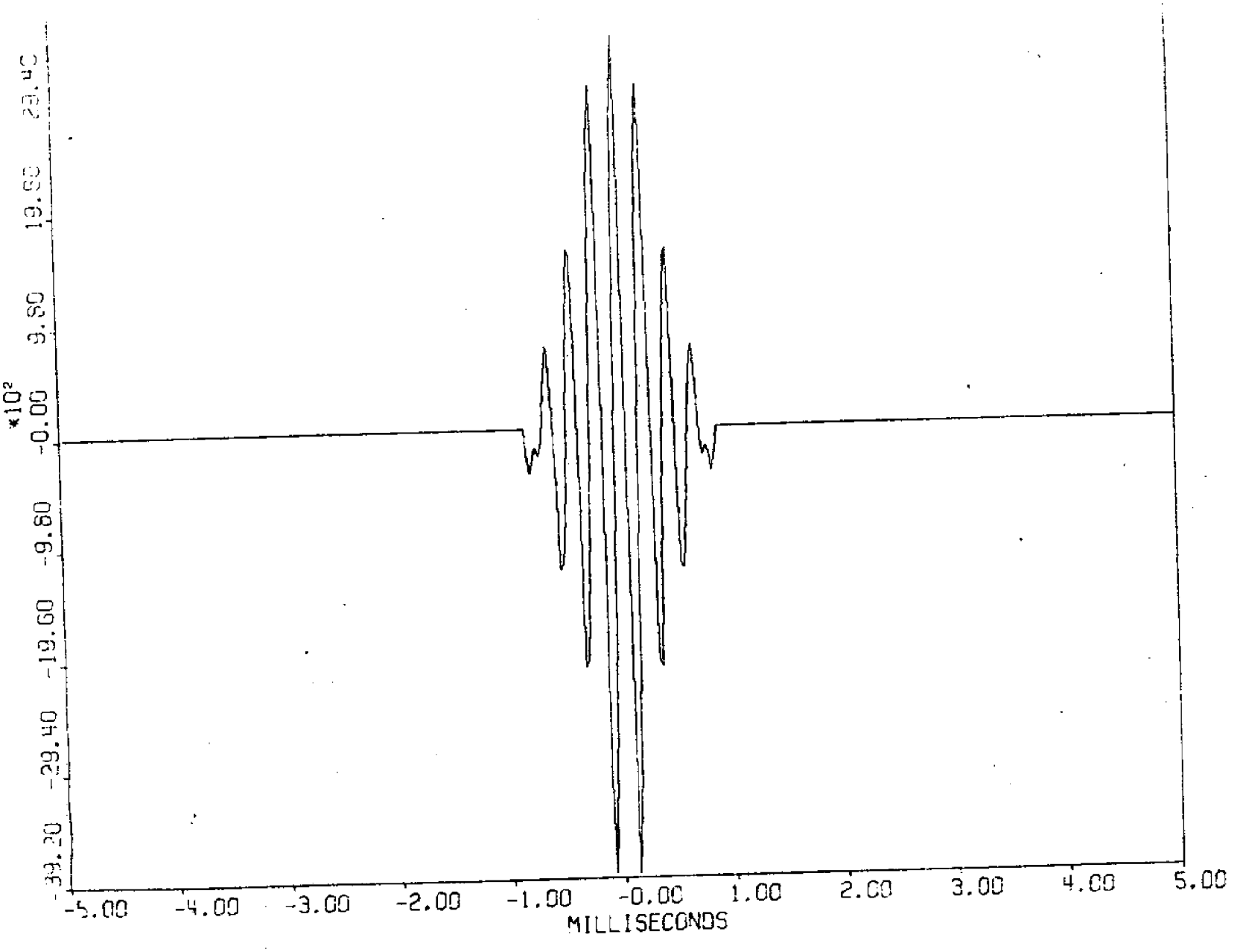
*10²
9.80
-0.00
-9.80
-19.60
-29.40
-39.20
-5.00
-4.00
-3.00
-2.00
-1.00
-0.00
1.00
2.00
3.00
4.00
5.00
MILLISECONDS

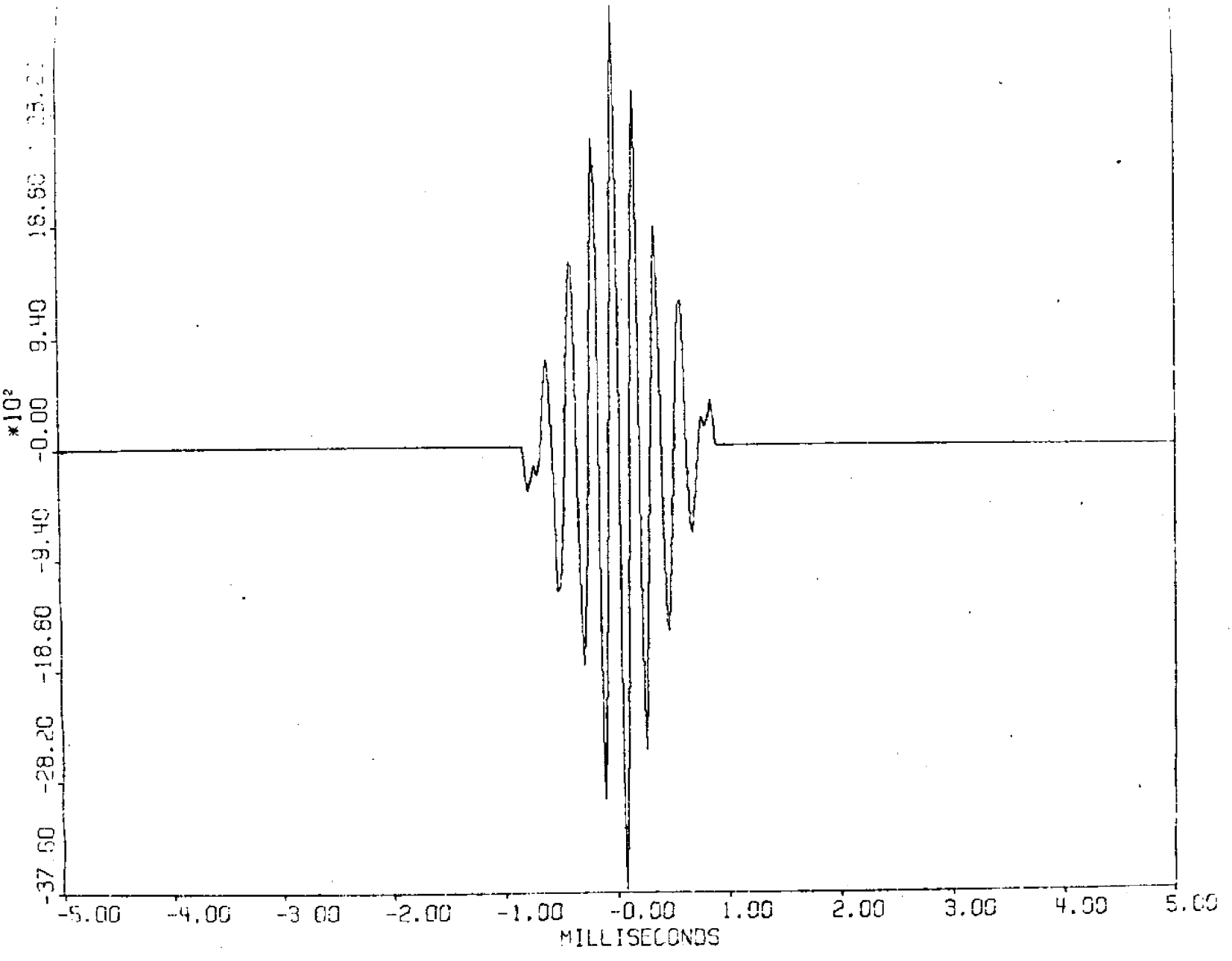
*10²
-0.00
-9.40
-18.80
-28.20
-37.60
-5.00
-4.00
-3.00
-2.00
-1.00
-0.00
1.00
2.00
3.00
4.00
5.00
MILLISECONDS

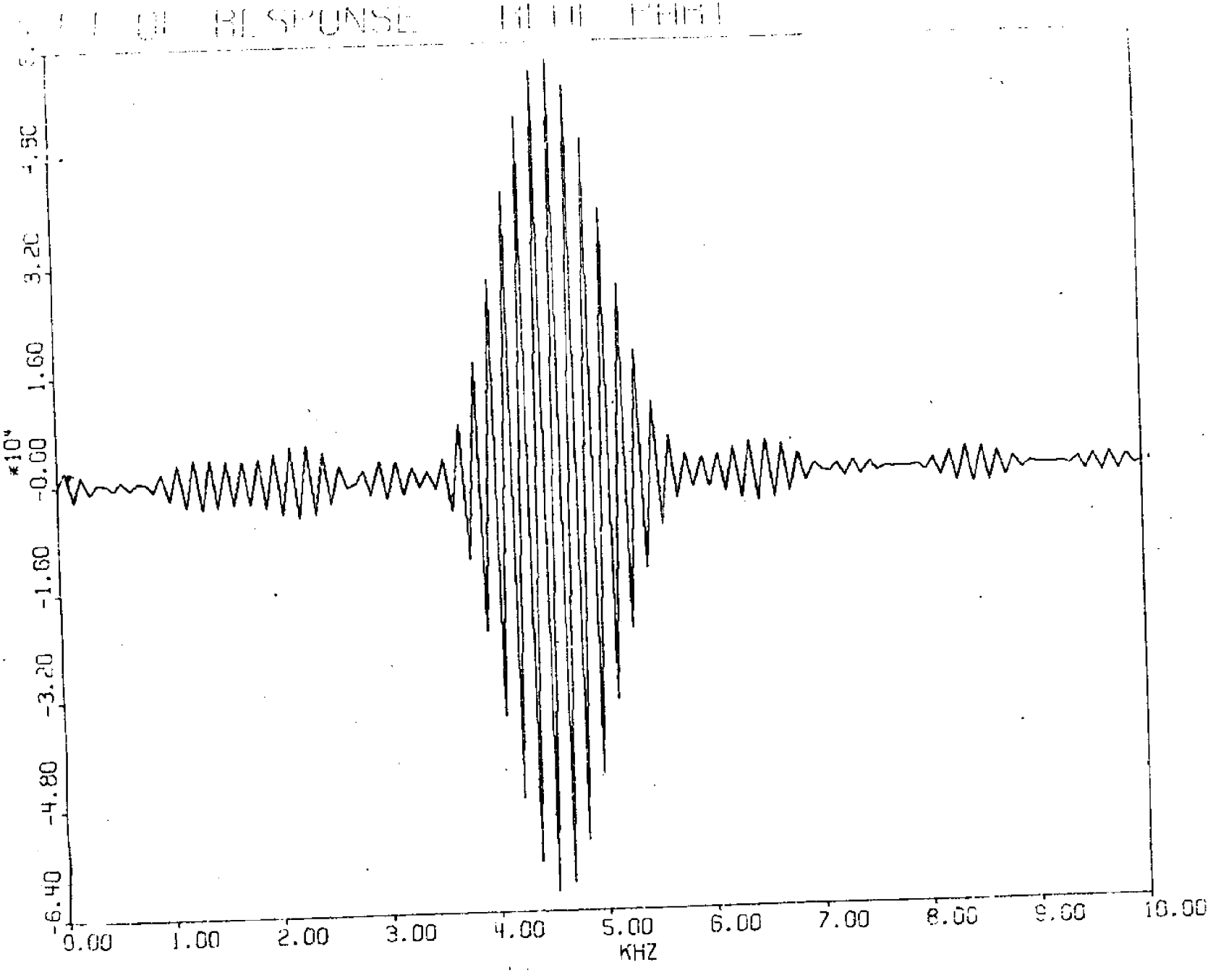
4.80
3.20
1.60
*10⁴
-0.00
-1.60
-3.20
-4.80
-6.40
0.00
1.00
2.00
3.00
4.00
5.00
6.00
7.00
8.00
9.00
10.00
KHZ

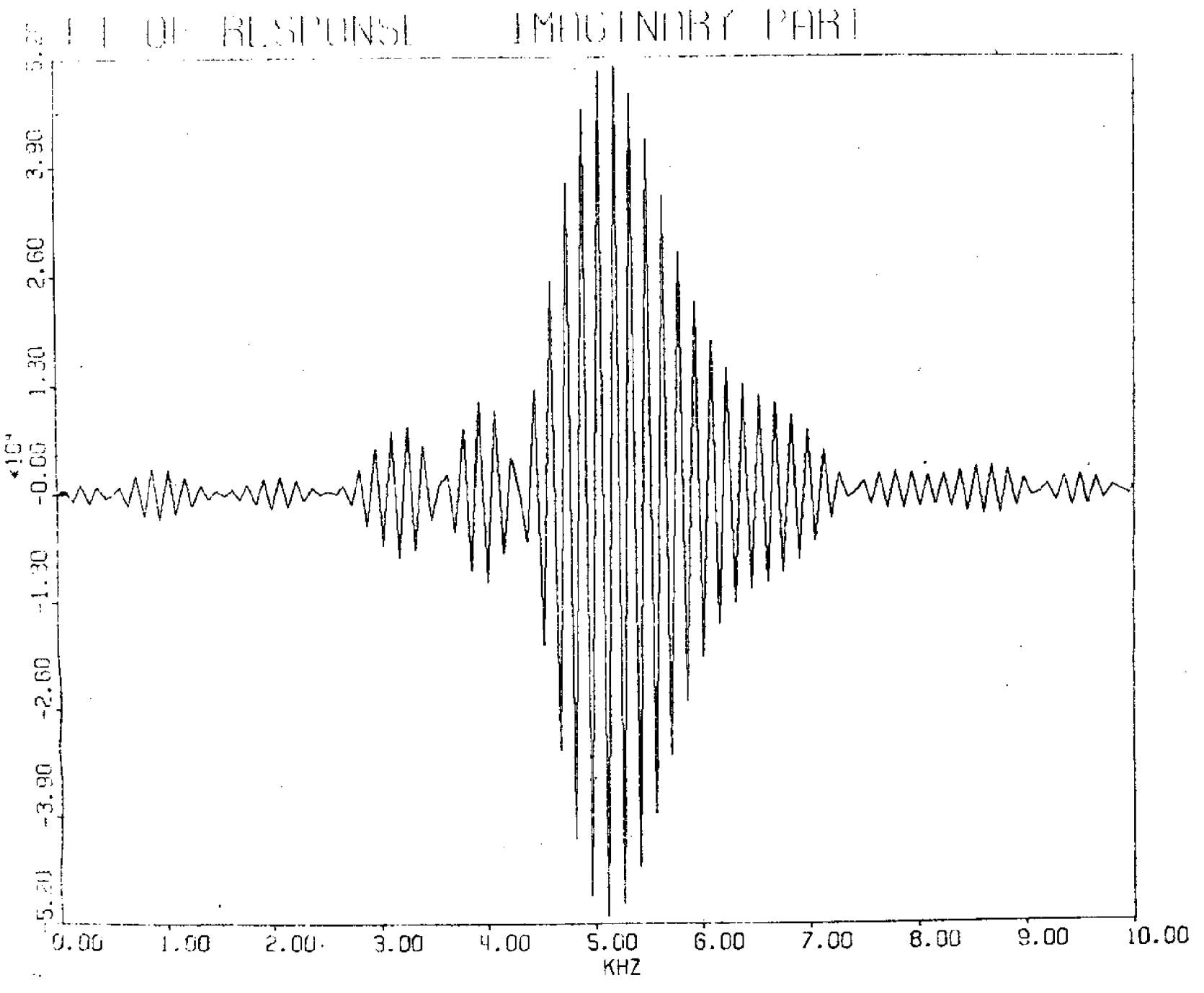
IMAGINARY PART
*10^
5.20
3.90
2.60
1.30
-0.00
-1.30
-2.60
-3.90
-5.20
0.00
1.00
2.00
3.00
4.00
5.00
6.00
7.00
8.00
9.00
10.00
KHZ

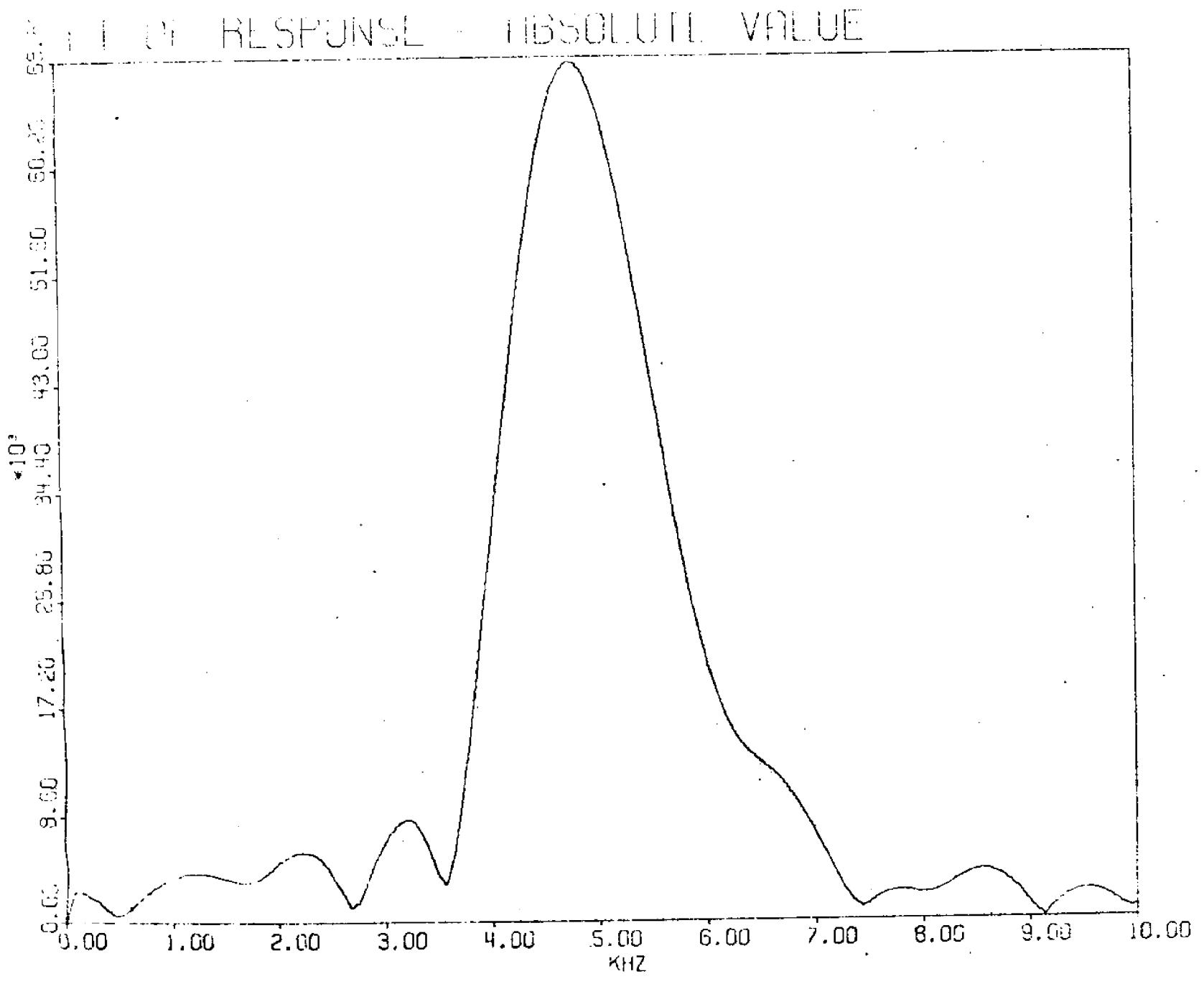
RESPONSE - ABSOLUTE VALUE
*10³
51.30
43.05
34.40
25.80
17.20
9.60
0.00
1.00
2.00
3.00
4.00
5.00
6.00
7.00
8.00
9.00
10.00
KHZ

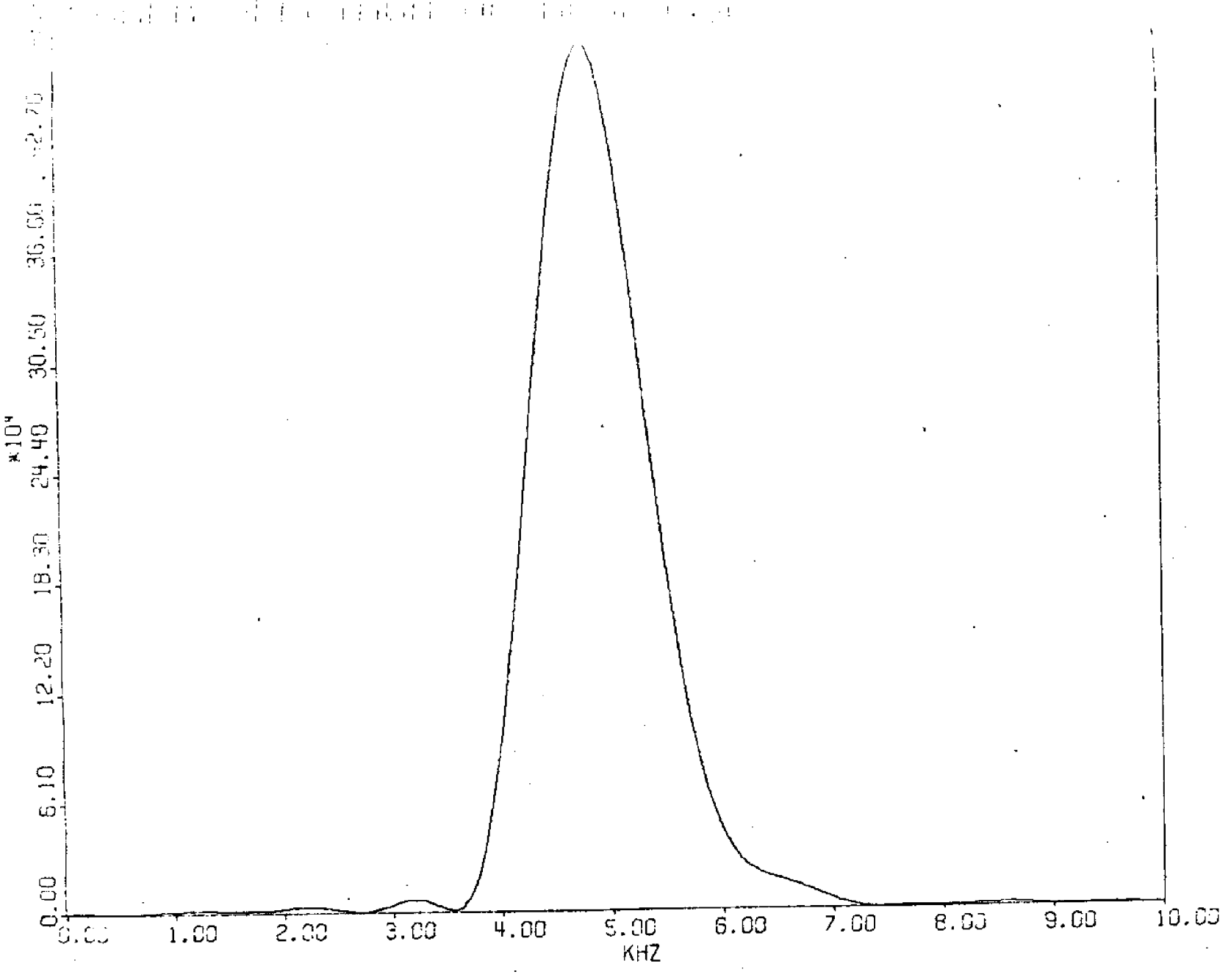
x10⁴
0.00
6.10
12.20
18.30
24.40
30.50
36.60
1.00
2.00
3.00
4.00
5.00
6.00
7.00
8.00
9.00
10.00
KHZ

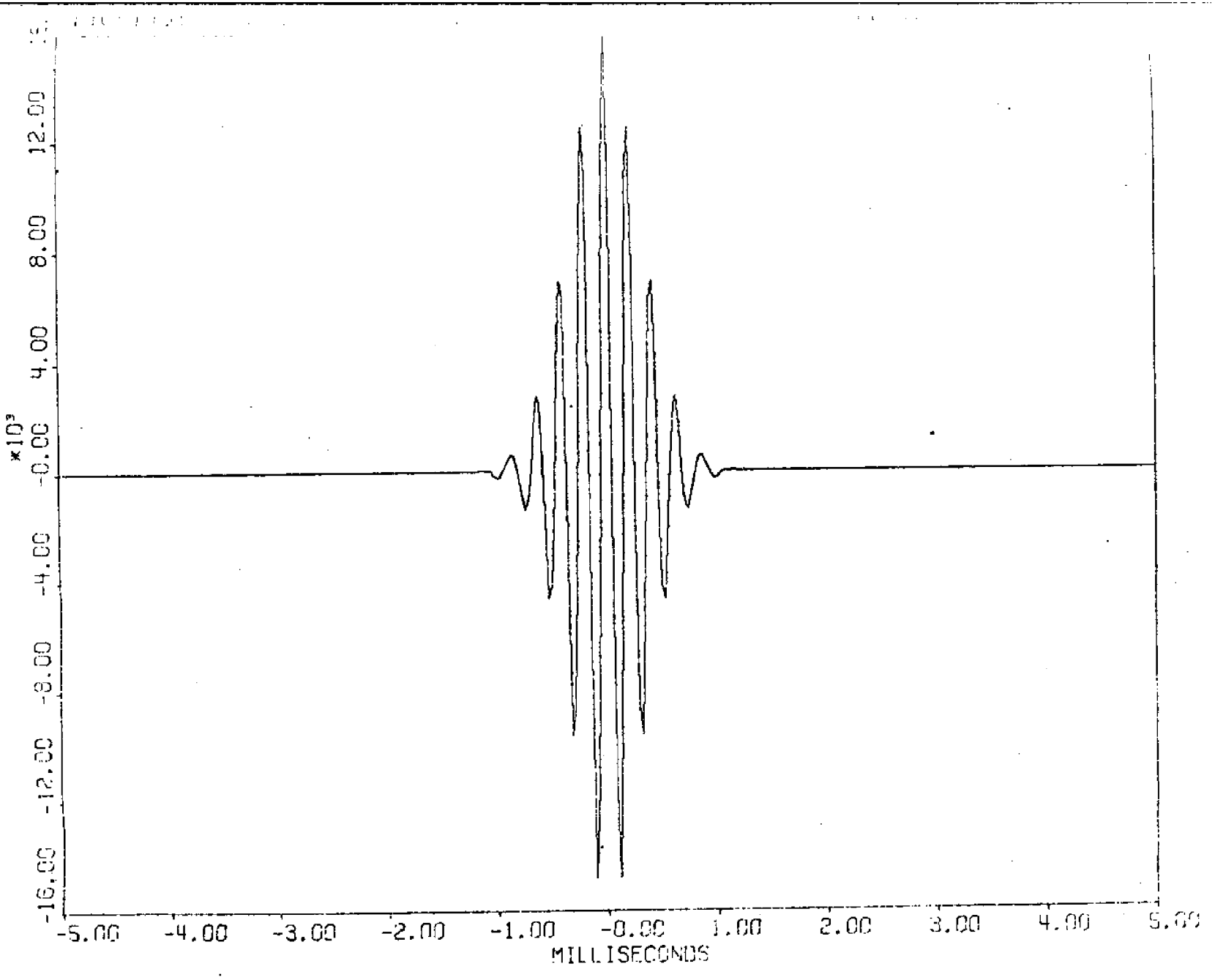
12.00
8.00
4.00
-0.00
-4.00
-8.00
-12.00
-16.00
*10³
-5.00
-4.00
-3.00
-2.00
-1.00
-0.00
1.00
2.00
3.00
4.00
5.00
MILLISECONDS

FIGURE (36)

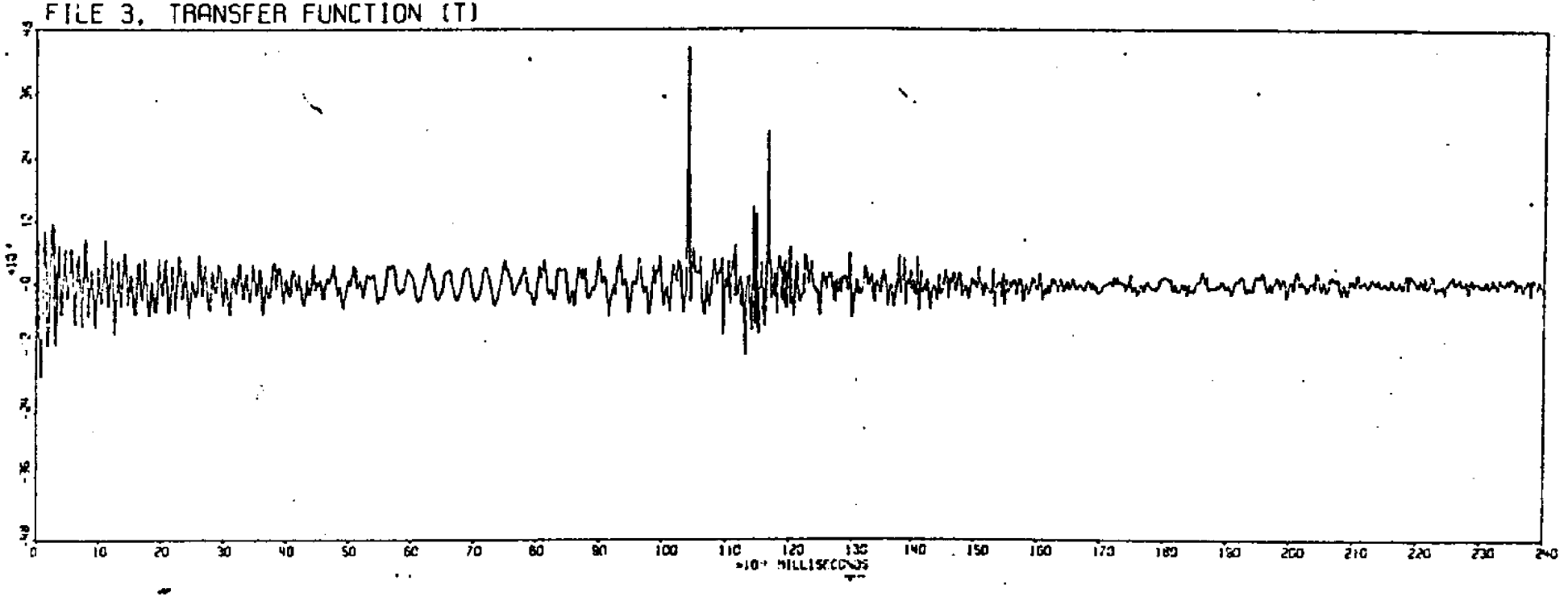
FILE 3, TRANSFER FUNCTION (T)
0
10
20
30
40
50
60
70
80
90
100
110
120
130
140
150
160
170
180
190
200
210
220
230
240

FIGURE (37)

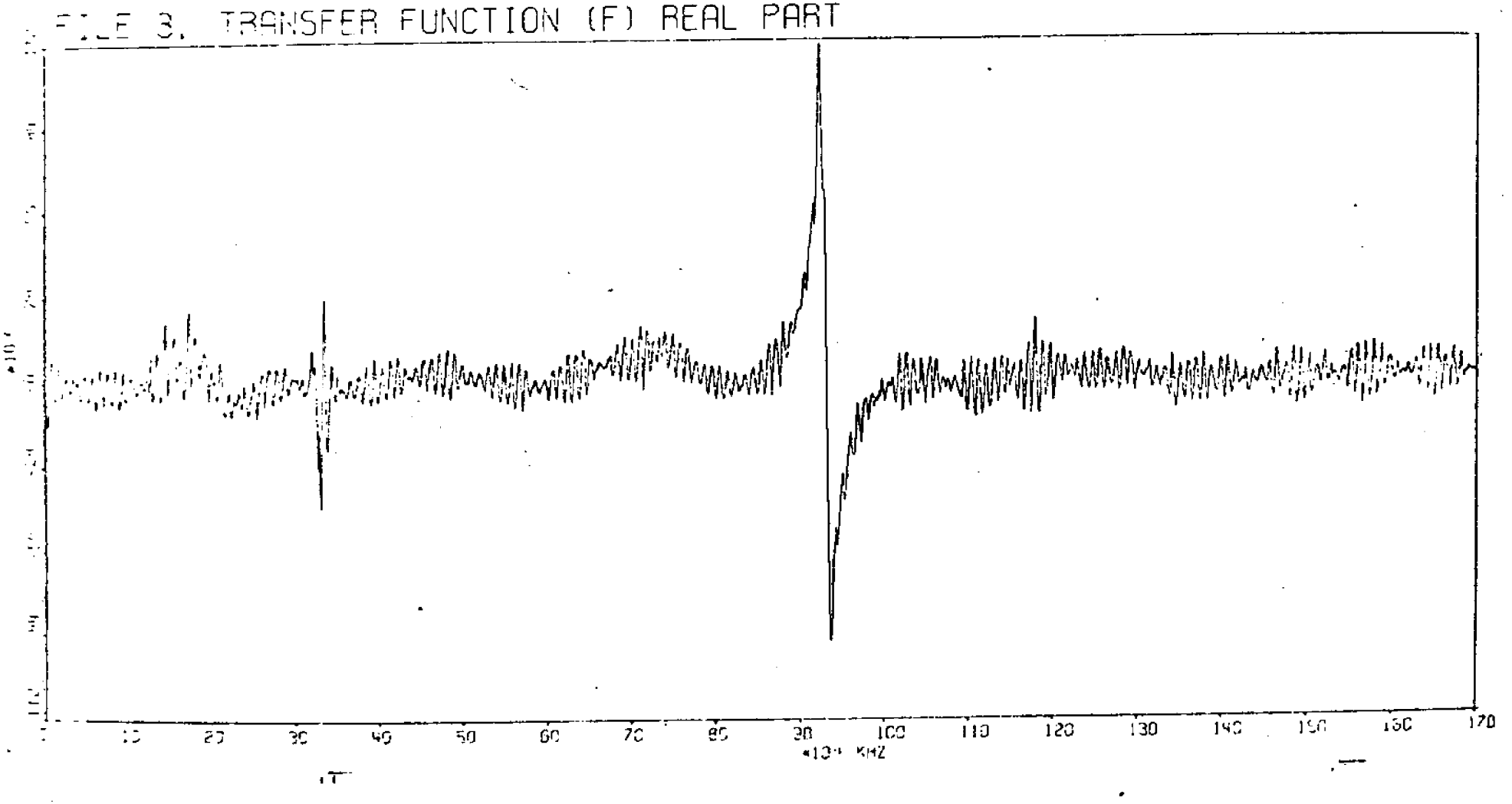
FILE 3. TRANSFER FUNCTION (F) REAL PART
10
20
30
40
50
60
70
80
90
100
110
120
130
140
150
160
170
*10** KHZ

FIGURE (38)

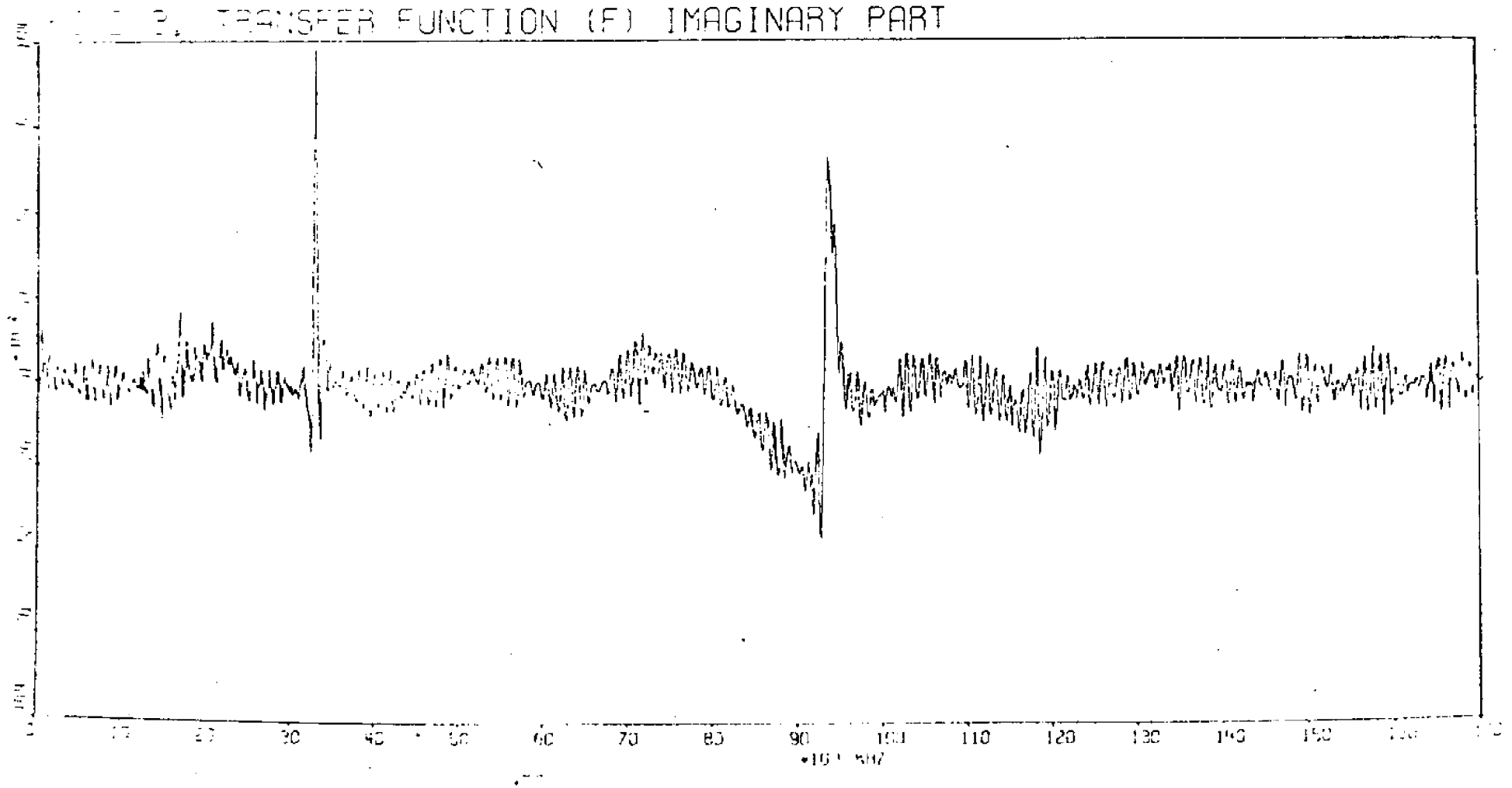
TRANSFER FUNCTION (F) IMAGINARY PART
30
40
50
60
70
80
90
110
120
130

FIGURE (39)

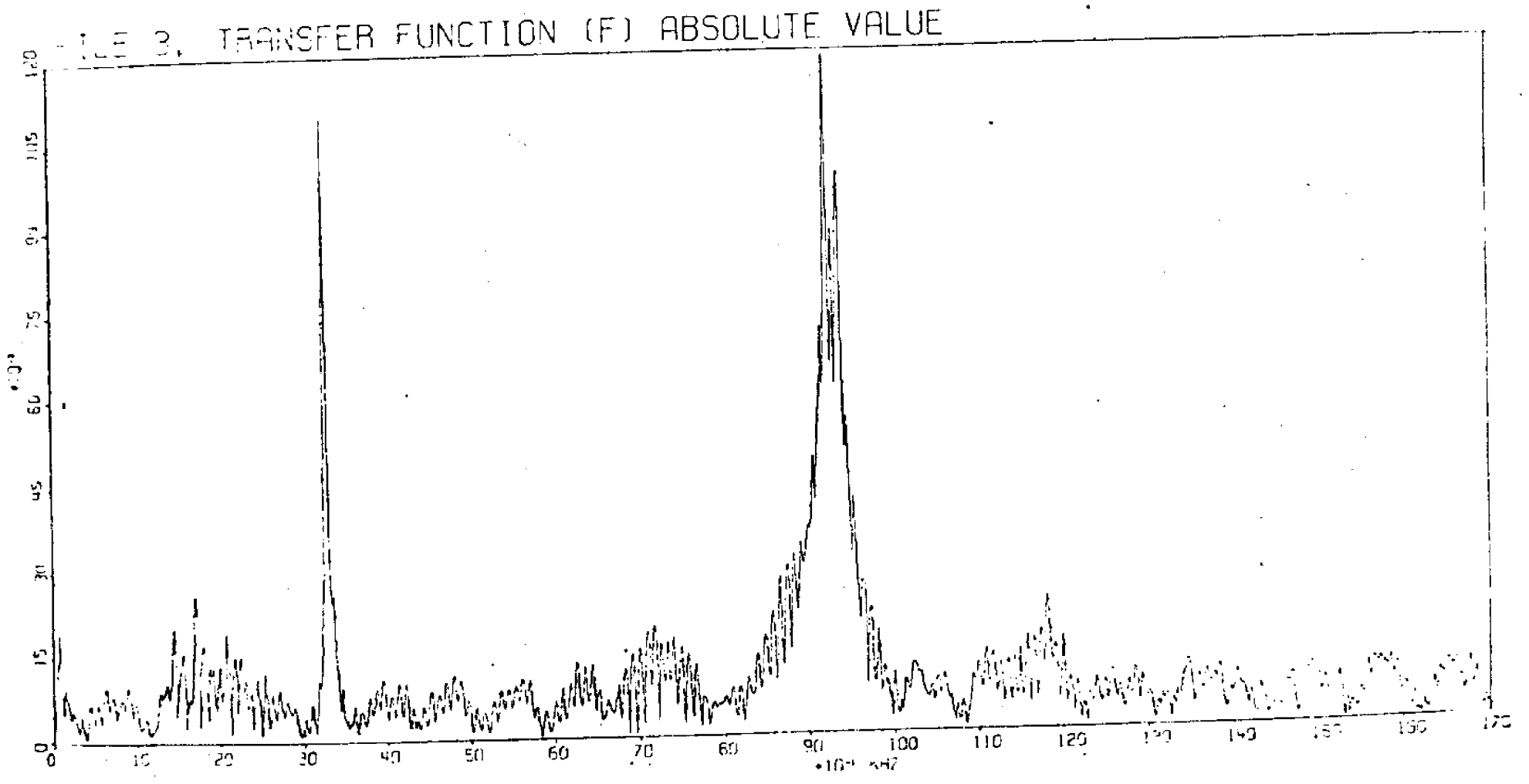
TRANSFER FUNCTION (F) ABSOLUTE VALUE
0
15
30
45
60
75
90
105
120
0
10
20
30
40
50
60
70
80
90
100
110
120
130
140
150
160

APPENDIX

MEASUREMENT OF SPECTRAL DENSITY OF RAW DATA

Let r(t) be the time history of a subbottom soil of interest. We assume that the data available to us may be assumed to be a representative sample of a stationary random process, and we like to evaluate the mean-square spectral density of the process from measurements of the data.

By employing the Fourier transform, the theoretical spectral density $P(\omega, k, \mu, \lambda)$ is evaluated according to the prescription:

$$P(\omega; k, \mu, \lambda) = \int_{-\infty}^{\infty} d\tau e^{i\omega\tau} \langle r(t)r(t+\tau)\rangle \qquad (1)$$

where $\langle r(t)r(t+\tau)\rangle$ is an ensemble average. The theoretical spectral density cannot be measured experimentally over a finite time exactly, since an average over an infinite data is needed. Therefore, the experimenter can at best measure a statistical estimate.

The experimenter will most probably follow the procedure as outlined in Figure (1) in data processing for measuring spectral density. The sample data is screened, leaving only those frequency values in the neighborhood of ω_c.

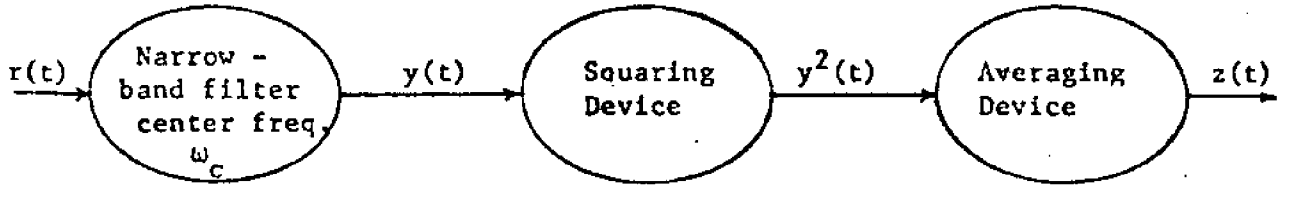

Figure (1): Block Diagram for Spectral Density Measurement

They are squared and later averaged to provide an estimate of the spectral density $P(\omega; k, \mu, \lambda)$. In the following paragraphs, we shall show how the procedures in Figure (1) can give such an estimate and show how a statistical estimate

can be changed by the filter parameters and by the "record length" of the chosen data. In order to show this, we first assume that we have an infinite time interval and that r(t), y(t), and z(t) in Figure (1) can be assumed to represent a stationary process. We shall then do a more detailed description of the filter and averager in Figure (1).

The characteristics of the filter can be understood either in the frequency domain or in the time domain. In the frequency domain, the filter is described by its transfer function or complex frequency response $G(\omega; k, \mu, \lambda)$, which is the complex amplitude of the output y when the input is $r = e^{i\omega t}$. The graph of $|G(\omega; k, \mu, \lambda)|$ is sketched in Figure (2). In order to simplify the procedure, we shall take the filter to have unit gain at the center frequency.

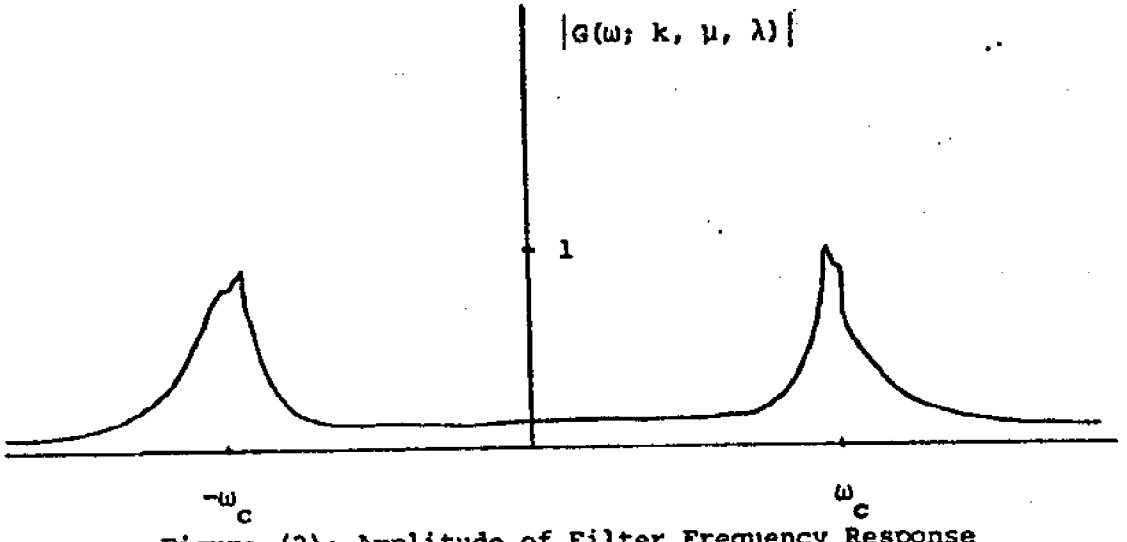

Figure (2): Amplitude of Filter Frequency Response

However, in actual experiment a scaling factor would have to be introduced to account for the filter gain. In the time domain, the filter is described by its impulse response $g(t; k, \mu, \lambda)$, which is the output y(t) when the input is the unit impulse or Dirac delta function $r(t) = \delta(t)$. The general form of $g(t; k, \mu, \lambda)$ is sketched in Figure (3). It should be noted that $g(t; k, \mu, \lambda)$ for $t<0$. This is a physical requirement, since a system cannot respond before it has been excited.

For all intensive purposes, the impulse response is a decaying harmonic function.

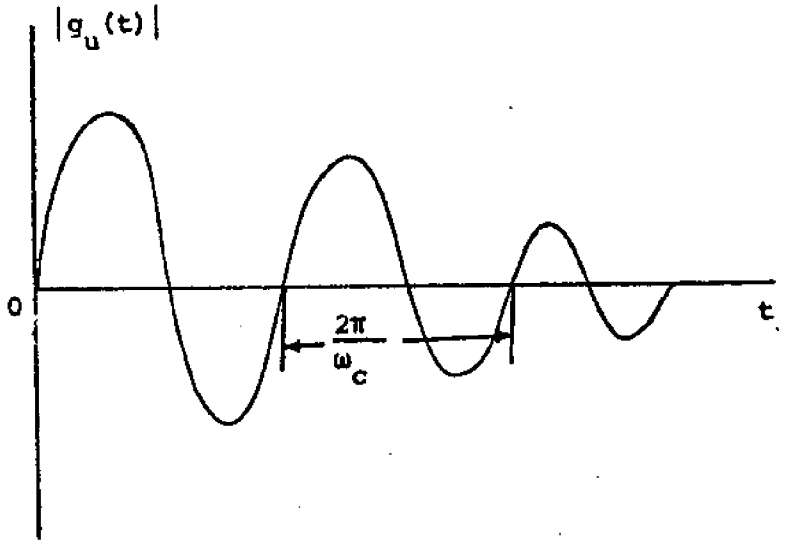

Figure (3): Filter Impulse Response Function

The frequency response and impulse response functions for the same filter are Fourier transforms on one another, and are described by

$$G_u(\omega;\ k,\ \mu,\ \lambda) = \int_{-\infty}^{\infty} g_u(t;\ k,\ \mu,\ \lambda)\ e^{-i\omega t}dt \qquad (2)$$

$$g_u(t;\ k,\ \mu,\ \lambda) = \frac{1}{2\pi} \int_{-\infty}^{\infty} G_u(\omega;\ k,\ \mu,\ \lambda)\ e^{i\omega t}d\omega$$

Hence, $G_u(\omega;\ k,\ \mu,\ \lambda)$ and $g_u(t;\ k,\ \mu,\ \lambda)$ contain the same information. We have stated that the center frequency in Figure (2) appears as the main oscillation frequency in Figure (3). Furthermore, the filter bandwidth in Figure (2) and the decay time in Figure (3) are related to each other uniquely depending on the characteristics of the filter.

We shall now assume the low pass filter characteristics shown in Figure (4) are in the averaging device shown in Figure (1). The assumed filter passes the steady-state average value

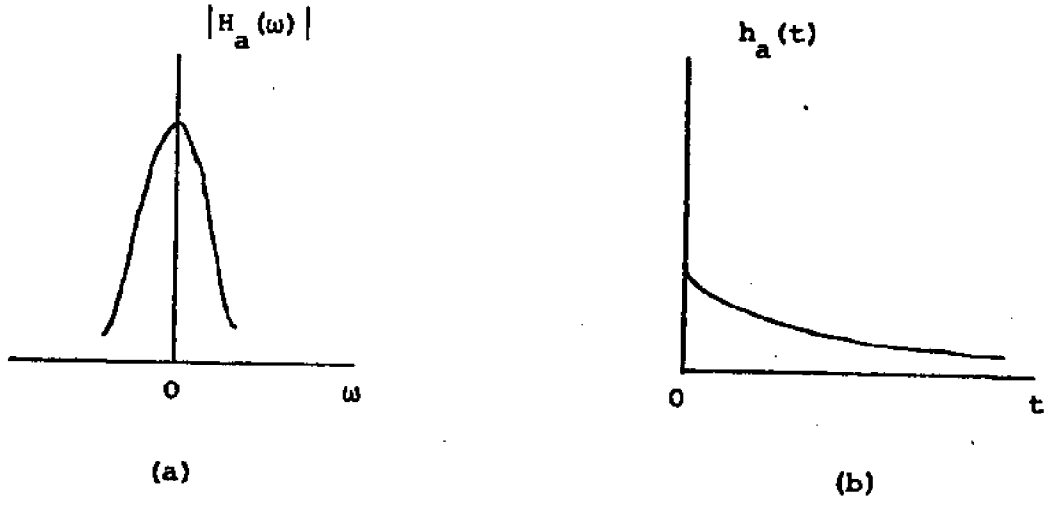

Figure (4): (a) Frequency and (b) Time Domain Characteristics of Low-pass Averaging Filter; Subscript "a" Stands for Averaging

of a signal with a minimum of additional low-frequency noise. Here, we require the averaging device to have <u>unit</u> gain at zero frequency. Since the frequency and impulse response functions are Fourier transforms of one another

$$H_a(\omega) = \int_{-\infty}^{\infty} h_a(t)\, e^{-i\omega t} dt$$

$$h_a(t) = \frac{1}{2\pi} \int_{-\infty}^{\infty} H_a(\omega)\, e^{i\omega t} d\omega \qquad (3)$$

the assumption for a unit gain at $\omega = 0$ implies that the area under the curve in

Figure (3) is also unity; in other words

$$\int_{-\infty}^{\infty} h_a(t)\, dt = 1 \tag{4}$$

which can be derived from setting $\omega = 0$ in the first equation of (3).

Now we return to the analytic descriptions of the operations performed in the data-processing as shown in Figure (1). In time domain, the filter output is given by the convolution integral

$$y(t) = \int_{-\infty}^{\infty} g_u(\tau;\, k,\, \mu,\, \lambda) r(t-\tau)\, d\tau \tag{5}$$

after squaring, we have

$$y^2(t) = \int_{-\infty}^{\infty}\int_{-\infty}^{\infty} g_u(\tau_1;\, k, \mu, \lambda) g_u(\tau_2;\, k, \mu, \lambda) r(t - \tau_1) r(t - \tau_2)\, d\tau_1 d\tau_2 \tag{6}$$

Thus, the output of the averager is

$$\begin{aligned} z(t) &= \int_{-\infty}^{\infty} h_a(\tau)\, y^2(t - \tau)\, d\tau \\ &= \int_{-\infty}^{\infty}\int_{-\infty}^{\infty}\int_{-\infty}^{\infty} h_a(\tau) g_u(\tau_1;\, k, \mu, \lambda) g_u(\tau_2;\, k, \mu, \lambda) r(t - \tau - \tau_2)\, d\tau_1 d\tau_2 d\tau \end{aligned} \tag{7}$$

Hence, we have derived a formal expression for the measured quantity z(t) in terms of the received data r(t). The problem is then to determine how z(t) represents the spectral density $P(\omega_c)$ of the random process.

MEAN VALUE OF THE MEASUREMENT

Assume that at a particular instant of time t we read z(t). Now we would like to show that if the complete samples of data r(t) are available, then the statistical average E[z] would bear close relationship to the desired spectral density $P(\omega_c)$. We first assume that Equation (7) has been written for each member of the data samples and after averaging across the data, we obtain

$$E[z] = \int_{-\infty}^{\infty} h_a(\tau)\ E[y^2(t-\tau)]d\tau \tag{8}$$

Hence, the expectation of a sum is the sum of the expectations and the terms containing y are the only ones that vary across the data sample. Now, since Y(t) is a stationary process, so is $y^2(t)$ and therefore, Equation (8) can be re-written as

$$E[z] = E[y^2] \int_{-\infty}^{\infty} h_a(\tau)d\tau = E[y^2] \tag{9}$$

following the use of Equation (4). The statistical average of the data reading z is just the mean-aquare of y. We shall now relate the mean-square of y to r(t) by utilizing Equation (5). We first form

$$y(t)y(t+\tau) = \int_{-\infty}^{\infty}\int_{-\infty}^{\infty} g_u(\tau_1;k,\lambda,\mu)g_u(\tau_2;k,\lambda,\mu)r(t-\tau_1)r(t+\tau-\tau_2)d\tau_1 d\tau_2 \tag{10}$$

by two applications of Equation (5). Then, we take the statistical average

$$E[y(t)y(t+\tau)] = \int_{-\infty}^{\infty}\int_{-\infty}^{\infty} g_u(\tau_1;k,\mu,\lambda)g_u(\tau_2;k,\mu,\lambda)R(\tau+\tau_1-\tau_2)d\tau_1 d\tau_2 \tag{11}$$

making use of the definition Equation (2) of the autocorrelation function. Utilization of the Fourier transformations given in Equations (1) and (2), Equation (11) can be rewritten. We commence by rewriting the second of Equation (2) as

$$g_u(\tau_1;k,\mu,\lambda) = \frac{1}{2\pi}\int_{-\infty}^{\infty} G(-\omega;k,\mu,\lambda)\ e^{-i\omega\tau_1}d\omega \tag{12}$$

by writing $-\omega$ for ω, and substituting it into Equation (11), changing the order of integration, and the insertion of the exponentials $e^{i\omega\tau}$, $e^{-i\omega\tau_2}$, and $e^{-i\omega(\tau-\tau_2)}$

results in the expression

$$E[y(t)y(t+\tau)] = \int_{-\infty}^{\infty} G(-\omega;\ k, \mu, \lambda) e^{i\omega\tau} d\omega \int_{-\infty}^{\infty} g(\tau_2;\ k, \mu, \lambda)\ e^{-i\omega\tau_2} d\tau_2 \cdot \tag{13}$$

$$\cdot \frac{1}{2\pi} \int_{-\infty}^{\infty} e^{-i\omega(\tau+\tau_1-\tau_2)} R(\tau+\tau_1-\tau_2) d\tau_1$$

The second integral is recognized as $G(\omega;\ k,\ \mu,\ \lambda)$ according to the first of Equations (2), and the third integral is recognized as $P(\omega,\ k,\ \mu,\ \lambda)$ according to Equation (1), since τ and τ_2 are treated as constants in the integration over τ_1. Hence, a useful result is obtained

$$E[y(t)y(t+\tau)] = \int_{-\infty}^{\infty} |G_u(\omega;\ k, \mu, \lambda)|^2\ P(\omega;\ k, \mu, \lambda)\ e^{i\omega\tau} d\omega \tag{14}$$

from on which setting $\tau = 0$, we get

$$E[z] = E[y^2] = \int_{-\infty}^{\infty} |G_u(\omega;\ k, \mu, \lambda)|^2\ P(\omega;\ k, \mu, \lambda) d\omega \tag{15}$$

The statistical average of the data-readings is thus not the spectral density $P(\omega_c;\ k,\ \mu,\ \lambda)$ directly, but the total mean-square response that filters through a narrow spectral window centered on ω_c. An estimate $P_1(\omega_c;\ k,\ \mu,\ \lambda)$ of the actual density $P(\omega_c;\ k,\ \mu,\ \lambda)$ is given by the relation

$$P_1(\omega_c;\ k, \mu, \lambda) = \int_{-\infty}^{\infty} |G_u(\omega;\ k, \mu, \lambda)|^2 P(\omega; k, \mu, \lambda) d\omega \Big/ \int_{-\infty}^{\infty} |G_u(\omega;\ k, \mu, \lambda)|^2 d\omega \tag{16}$$

$$= E[z] \Big/ \int_{-\infty}^{\infty} |G_u(\omega;\ k, \mu, \lambda)|^2 d\omega$$

As shown in Figure (4), the function $P_1(\omega_c;\ k,\ \mu,\ \lambda)$ is close to unity in the

vicinity of ω_c and nearly zero elsewhere. If $P(\omega; k, \mu, \lambda)$ is smooth and nearly constant over a frequency band that is wide in comparison with the filter bandwidth, then $P_1(\omega_c; k, \mu, \lambda)$ gives a good approximation to $P(\omega_c; k, \mu, \lambda)$, but if $P(\omega; k, \mu, \lambda)$ changes drastically up and down within the filter bandwidth, then the measurement will not have sufficient resolution to detect such a small detail. Hence, we can conclude that if the bandwidth of the filter is narrower, then the resolution of the measurement is better.

Now we shall discuss equivalent bandwidths for the filter. Equivalent bandwidth for the filter can be simply defined as the denominator of Equation (16). For example, consider the ideal band-pass filter whose transfer function is sketched in Figure (5). Actually, this is not attainable in reality. However, it represents a limit that can be approached by real filters. For the above filter, the denominator integral in Equation (16) can be written as

$$\int_{-\infty}^{\infty} |H(\omega)|^2 d\omega = 2\Delta\omega_c \qquad (17)$$

where $\Delta\omega_c$ is the bandwidth and the factor 2 arises from the use of two-sided spectrum.

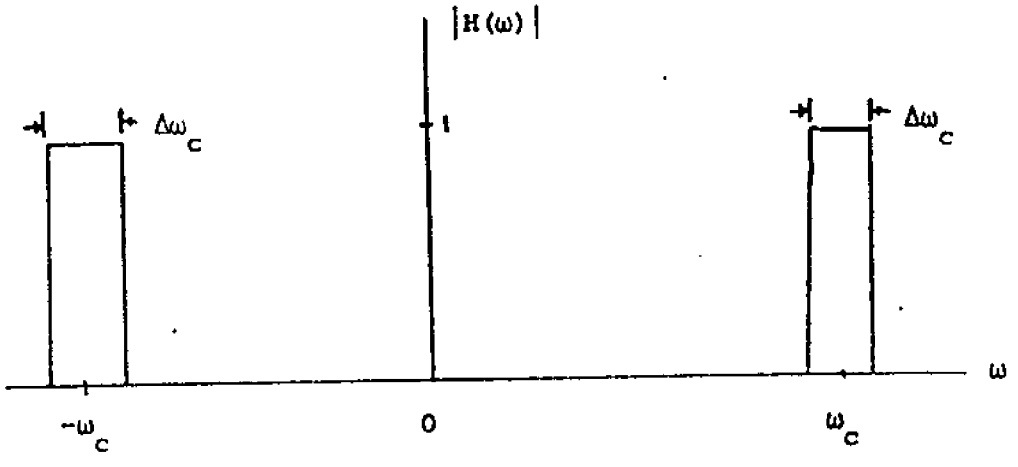

Figure (5): Amplitude of Frequency Response for Ideal Bandpass Filter

In general, the denominator integral in Equation (16) can be used to define an equivalent bandwidth $(\Delta\omega_c)_1$. For an arbitrary filter, we have

$$2(\Delta\omega_c)_1 = \int_{-\infty}^{\infty} |H(\omega)|^2 d\omega \tag{18}$$

and then we can rewrite Equation (16) as

$$E[z] = 2(\Delta\omega_c)_1 P_1(\omega_c;\ k, \mu, \lambda) \tag{19}$$

Thus, the statistical mean of the measurement is twice the equivalent bandwidth of the filter multiplied by an average spectral density.

As an example of an actual filter, consider the frequency response of the subbottom soil,

$$G(\omega;\ k, \mu, \lambda) = 2\zeta\omega_c^2 \ / \ \omega_c^2 - \omega^2 + i\omega^2\zeta\omega_c \tag{20}$$

where $\omega_c = k \cdot \left[\frac{\lambda' + 2\mu'}{\rho}\right]^{\frac{1}{2}}$, $\zeta = \frac{(\lambda'' + 2\mu'')k}{2[\lambda' + 2\mu') / \rho]^{\frac{1}{2}}}$, and where λ, μ, k, and ρ are the two Lamé parameters, wave number, and the density of the soil. In this case,

$$2(\Delta\omega_c)_1 = \int_{-\infty}^{\infty} |G(\omega;\ k, \mu, \lambda)|^2 d\omega = 2\pi\zeta\omega_c \tag{21}$$

The equivalent bandwidth is thus $\Delta\omega_c = \pi\zeta\omega_c$. It is noted that the half-power bandwidth for this case is $(\Delta\omega_c)_0 = 2\zeta\omega_c = \frac{\omega_c}{Q}$. In other words, for the purpose of evaluating Equation (19), the equivalent bandwidth of the simple resonant response is $\pi/2$ times the half-power bandwidth.

VARIANCE OF THE MEASUREMENT

In the previous section, we have shown that a single measurement of z(t) can be considered as a sample of a response whose mean value E[z] is associated to the

desired spectral density by Equation (16). We now look at the variance σ_z^2 of the distribution of z across the gathered statistical data. From definition

$$\sigma_z^2 = E[z^2] - (E(z))^2 \tag{22}$$

where each sample of z(t) is given by Equation (7). The mean E[z] has already been calculated in Equation (15). In order to obtain an expression for σ_z^2, we square Equation (7) and average across the gathered data

$$E[z^2] = \int_{-\infty}^{\infty}\int_{-\infty}^{\infty} h_a(\tau_1)h_a(\tau_2)E[y^2(t-\tau_1)y^2(t-\tau_2)]d\tau_1 d\tau_2 \tag{23}$$

Now, using the identity

$$E[x_1x_2x_3x_4] = E[x_1x_2]E[x_3x_4] + E[x_2x_3]E[x_1x_4] + E[x_1x_3]E[x_2x_4] \tag{23a}$$

which applies only to a normal (Gaussian) processes with zero mean to the integrand in (23) becomes

$$\begin{aligned} E[y^2(t-\tau_1)y^2(t-\tau_2)] &= E[y^2(t-\tau_1)]E[y^2(t-\tau_2)] + \\ &+2E[y(t-\tau_1)y(t-\tau_2)]E[y(t-\tau_1)y(t-\tau_2)] = \\ &= (E[y^2])^2 + 2(E[y(t)y(t+\tau_1-\tau_2)])^2 \end{aligned} \tag{24}$$

On substituting Equation (24) into (23), the expression in (23) becomes

$$\sigma^2_z = 2\int_{-\infty}^{\infty}\int_{-\infty}^{\infty} h_a(\tau_1)h_a(\tau_2)(E[y(t)y(t+\tau_1-\tau_2)])^2 d\tau_1 d\tau_2 \tag{25}$$

where we have used Equation (9) and (4). The expectation value in Equation (25) is related to the spectral density of r(t) by Equation (14). Squaring Equation (14),

substituting in Equation (25), and the inversion of the order on integration yields

$$\sigma_z^2 = 2\int_{-\infty}^{\infty} |G(\omega_1;\, k,\, \mu,\lambda)|^2 P(\omega_1;\, k,\, \mu,\lambda)d\omega_1 \int_{-\infty}^{\infty} |G(\omega_2;\, k,\, \mu,\lambda)|^2 P(\omega_2;\, k,\, \mu,\lambda)d\omega_2 \cdot$$

$$\cdot \int_{-\infty}^{\infty} h_a(\tau_1) e^{i(\omega_1+\omega_2)\tau_1} d\tau_1 \int_{-\infty}^{\infty} h_a(\tau_2) e^{-i(\omega_1+\omega_2)\tau_2} d\tau_2 \qquad (26)$$

$$= 2\int_{-\infty}^{\infty}\int_{-\infty}^{\infty} |G(\omega_1;\, k,\, \mu,\lambda)|^2 \, |G(\omega_2;\, k,\, \mu,\lambda)|^2 \, |H_a(\omega_1+\omega_2)|^2 \, P(\omega_1;\, k,\, \mu,\lambda) \cdot$$

$$\cdot P(\omega_2;\, k,\, \mu,\lambda)\, d\omega_1 d\omega_2$$

where in the last step we used Equation (3). Thus, a formal expression relating the variance of the measurement to the spectral density under measurement and the frequency responses of the filter and averager. In reality, Equation (26) is never evaluated and hence, an asymptotic approximation is obtained by the utilization of the narrow-band character of the filters.

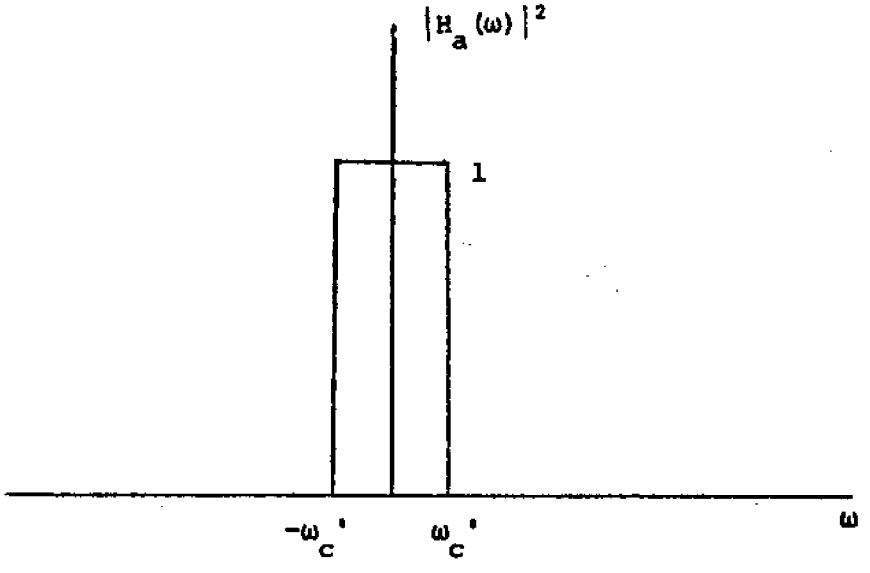

Figure (6): Amplitude of Frequency Response of Ideal Low-pass Filter with Cut-off Frequency ω_c'

It can be shown that if $\omega_c << \Delta\omega_c$, this area is approximately $4\Delta\omega_c\omega_c$, and if $P(\omega; k, \mu, \lambda)$ is flat in the neighborhood of ω_c, we have a good approximation to Equation (26).

$$\sigma_z^2 = 8\,\Delta\omega_c\omega_c'\,P^2(\omega_c; k, \mu, \lambda) \tag{27}$$

Now, the relation of the variance in Equation (27) for the ideal low-pass system to the corresponding mean E[z] is done by assuming that $P(\omega; k, \mu, \lambda)$ is flat in one neighborhood of ω_c. Upon substitution in Equations (16) and (17), we obtain

$$E[z] = 2\,\Delta\omega_c P(\omega_c; k, \mu, \lambda) \tag{28}$$

Thus, a relative deviation from one mean is

$$\frac{\sigma_z}{E[z]} = \left[\frac{2\omega_c'}{\Delta\omega_c}\right]^{1/2} \tag{29}$$

The actual distribution of z across the ensemble is unknown; but if we assume it is of chi-square type, i.e., $\chi^2_k = z_1^2 + z_2^2 + \ldots z^2_k$, then the equivalent number of statistical degrees of freedom can be shown to be given by

$$k_{eq.} = \frac{\Delta\omega_c}{\omega_c'} \tag{30}$$

This is a very important result. It states that in order to have a large number of degrees of freedom and hence, a high assurance that the measured value lies close to the true value, the bandwidth $\Delta\omega_c$ of the filter centered at ω_c must be very much wider than the low-pass averaging filter with cut-off frequency ω_c'.

within the filter bandwidth $\Delta\omega_c$, each subband of ω_c' equal to the averager bandwidth may be considered to represent an independent statistical degree of freedom. Hence, the main problem in spectral density measurement is revealed. In order to obtain high resolution, $\Delta\omega_c$ should be small; however, in order to achieve statistical accuracy, $\Delta\omega_c$ should be large compared to ω_c'. In theory, both requirements can be met by decreasing ω_c' sufficiently.

EQUIVALENT BANDWIDTHS

As mentioned in the previous section, we shall attempt to evaluate Equation (26) by the use of the narrow-band character of the filter. In order to get an asymptotic approximation to (26). We assume that in the first integration with respect to ω_2, the only contributions occur in a narrow strip centered on $\omega_2 = -\omega_1$, which is based on the narrowness of the low-pass averaging filter. We further assume that for fixed ω_1, the only term in the integrand that varies significantly as traverses this strip is the rapidly varying term $|H_a(\omega_1+\omega_2)|^2$. Therefore, we place $|H_a(\omega_1+\omega_2)|^2$ in the ω_2-integral and place all other terms in the ω_1-integral after substituting $-\omega_1$ for ω_2. Thus, the approximation to Equation (26) takes the form:

$$\sigma_z^2 = 2\int_{-\infty}^{\infty} |G(\omega_1;k,\mu,\lambda)|^4\, P^2(\omega_1;k,\mu,\lambda)\, d\omega_1 \int_{-\infty}^{\infty} |H_a(\omega_1+\omega_2)|^2\, d\omega_2 \qquad (31)$$

where we have taken the advantage of the fact that $|H(\omega_1; k, \mu, \lambda)|^2$ and $P(\omega_1; k, \mu, \lambda)$ are even functions. In order to have an interpretation of this approximation, we define the following equivalent bandwidths:

$$
\begin{aligned}
2\ (\Delta\omega_c)_1 &= \int_{-\infty}^{\infty} |G(\omega;k,\lambda,\mu)|^2\ d\omega \\
2(\Delta\omega_c)_2 &= \int_{-\infty}^{\infty} |G(\omega;k,\mu,\lambda)^{\ 4}\ d\omega \\
2(\omega_c')_1 &= \int_{-\infty}^{\infty} |H_a(\omega)|^2\ d\omega
\end{aligned}
\tag{32}
$$

and the following weighted average spectral densities

$$
\begin{aligned}
P_1(\omega_c;k,\mu,\lambda) &= \frac{1}{2(\Delta\omega_c)_1} \int_{\infty}^{\infty} |G(\omega;k,\mu,\lambda)|^2\ P(\omega;k,\mu,\lambda)\ d\omega \\
P_2^2(\omega_c;k,\mu,\lambda) &= \frac{1}{2(\Delta\omega_c)_2} \int_{\infty} |G(\omega;k,\mu,\lambda)|^4\ P^2(\omega;k,\mu,\lambda)\ d\omega
\end{aligned}
\tag{33}
$$

In order to be complete, we have restated Equations (18) and (16) in the preceding definitions. Hence, using Equations (32) and (33), Equation (31) can be written as

$$
\sigma_z^2 = 8(\Delta\omega_c)_2\ (\omega_c')_1\ P_2^2(\omega_c;k,\mu,\lambda) \tag{34}
$$

which may be considered as a generalization of Equation (27). Both $P_1(\omega_c;\ k,\ \mu,\ \lambda)$ and $P_2(\omega_c;\ k,\ \mu,\ \lambda)$ will be good approximations to $P(\omega_c;\ k,\ \mu,\ \lambda)$, if the selective filter is in fact narrow and the actual spectral density is smooth. The equivalent bandwidths $(\Delta\omega_c)_1$, $(\Delta\omega_c)_2$, and ω_c' may differ somewhat from the bandwidths usually assigned to the filters involved.

The relative deviation from the mean is obtained from Equations (34) and (19) as

$$
\frac{\sigma_z}{E[z]} = \frac{2(\Delta\omega_c)_2(\omega_c')_1}{(\Delta\omega_c)_1^2} \cdot \frac{P_2(\omega_c;k,\mu,\lambda)}{P_1(\omega_c;k,\mu,\lambda)} \tag{35}
$$

which can be considered as a generalization of Equation (29). Finally, the equivalent number of statistical degrees of freedom is

$$k_{eq} = \frac{(\Delta\omega_c)_1^2}{(\Delta\omega_c)_2 (\omega_c')_1} \cdot \frac{P_1^2(\omega_c;k,\mu,\lambda)}{P_2^2(\omega_c;k,\mu,\lambda)} \tag{36}$$

As an example of an actual selective filter, we have the simple linear resonant system with the frequency response of Equation (20). The equivalent bandwidths are

$$\begin{aligned} (\Delta\omega_c)_1 &= \pi\zeta\omega_c \\ (\Delta\omega_c)_2 &= \frac{\pi}{2}\zeta\omega_c\,(1+4\zeta^2) \end{aligned} \tag{37}$$

as compared with the half-power bandwidth $\Delta\omega_c = 2\zeta\omega_c$. The frequency response of a first order averaging filter circuit with unit gain at zero frequency is

$$H_a(\omega) = \frac{1}{1 + i\omega T_c} \tag{38}$$

where T_c is time constant. The equivalent low-pass cut-off frequency can be determined to be

$$(\omega_c')_1 = \frac{\pi}{2T_c} \tag{39}$$

whereas the half-power frequency is $\omega_c = 1/T_c$.

Now, going back to Figure (1), we shall assume the data processing chain to consist of simple linear resonant filter, Equation (20), and we further assume it

contains the first order averaging circuit given by Equation (38). Then, the number of equivalent statistical degrees of freedom is given by

$$k_{eq} = \frac{(\Delta\omega_c)_1^2}{(\Delta\omega_c)_2(\Delta\omega_c)_1} = \frac{4\zeta\,\omega_c\,T_c}{1+4\zeta^2} \tag{40}$$

if we assume that $P_1(\omega_c;\ k,\ \mu,\ \lambda) = P_2(\omega_c;\ k,\ \mu,\ \lambda)$. This can be expressed in terms of the half-power bandwidths as

$$k_{eq} = \frac{2(\Delta\omega_c)_o}{(\omega'_c)_o} \cdot \frac{1}{1+4\zeta^2} \tag{41}$$

If the above expression is compared with Equation (30) for the ideal filter system, it is seen that if the half-power bandwidths of both systems are the same, then the real system just described has nearly twice as many statistical degrees of freedom as the ideal system. However, this gain in statistical reliability is obtained at the expense of resolving power because the bandwidth $(\Delta\omega_c)_1$, to be used in Equation (19) is $\pi/2$ times the half-power bandwidth $(\Delta\omega_c)_o$.

b) *Measurement of Autocorrelation of Raw Data*

Since the spectral density and the autocorrelation function are Fourier transforms of each other, from a theoretical point of view they both contain the same information. However, it is not easy to go from one to another from an experimental point of view, since the Fourier transform seems to be inappropriate procedure for numerical evaluation. If both are required, then it is usually best to obtain them separately from the original data.

For stationary ergodic phenomena which we have sasumed, the concept of autocorrelation is defined as

$$R(\tau) = \lim_{T\to\infty} \frac{1}{2T} \int_{-T}^{T} r(t)r(t+\tau)dt$$

where $R(\tau)$ is a function only of the time difference $t_2 - t_1 = \tau$.

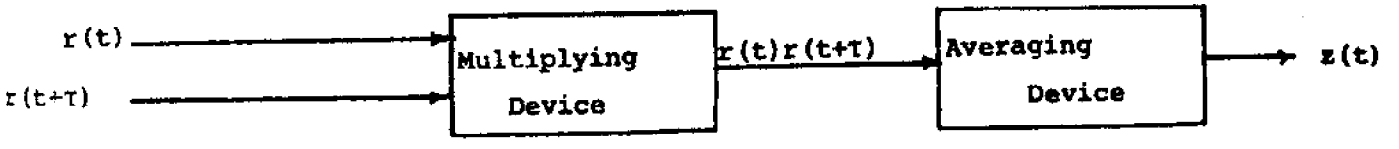

Figure (7): Block Diagram for Autocorrelation Function

The procedure to measure autocorrelation is shown schematically in Figure (7). First, the data signal is delayed by a lag time τ, then the original data is multiplied by the delayed signal and the result averaged to provide the measured quantity $z(t)$. To simplify the analysis, we assume that a continuously averaging filter is used and that $r(t)$ and $z(t)$ are stationary process. Just as was the case for spectrum measurements, a true average over an interval T can be used, even though there are similar problems associated with restrictions of the "record length" of the signal.

A formal representation of the output $z(t)$ in Figure (7) can be written as

$$z(t) = \int_{-\infty}^{\infty} h_2(\tau_1) r(t-\tau_1) r(t+\tau-\tau_1) d\tau_1 \tag{42}$$

where the properties of the continuously averaging filter are given in Equations (3) and (4).

As before, we consider an ensemble of such measurements at a fixed instant of time. The ensemble mean or expected value is

$$E[z] = \int_{-\infty}^{\infty} h_a(\tau_1) E[r(t-\tau_1) r(t+\tau-\tau_1)] d\tau_1 = R(\tau) \tag{43}$$

on using Equations (1) and (4). Thus, the ensemble average of the measurements is the desired autocorrelation. Next, we shall estimate the statistical importance of a single measurement by determining the variance of $z(t)$. The mean-square is found by squaring (42) and taking the statistical average. The variance, Equation (22), then follows as

$$\sigma_z^2 = \int_{-\infty}^{\infty} \int_{-\infty}^{\infty} h_a(\tau_1) h_a(\tau_2) \{ E[r(t-\tau_1) r(t+\tau-\tau_1) r(t-\tau_2) r(t+\tau-\tau_2)] - R^2(\tau) \} d\tau_2 \tag{44}$$

Now, assuming the normal process identity of Equation (23a) can be applied to

the process r(t), Equation (44) can be reduced further to obtain

$$\sigma_z^2 = \int_{-\infty}^{\infty}\int_{-\infty}^{\infty} h_a(\tau_1)h_a(\tau_2)[R^2(\tau_1-\tau_2)+ R(\tau_1-\tau_2+\tau)R(\tau_1-\tau_2-\tau)]d\tau_1 d\tau_2 \qquad (45)$$

Eventhough this can be studied in time domain in order to compare with previous analysis of the spectral density, we shall go into the frequency domain. Using the inverse Fourier relation of Equation (1)

$$R(\tau) = \int_{-\infty}^{\infty} P(\omega)e^{i\omega t}\, d\omega \qquad (46)$$

Equation (45) becomes upon interchanging the order of integration

$$\sigma_z^2 = \int_{-\infty}^{\infty}\int_{-\infty}^{\infty} P(\omega_1)P(\omega_2)(1 + e^{i(\omega_1-\omega_2)\tau})d\omega_1 d\omega_2 \quad \times$$

$$\times \int_{-\infty}^{\infty} h_a(\tau_1)e^{i(\omega_1+\omega_2)\tau_1} d\tau_1 \int_{-\infty}^{\infty} h_a(\tau_2)e^{-i(\omega_1+\omega_2)\tau_2} d\tau_2 \qquad (47)$$

The last two integrals are identified with the help of Equation (2), so that we have

$$\sigma_z^2 = \int_{-\infty}^{\infty}\int_{-\infty}^{\infty} [(1+\cos(\omega_1-\omega_2)\tau] \; | \; H_a(\omega_1+\omega_2) |^2 \; P(\omega_1)P(\omega_2)d\omega_1 d\omega_2 \qquad (48)$$

which is somewhat similar to Equation (26) . A good approximation to Equation (48) can be had if the averaging filter has a very narrow passband in the neighborhood of $\omega_1+\omega_2 = 0$. We only consider $H_a(\omega_1+\omega_2)$ variation during the ω_2 integration and set $\omega_2 = -\omega_1$ in the remaining terms. In this procedure, we find

$$\sigma_z^2 = \int_{-\infty}^{\infty} \int_{-\infty}^{\infty} (1+\cos 2\omega_1\tau)\ P^2(\omega_1)d\omega_1 \int_{-\infty}^{\infty} |\ H_a(\omega_1+\omega_2)\ |^2 d\omega_2 \qquad (49)$$

$$= 4(\omega_c')_1 \int_{-\infty}^{\infty} \cos^2\omega\tau\ P^2(\omega)d\omega$$

The latter expression is obtained following Equation (22) and the trigonometric identity for the cosine of the double angle.

The variance of the spectral density measurement, (Equation (34)), depends only on the local behavior of the input spectrum at $\omega=\omega_c$, whereas the variance of the autocorrelation measurement for any τ depends on the complete spectrum of the input process r(t).

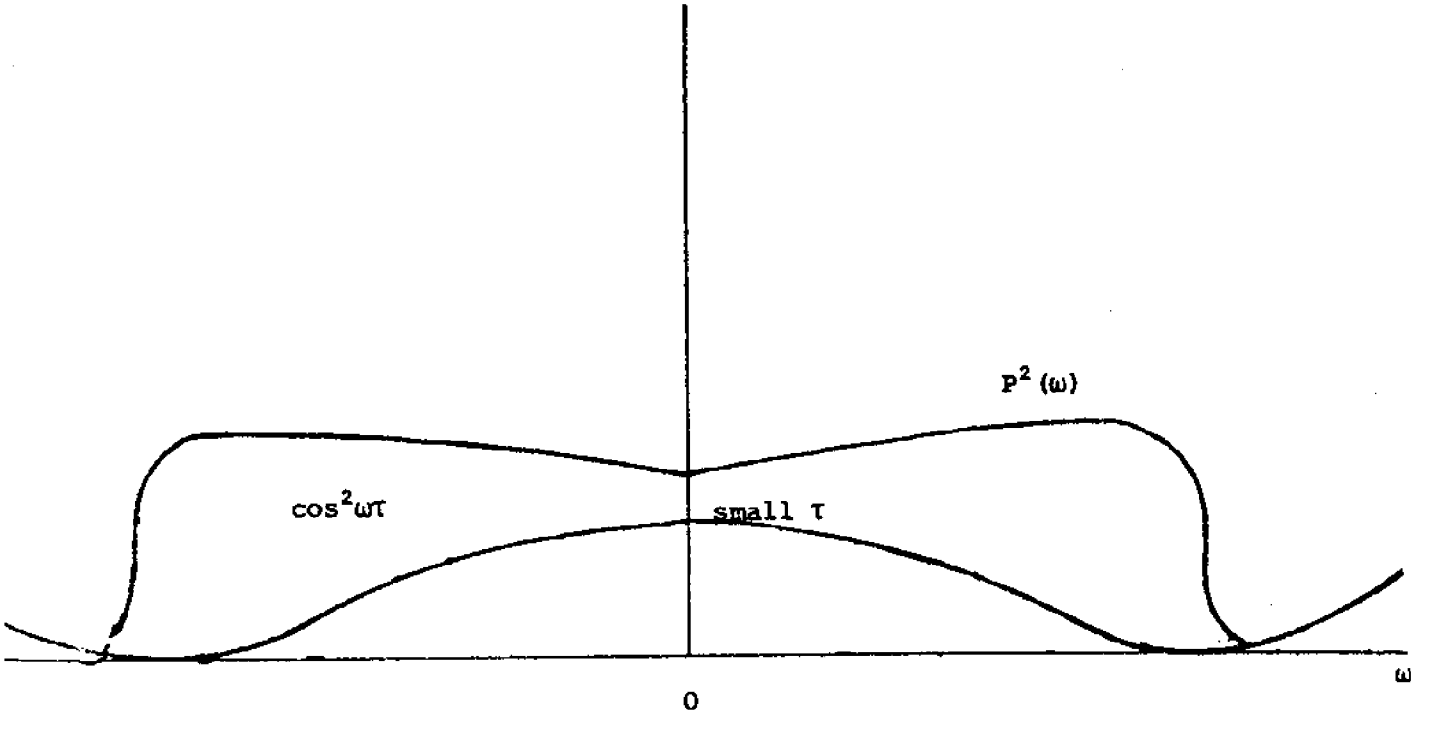

Figure (8): Illustrating the Terms in the Integrand for the Variance in the Measurement of the Autocorrelation R(τ).

The terms in the integrand of Equation (49) are sketched in Figure (8). It is seen that there is some dependance on τ, although this dependance is not very much. The greatest variance is obtained for $\tau = 0$

$$\sigma_z^2 \ (\tau=0) = 4(\omega_c')_1 \int_{-\infty}^{\infty} P^2(\omega)\,d\omega \tag{50}$$

When τ is very large, the fluctuation of $\cos^2\omega\tau$ are much more rapid than those of $P^2(\omega)$, so integrating $\cos^2\omega\tau$ cycle by cycle, we have

$$\sigma_z^2(\tau \to \infty) = 2(\omega_c')_1 \int_{-\infty}^{\infty} P^2(\omega)\,d\omega \tag{51}$$

which is just half of Equation (50). For intermediate values of τ, we have

$$\sigma_z^2(\tau \to \infty) > \sigma_z^2 < \sigma_z^2(\tau = 0)$$

In order to obtain a measure of the statistical reliability, the expected deviation of the measurement against a reference value must be compared. For quantities that are essentially positive, such as the spectral density, the natural reference is the mean value of the measurement. However, the autocorrelation function can be negative as well as positive. The mean value of the measurement may be zero, in which case, although the variance is finite, the relative variation is infinite. Therefore, it is more appropriate to use R(0) which is the mean value of the measurement for $\tau = 0$, as the reference. The uncertainty of the autocorrelation measurement is then indicated by the ratio

$$\frac{\sigma_z(\tau)}{R(0)} = \left[4(\omega_c') \int_{-\infty}^{\infty} \cos^2\omega\tau \ P^2(\omega)\,d\omega\right]^{\frac{1}{2}} \Big/ \int_{-\infty}^{\infty} P(\omega)\,d\omega \tag{52}$$

where we have used Equation (46) to represent R(0).

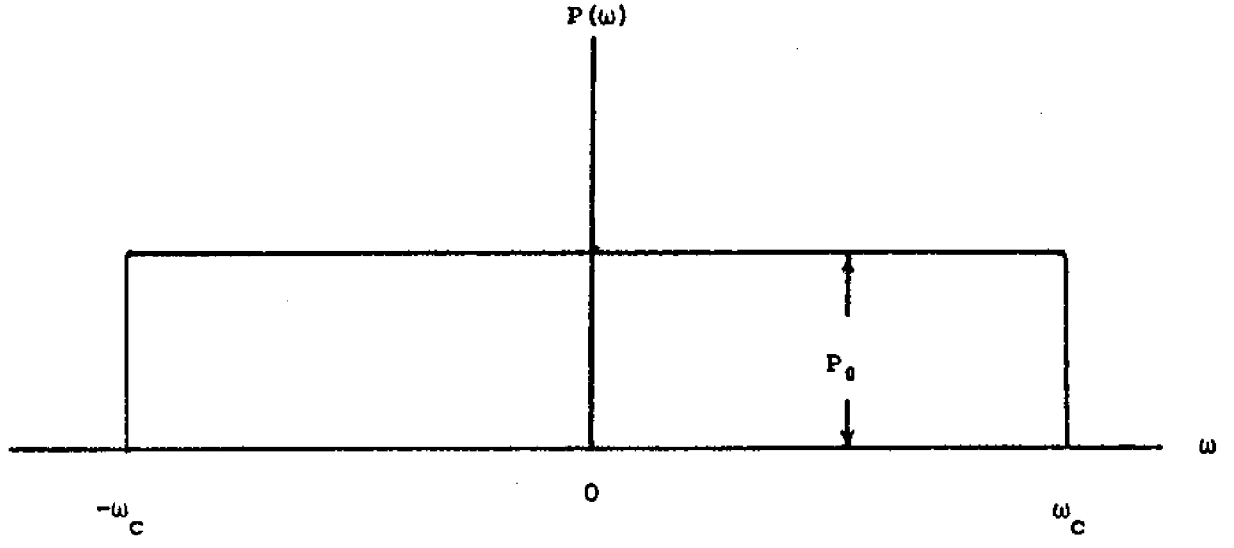

Figure (9): Spectral Density of Band Limited White Noise with cut-off Frequency ω_c.

The uncertainty Equation (52) depends on the entire spectrum of the process r(t). As an example, consider that r(t) has the spectral density sketched in Figure (9). In this case, it is an easy matter to evaluate the integrals in Equation (52) to find

$$\frac{\sigma_z(t)}{R(0)} = \frac{(\omega_c')_1}{\omega_c}\left(1 + \frac{\sin 2\omega_c\tau}{2\omega_c\tau}\right) \tag{53}$$

In the case of the measurement of R(0) itself, the uncertainty is

(54)

$$\frac{\sigma_z(0)}{R(0)} = \sqrt{\frac{2(\omega_c')_1}{\omega_c}}$$

and the equivalent number of statistical degrees of freedom is just

$$keq = \frac{\omega_c}{(\omega_c')_1} \tag{55}$$

which is exactly of the form of Equation (30). In both cases, the denominator gives the bandwidth of the averaging device. In the spectral density measurement, the numerator is the bandwidth of the selective filter, while in the measurement of autocorrelation, the numerator is the bandwidth of the entire input process. Therefore, we conclude that in measuring wide-band processes, each individual measurement of $R(\tau)$ should take much less time than each individual measurement of $P(\omega)$ if both are to have the same statisitical reliability or that an individual measurement of $R(\tau)$ is much more reliable than a single measurement of $P(\omega)$ if the same averaging filter is used in both measurement.

The above analysis was based onthe assumption that the duration of $r(t)$ was unlimited and that a continuously averaging filter was employed. When the sample length is limited, a true average over an interval T can be used. Since a lag time is inherent in an autocorrelation measurement, the duration of the sample must be at least $T + \tau$ in order to utilize a true average over an interval T.

ANALOG-TO-DIGITAL CONVERSION:

Even though machinery performing digital processing is usually costlier, bulkier, and less reliable than its analog counterpart, the ease and flexibility of programming often decide in its favour. Once the analog-to-digital conversion, is performed, the overall computation accuracy no longer depends on the number of operations, but only on the arbitrary number of digits carried. In particular, multiplication and addition, which are basic to spectral analysis, can be programmed to carry all significant numbers throughout the whole operation. basic converters will be described in the following pages.

(a). Time-Base Conversion

The output of a precision saw-tooth generator is compared with the input signal, stretched in time, and equality is detected by the discriminator. At equality, the discriminator reads out a time-counter that has been initiated at the same time as the saw-tooth signal. Automatic counter is programmed.

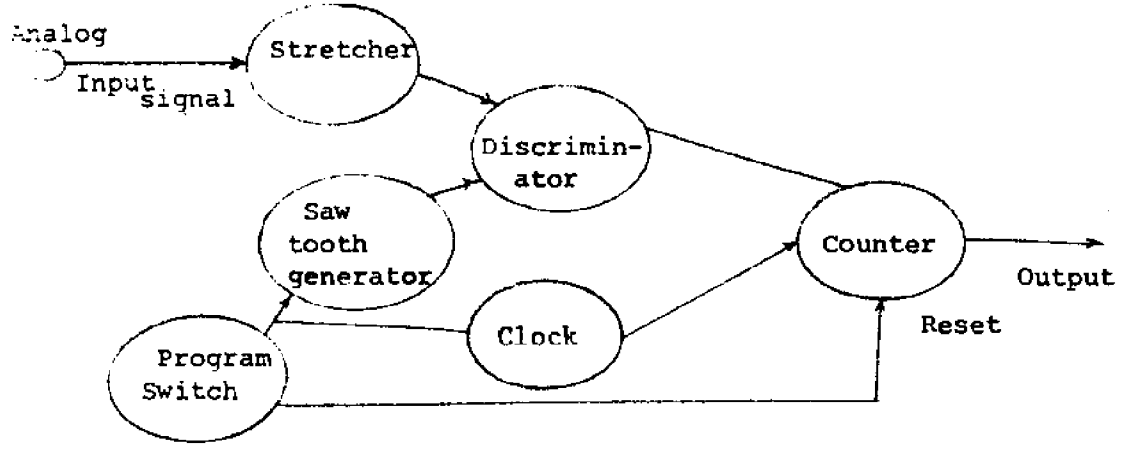

Time-base Analog-to-digital Conversion

(b). Voltage-Base Conversion

Instead of depending on the accuracy and linearity of the saw-tooth wave form, it has been expedient to govern a servo-generator by means of the counter output. This could be ideally a series of precision current of voltage sources switched by means of gates commanded by the output counter. The comparison with the input is once again performed through the discriminator which also operates the clock reset.

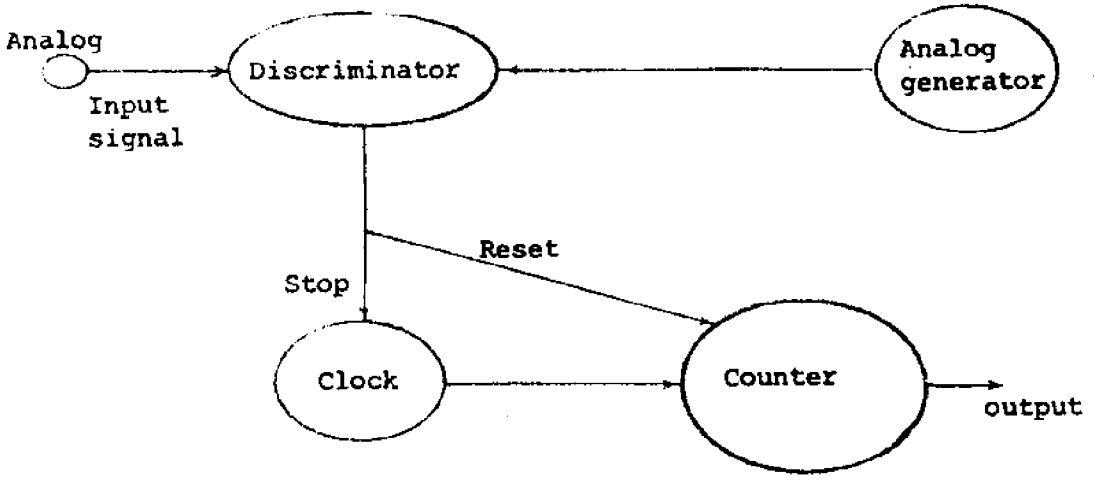

Voltage-base Analog-to-digital Conversion

PROBABILITY DISTRIBUTION:

In this section, we are interested in the determination of the probability at any instant of a random time function r(t) lying between, say, r_1 and $r_1+\Delta r$. We determine an expression for a random function with the aid of the figure shown below.

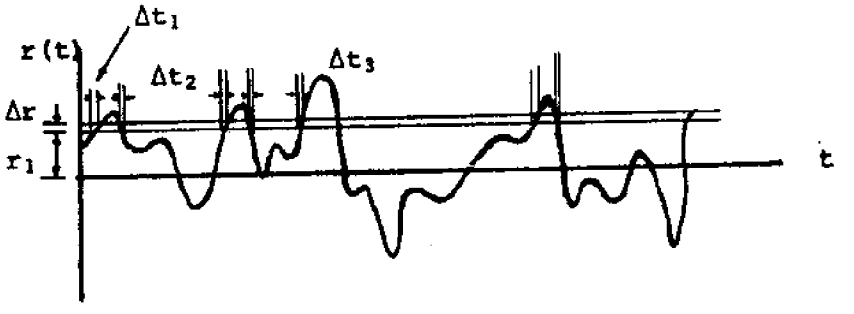

Figure (10): Probability Determination for a Random Function

As shown in the graph, two horizontal lines at r_1 and $r_1 + \Delta r$ are drawn and the time intervals Δt during which r(t) occupies this interval are summed. The sum, divided by the total time, then represents the fraction of the time that r(t) remained in the amplitude interval r_1 to $r_1 + \Delta r$, which is the probability that r(t) will be found within this interval.

We can obtain the same information as out lined in the previous paragraph by another method. We start at a very large negative value of r_1 and counting the time intervals for which r(t) exceeded this amplitude, i.e., $r(t)<r_1$. If r_1 is chosen large enough, none of the curve will lie beyond it and hence, $(1/t)\Sigma\Delta t$ will be zero. As r_1 is reduced, r(t) will exceed the specified value of r more frequently and $(1/t)\Sigma\Delta t$ will tend to increase, as indicated in Figure (2). Such

a curve at any r, then, gives the probability that r(t) will lie on the negative side of r. As $r \to \infty$, the entire curve will lie in the region less than $r = \infty$, and thus, the probability of r(t) being less that $r = \infty$ is certain or $(1/t)\Sigma\Delta t=1$.

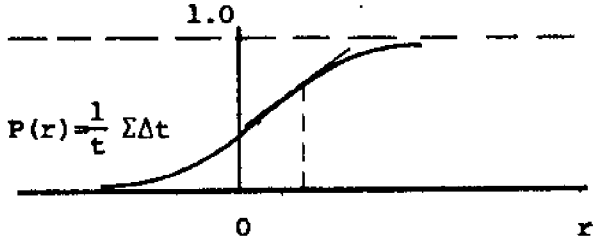

Figure (11): Cumulative Probability Curve

In Figure (11), the curve increases monotonically from zero at $r = -\infty$ to 1 at $r = \infty$, and is called the cumulative probability curve. Stated in mathematical terms, we have

$$P(-\infty) = 0 \quad , \quad 0 \leq P(r) \leq 1 \quad , \quad P(\infty) = 1$$

From P(r) we can define another function p(r) called the probability density curve as

$$p(r) = \frac{d}{dr} P(r)$$

and it is plotted in Figure (3). It is also evident that

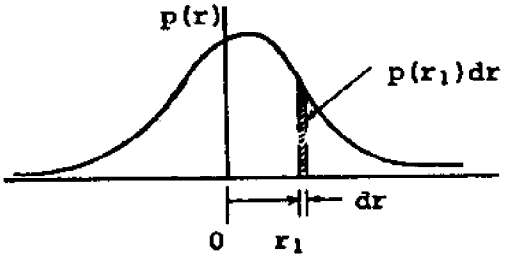

Figure (12): Probability Density Curve

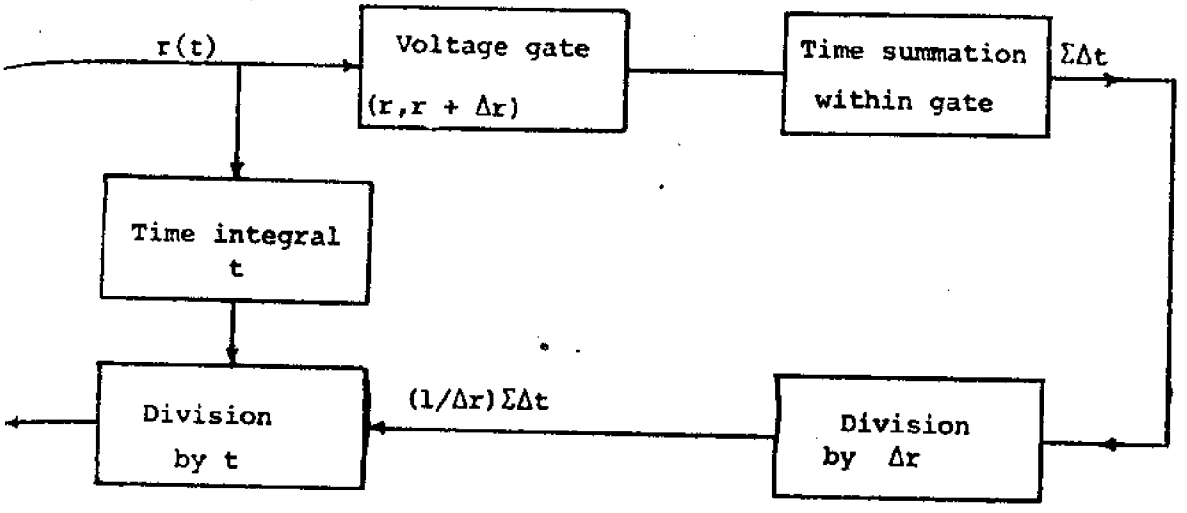

Figure (13): Probability Density Analyzer $p(r) = \lim_{t\to\infty;\Delta r\to 0} \lim (1/t\Delta r)\Sigma\Delta t$

$$P(r_1) = \int_{-\infty}^{r_1} p(r)dr$$

and

$$P(\infty) = \int_{-\infty}^{\infty} p(r)dr = 1.0 \quad .$$

Figure (13) shows a block diagram which will determine the probability density electronically.

In this section, we are assuming that the sample lenghts of records of sufficient length all result in the same statistical properties, i.e., the record is stationary. The stationary random phenomena has the ergodic property which implies that time averaging and ensemble averaging lead to the same statistical result.

For the viscoelastic model of the subbottom soil, we have for all intents

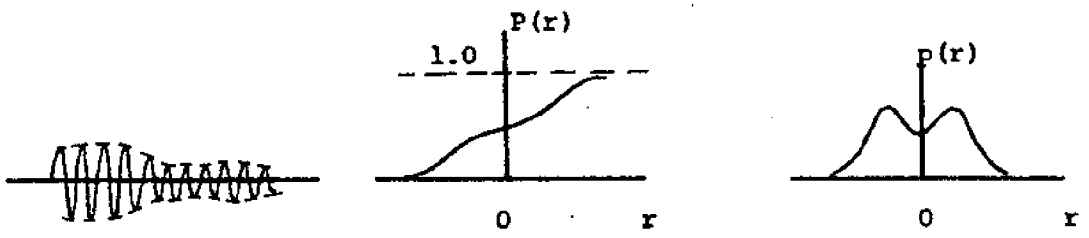

Figure (14): Probability Functions of a Narrow Band record.

and purposes, a narrow band time record. The time record, the cumulative density and probability density of a narrow band process are shown respectively in Figure(5).

Another quantity of great interest is the distribution of the peak values. Rice, in his classic paper, shows that the distribution of the peak values depends on a quantity $N_o/2M$ where N_o is the number of zero crossings and 2M is the number of positive and negative peaks. For a narrow band, $N_o = 2M$, hence, $N_o/2M = 1$, then the probability density distribution of the peak values is given by a Rayleigh distribution expressed as

$$p(r_p) = r_p e^{-(1/2)r_p^2}$$

and is shown in Figure (6).

It should also be noted that the mean value is given by

$$\bar{r} = \int_{-\infty}^{\infty} r\, p(r)dr$$

which for a stationary random process becomes

$$\bar{r} = \lim_{T\to\infty} \frac{1}{2T} \int_{-T}^{T} r(t)dt$$

The mean square values are determined in the same manner.

Finally, we should note that for nonstationary phenomena, the above procedures of time averaging cannot be used and the statistical properties must be determined at any time t_1 by analyzing a large ensemble of random records belonging to the same phenomena.

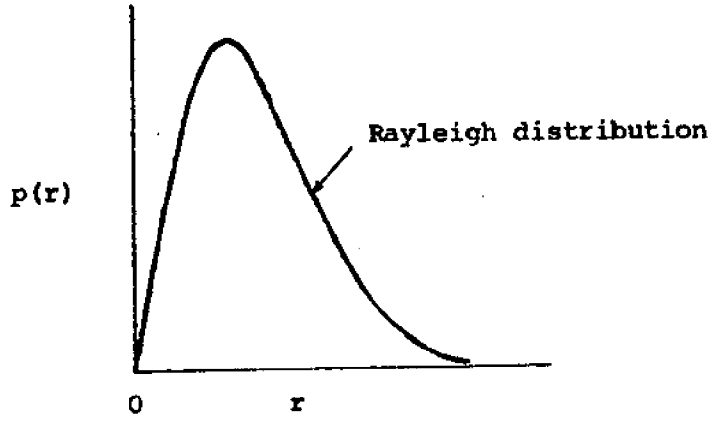

Figure (15): Probability Density Distribution for Peak Values of a Narrow Band Process

NON-STATIONARY RANDOM PROCESSES

This is probably the most important section in analyzing the Raytheon acoustic response signatures from the subbottom ocean. The data obtained from the experiment indicates that the process is a non-stationary random one, since the statistical properties of the data change with time. The time varying properties of the data can be determined only by performing instantaneous averages over the ensemble of sample responses forming the process. In actual analysis, it is sometimes not necessary to obtain a huge number of sample records to allow an accurate measurement of soil properties by ensemble averaging. The non-stationary random data produced by this actual physical phenomena can be classified into a special category of non-stationary which simplify the measurement and analysis. This particular experiment results in a random data which is a result of a non-stationary random process input $\{s(t)\}$ where each sample input function is given by $s(t) = e(t)n(t)$. Here, $n(t)$ is a sample noise function from a stationary random process $\{n(t)\}$ and $e(t)$ is a deterministic envelope (signal) multiplication factor. Since the non-stationary random data from the experiment is a result of this particular input, ensemble averaging is not always needed to describe the data. The various desired properties can then be estimated from a single sample signature, as is valid for ergodic stationary data.

An adequate methodology does not seem to exist for the analysis of all types of non-stationary data. This is mainly due to the fact that a non-stationary conclusion is generally a negative statement stating the lack of stationary properties, rather than a positive statement defining the precise nature of the non-stationarity. Hence, it follows that special techniques must be developed for non-stationary

data which only apply to limited classes of data. Some examples of different types of non-stationary data are: (a) time-varying mean value; (b) time-varying mean square value, and (c) time-varying frequency value.

The statistical properties of a single non-stationary process at different times can be described by its (1) non-stationary probability density function, (2)non-stationary auto-correlation function, and (3) non-stationary spectral density function. Furthermore, the determination of input-output relations for non-stationary data passing through physical systems. These items shall be discussed in the following sections.

PROBABILITY DENSITY OF NON-STATIONARY DATA

In a non-stationary random process $\{r(t)\}$, the statistical properties over the ensemble at any time t are not invariant with respect to translations in t. Therefore, at any time $t = t_1$, the probability structure of the random variable $r(t_1)$ would be a function of t_1. Mathematically, the non-stationary probability density function $p(r,t_1)$ of $\{r(t)\}$ can be stated as

$$p(r,t_1) = \lim_{\Delta r \to 0} \frac{\text{Prob } [r < r(t_1) \leq r+\Delta r]}{\Delta r} \qquad (1)$$

and has the following basic properties for any t.

$$\int_{-\infty}^{\infty} r(r,t)dr = 1$$

$$E[r(t)] = \int_{-\infty}^{\infty} r\ p(r,t)dr \qquad \text{(mean)}$$

$$E[r^2(t)] = \int_{-\infty}^{\infty} r^2\ p(r,t)dr$$

$$\sigma_r^2(t) = E[\{r(t) - E[r(t)]\}^2] \qquad \text{(mean square value)} \tag{2}$$

The above formulas also apply to stationary case where $p(r,t) = p(r)$, independent of time t.

The non-stationary probability distribution function $P(r,t_1)$ is defined by

$$P(r, t_1) = \text{Prob}[-\infty < r(t_1) \leq r] \quad . \tag{3}$$

As usual similar relationships hold true for the stationary probability distribution function $P(r)$ as discussed in previous sections.

Now, we would like to give some examples on how the probability density function can be prescribed to non-stationary random process $\{r(t)\}$. Let us assume that the non-stationary random process $\{r(t)\}$ is Gaussian at $t=t_1$, then $p(r,t_1)$ takes the form

$$p(r,t_1) = [\sigma_r(t_1)(2\pi)^{\frac{1}{2}}]^{-1} \exp\left(\frac{-\{r-E[r(t_1)]\}^2}{2\sigma_r^2(t_1)}\right) \tag{4}$$

which is solely determined by the non-stationary mean and mean square values of $r(t)$ and t_1. Hence, (4) indicates that the measurement of these two quantities are significant in understanding and analyzing the non-stationary data. Now, for a pair of times t_1 and t_2, the second-order non-stationary probability density function of $r(t_1)$ and $r(t_2)$ can be stated as

$$p(r_1,t_1;r_2,t_2) = \lim_{\substack{\Delta r_1 \to 0 \\ \Delta r_2 \to 0}} \frac{\text{Prob}[r_1 < r(t_1) \leq r_1 + \Delta r_1 \text{ and } r_2 < r(t_2) \leq r(t_2) \leq r_2 + \Delta r_2]}{(\Delta r_1)(\Delta r_2)} \tag{5}$$

and has the following basic preperties for any t_1 , t_2 .

$$\int_{-\infty}^{\infty}\int_{-\infty}^{\infty} p(r_1,t_1;r_2,t_2)dr_1dr_2 = 1$$

$$p(r_1,t_1) = \int_{-\infty}^{\infty} p(r_1,t_1;r_2,t_2)dr_2$$

$$p(r_2,t_2) = \int_{-\infty}^{\infty} p(r_1,t_1;r_2,t_2)\ dr_1$$

$$R_r(t_1,t_2) = E[r(t_1)r(t_2)] = \int_{-\infty}^{\infty}\int_{-\infty}^{\infty} r_1r_2\ p(r_1,t_1;r_2,t_2)dr_1dr_2 \qquad (6)$$

Continuing in this manner, higher-order non-stationary probability distribution and density functions can be defined which describe the non-stationary random process $\{r(t)\}$ in greater and greater detail. This procedure gives a rigorous characterization for the non-stationary random process $\{r(t)\}$.

The measurement of non-stationary probability density functions can be a difficult task. Even for the first-order density function given in Eq. (1), all possible combinations of r and t_1 must be considered. This, obviously, will require analysis of a large collection of sample signatures.

In practice, it often happens that for only one or a very few sample records of data are available for a non-stationary random process under investigation. One can be easily tempted in such cases to analyse the data by time averaging procedures, as would be appropriate if the data were a sample signature from a stationary (ergodic) random process. For some non-stationary data parameters, time averaging analysis procedures can produce meaningful results in certain special cases, as will be discussed later. However, for the case of probability density

functions, time averaging procedures will generally produce several distorted results. For example, the probability density function computed by time averaging data with a non-stationary mean square value will tend to exaggerate the probability density of low and high amplitude values at the expense of intermediate values.

NON-STATIONARY MEAN VALUES

Let us consider the problem of estimating the time varying mean value of non-stationary data. Given a collection of sample signatures $r_i(t)$; $0 \leq t \leq T$: $i = 1,2, \ldots, N$, from a non-stationary process $\{r(t)\}$, the mean value at any time t is estimated by the ensemble average

$$\hat{E}[r(t)] = \frac{1}{N} \sum_{i=1}^{N} r_i(t) \tag{7}$$

The estimate $E[r(t)]$ will differ over different choices of the N samples $\{r_i(t)\}$. Thus, one must investigate for every t how closely an arbitrary estimate will approximate the true mean value. The expected value of $\hat{E}[r(t)]$ is given by

$$E\{\hat{E}[r(t)]\} = \frac{1}{N} \sum_{i=1}^{N} E[r_i(t)] = E[r(t)] \tag{8}$$

where $E[r(t)]$ is the true mean value of the non-stationary process at time t. Thus, $\hat{E}[r(t)]$ is an unbiased estimate of $E[r(t)]$ for all t, independent of N.

NON-STATIONARY MEAN SQUARE VALUES

Now consider the problem of estimating the time varying mean square value of non-stationary data. Given a collection of sample response signatures $r_i(t)$; $0 \leq t \leq T$; $i = 1,2, \ldots, N$, from a non-stationary process $\{r(t)\}$, the mean square

value at time t is estimated by the ensemble average

$$\hat{E}[r^2(t)] = \frac{1}{N} \sum_{i=1}^{N} r_i^2(t) \tag{9}$$

Independent of N, the quantity $\hat{E}[r^2(t)]$ is an unbiased estimate of the true mean square value of the non-stationary process $\{r(t)\}$ at any time t since the expected value

$$E[E[r\ (t)]] = \frac{1}{N} \sum_{i=1}^{N} E[r_i^2(t)] = E[r^2(t)] \tag{10}$$

where

$$E[r_i^2(t)] = E[r(t)]^2 + \sigma_r^2(t) \tag{11}$$

is the true mean square value of the non-stationary process at time t.

To arrive at the variance of the estimate $\hat{E}[r^2(t)]$, assume the N sample signatures $r_i(t)$ are independent so that for all i and j

$$E[r_i(t)r_j(t)] = E[r_i(t)]E[r_j(t)] = E[r(t)]^2 \tag{12}$$

It follows that

$$\text{var}\ \hat{E}[r^2(t)] = E[\{\hat{E}[r^2(t)] - E[r^2(t)]\}^2] =$$

$$= E[\{\hat{E}[r^2(t)]\}^2] - E[r^4(t)] \tag{13}$$

where $E[r^2(t)]$ is given by Equation (11) and

$$E[\{\hat{E}[r^2(t)]\}^2] = \frac{1}{N^2} \sum_{i,j=1}^{N} E[r_i^2(t)r_j^2(t)] =$$

$$= \frac{1}{N^2} \left(\sum_{i=1}^{N} E[r_i^4(t)] + \sum_{\substack{i,j=1 \\ i \neq j}}^{N} E[r_i^2(t)r_j^2(t)] \right) \tag{14}$$

Hence, the problem reduces to the evaluation of the expected values appearing in Eq. (14).

Since reasonable closed-form answers are desired, we shall assume that the random process $\{r_i(t)\}$ at any time t follows a Gaussian distribution with mean value $E[r(t)]$ and variance $\sigma_r^2(t)$. It can be shown that

$$E[r_i^4(t)] = 3E[r^4(t)] - 2\,E[r(t)]^4 \tag{15}$$

$$E[r_i^2(t)r_j^2(t)] = E[r^4(t)] \qquad \text{for } i \neq j \quad . \tag{16}$$

The derivation of Eqs. (15) and (16) is based upon a non-stationary form of the fourth-order Gaussian relation given by

$$\begin{aligned} E[r_i(t)r_j(t)r_m(t)] = {} & E[r_i(t)r_j(t)]E[r_m(t)r_n(t)] \quad + \\ & + \; E[r_i(t)r_m(t)]E(r_j(t)r_n(t)] \quad + \\ & + \; E[r_i(t)r_n(t)]E[r_j(t)r_m(t)] - 2\,E[r(t)]^4 \end{aligned} \tag{17}$$

Substitution into Eqs. (13) and (14) gives the result

$$\text{var}\;\hat{E}[r^2(t)] = \frac{2}{N}\;[E[r^4(t)] - E[r(t)]^2\;] \tag{18}$$

Thus, var $\hat{E}[r^2(t)] \to 0$ as $N \to \infty$ proving that $\hat{E}[r^2(t)]$ is a consistent estimate of $E[r(t)]^2$ for all t.

Mean square values of non-stationary random processes can be estimated with the ensemble averaging device shown in Fig. (1). Two main steps are involved in the measurement.

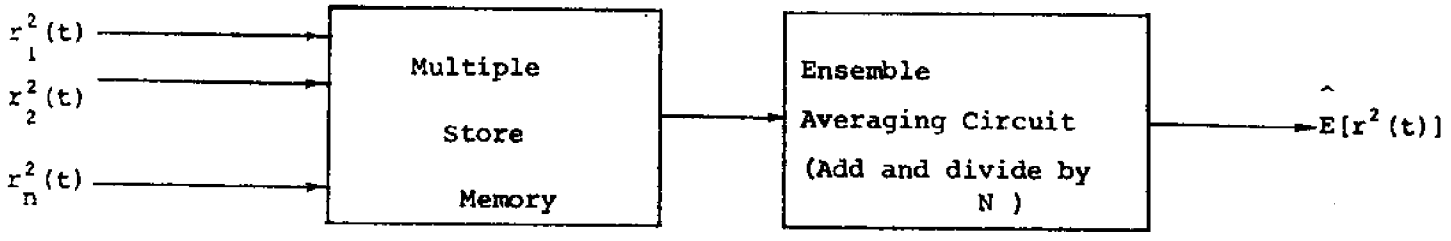

Figure (16): Procedure for Non-stationary Mean Square Value Measurement

The first step is to obtain and store each record $r_i^2(t)$ as a function of t. This may be done continuously for all t in the range $0 \leq t \leq T$, or discretely by some digitizing procedure. After this has been done for N records, the next step is to perform an ensemble average by adding the records together and dividing by N. If each $r_i^2(t)$ is digitized in L steps, then the total number of stored values would be LN.

AUTOCORRELATION FUNCTION OF NON-STATIONARY DATA

For non-stationary random process $\{r(t)\}$ the mean values at arbitrary fixed values of time t are defined by the expected values, i.e., ensemble averages, $E[r(t)]$. The autocorrelation function of a non-stationary random process is given by

$$R_r(t_1,t_2) = E[r(t_1)r(t_2)] \tag{19}$$

Let us now consider the problem of estimating $R_r(t_1,t_2)$ using a set of N sample signatures, $r_i(t)$; i = 1,2, ...,N, from the non-stationary random process. In place of Eq. (19), the experimenter should compute the ensemble averaged estimate

$$\hat{R}_r(t_1,t_2) = \frac{1}{N} \sum_{i=1}^{N} r_i(t_1) r_i(t_2) \quad . \tag{20}$$

A good procedure is to hold t_1 fixed and to vary t_2. Let $t_1 = t$ and let $t_2 = t - \tau$ where τ is a fixed time delay value. This gives

$$R_r(t,t-\tau) = \frac{1}{N} \sum_{i=1}^{N} r_i(t) r_i(t-\tau) \tag{21}$$

which for a stationary processes would be a function of τ only, but for non-stationary processes would be a function of both τ and t. The procedure is for each fixed delay value τ and each signature $r_i(t)$, calculate and store the product $r_i(t)r_i(t-\tau)$. This should be repeated for N signatures and then perform an ensemble average to yield the estimate of Eq. (21). This entire operation should be repeated for every different τ of concern . Figure (17) illustrates this procedure for the computation of non-stationary autocorrelation functions.

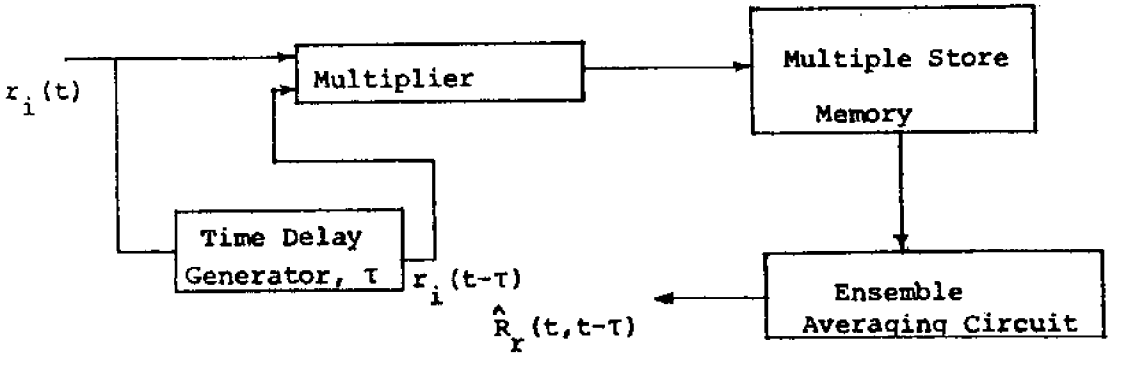

Figure (17): Procedure for Non-stationary Autocorrelation Measurement

It should be noted that the autocorrelation functions for a non-stationary process will vary with both t_1 and t_2 and for a stationary process these results would be a function of the time difference t_2-t_1 .

SPECTRAL STRUCTURE OF NON-STATIONARY DATA

In the stationary process, we have shown that the spectral density can be defined by the Fourier transform of a stationary autocorrelation function. In the non-stationary process, the spectral density can be defined by the double Fourier transform of the non-stationary autocorrelation function. Mathematically, with the usage of Eq. (19), we can define the double frequency (generalized) power spectral density of the process as

$$P(\omega_1,\omega_2) = \int_{-\infty}^{\infty} \int_{-\infty}^{\infty} R_r(t_1, t_2)\, e^{i(\omega_1 t_1 - \omega_2 t_2)}\, dt_1 dt_2 \quad .$$

We should note that $R_r(\omega_1,\omega_2)$ is complex valued and the angular frequencies ω_1 and ω_2 can take on arbitrary positive and negative values in the range $(-\infty,\infty)$. The inverse double Fourier transform gives

$$R_r(t_1,t_2) = \int_{-\infty}^{\infty} \int_{-\infty}^{\infty} P(\omega_1,\omega_2) e^{-i(\omega_1 t_1 - \omega_2 t_2)} \frac{d\omega_1}{2\pi} \frac{d\omega_2}{2\pi}$$

The double frequency spectral density function must be calculated from Fourier transform operations on non-stationary autocorrelation function. In general, $P(\omega_1,\omega_2)$ cannot be estimated by time averaging operations on individual sample response signatures (data), as can be done for stationary signatures.

We should note that short time averaging operations on individual sample records are often done to estimate time varying power spectra of non-stationary data. This can be done by segmenting the sample record into a series of very

subrecords, and then computing a power spectrum for each subrecord as if it were stationary. Eventhough an analysis of this type can produce useful qualitative information about the time varying spectral properties of the data, quantitative applications of the results should be approached with caution.

INPUT-OUTPUT RELATIONS FOR NON-STATIONARY DATA

Let us now assume that a sample input function $s(t)$ belonging to a non-stationary random process $\{s(t)\}$ excites a constant parameter linear system with Green's function $G(t)$ and frequency response function $G(\omega)$. For an arbitrary input sample $s(t)$, the sample response (output) function $r(t)$ belonging to $\{r(t)\}$ is given by

$$r(t) = \int_{-\infty}^{\infty} G(t')s(t-t')dt'$$

It is evident that $\{r(t)\}$ will be a non-stationary random process since its statistical properties will be a function of t. For a pair of times t_1, t_2, the product $r(t_1)r(t_2)$ is given to be

$$r(t_1)r(t_2) = \int_{-\infty}^{\infty}\int_{-\infty}^{\infty} G(t')G(\xi)s(t-t')s(t-\xi)dt'd\xi$$

and the expected value is given to be

$$R_r(t_1,t_2) = E[r(t_1)r(t_2)] = \int_{\infty}^{\infty}\int_{\infty}^{\infty} G(t')G(\xi)R_s(t_1-t',t_2-\xi)dt'd\xi$$

Finally, computing the double Fourier transform of the previous expression, we can define the non-stationary power spectrum of the response (output) as

$$P_r(\omega_1,\omega_2) = G^*(\omega_1)G(\omega_2)P_s(\omega_1,\omega_2)$$

where $G^*(\omega)$ is the complex conjugate of $G(\omega)$.

It should be stated that all of the electronic circuitry including the filter characteristics as described in the stationary random process can be used in analyzing non-stationary random process $\{r(t)\}$.

Finally, we should note that in the above sections, we have discussed four main types of statistical functions used to describe the basic properties of random data: (1) mean square values, (2) probability density functions, (3) autocorrelation functions, and (4) power spectral density functions. The mean square value gives a basic description of the intensity of the data. The probability density function gives information concerning the properties of the data in the amplitude domain. The autocorrelation function and the power spectral density function give similar information in the time domain and in the frequency domain, respectively.

MEAN SQUARE RESPONSE OF A SYSTEM TO NON-STATIONARY INPUT

Using previous section, we shall determine the mean square response of a system to non-stationary random input given by a specific s(t) to be later defined. We shall assume that the response is described by a non-stationary random process {r(t)} where each sample response function is given by

$$r(t) = \int_{-\infty}^{\infty}\int_{-\infty}^{\infty} G(\vec{r}-\vec{r}';t-t')s(t')d^3\vec{r}'dt' \tag{22}$$

Here, s(t) = e(t)n(t) is a input sample function of a stationary random process {s(t)} where n(t) is a sample noise function from a stationary random process {n(t)} with a zero mean and e(t) is a deterministic envelope mulitplication factor, and G is the Green's function, i.e., a unit impulse response function of the system under investigation. By taking a Fourier transform of Eq.(22), we can write

$$r(t) = \int_{-\infty}^{\infty} \frac{d\omega}{2\pi}\ G(\omega)s(\omega)e^{i\omega t} \tag{23}$$

Note that {r(t)} will be a non-stationary random process since its statistical properties will be a function of t.

We assume the autocorrelation function of the system response to non-stationary input force, as defined in previous sections, to be

$$R_r(t_1,t_2) = E[r(t_1)r(t_2)]. \tag{24}$$

Substituting (23) into (24), we get

$$R_r(t_1,t_2) = E\left[\int_{-\infty}^{\infty} \frac{d\omega_1}{2\pi}\ G^*(\omega_1)s^*(\omega_1)e^{-i\omega_1 t_1} \cdot \int_{-\infty}^{\infty} \frac{d\omega_2}{2\pi}\ G(\omega_2)s(\omega_2)e^{i\omega_2 t_2}\ d\omega_2\right]$$

$$= \int_{-\infty}^{\infty}\int_{-\infty}^{\infty} G^*(\omega_1)G(\omega_2)e^{-i(\omega_1 t_1-\omega_2 t_2)}\ \frac{E[s^*(\omega_1)s(\omega_2)]}{(2\pi)^2}\ d\omega_1 d\omega_2 \tag{25}$$

where we can define

$$P_s(\omega_1,\omega_2) = E[s^*(\omega_1)s(\omega_2)]/(2\pi)^2 \tag{26}$$

to be the generalized spectrum of the input excitation. Furthermore, we can define the spectral density of the sample response function as

$$P_r(\omega_1,\omega_2) = G^*(\omega_1)G(\omega_2)P_s(\omega_1,\omega_2) \quad . \tag{27}$$

We can write

$$s^*(\omega_1) = \int_{-\infty}^{\infty} s(t_1)e^{i\omega_1 t_1}dt_1$$

$$s(\omega_2) = \int_{-\infty}^{\infty} s(t_2)e^{-i\omega_2 t_2}dt_2$$

and hence, Equation (26) becomes

$$P_s(\omega_1,\omega_2) = \frac{1}{(2\pi)^2}\int_{-\infty}^{\infty}\int_{-\infty}^{\infty} e^{i\omega_1 t_1}e^{-i\omega_2 t_2}e(t_1)e(t_2)E[n(t_1)n(t_2)]dt_1dt_2 \tag{28}$$

But, $E[n(t_1)n(t_2)] = R_n(\tau)$ is the autocorrelation function of the noise with $\tau = t_2-t_1$. Taking the Fourier transform of the autocorrelation function, we have

$$R_n(\tau) = \int_{\infty}^{\infty} P_n(\omega)e^{i\omega\tau}\frac{d\omega}{2\pi} \; ; \quad \tau = t_2-t_1$$

$$R_n(\tau) = \int_{-\infty}^{\infty} P_n(\omega)e^{i\omega t_2}\, e^{-i\omega t_1}\, \frac{d\omega}{2\pi} \tag{29}$$

Upon substitution of (29) into (28) we obtain:

$$P_S(\omega_1,\omega_2) = \frac{1}{(2\pi)^2} \int_{-\infty}^{\infty}\int_{-\infty}^{\infty}\int_{-\infty}^{\infty} e^{-i(\omega-\omega_1)t_1}\, e^{-i(\omega_2-\omega)t_2}\, e(t_1)e(t_2) \times P_n(\omega)dt_1dt_2\frac{d\omega}{2\pi} \tag{30}$$

Now, defining envelope transformation functions to be

$$P_e(\omega-\omega_1) = \int_{-\infty}^{\infty} e(t_1)\, e^{-i(\omega-\omega_1)t_1}\, \frac{dt_1}{2\pi}$$

$$P_e(\omega_2-\omega) = \int_{-\infty}^{\infty} e(t_2)e^{-i(\omega_2-\omega)t_2}\, \frac{dt_2}{2\pi}$$

Equation (30) becomes

$$P_s(\omega_1,\omega_2) = \int_{-\infty}^{\infty} P_n(\omega)P_e(\omega-\omega_1)P(\omega_2-\omega)\, \frac{d\omega}{(2\pi)} \tag{31}$$

The mean square response is given to be

$$R_r(t,t) = E[r^2(t)]$$

so that via substituting (31) into Equation (25) and equating the times, $t_1=t_2=t$, we obtain

$$E[r^2(t)] = \int_{-\infty}^{\infty} \left(\int_{-\infty}^{\infty} G^*(\omega_1)P_e(\omega-\omega_1)\, e^{-i\omega_1 t}\, d\omega_1 \right) \times$$

$$\times \left(\int_{-\infty}^{\infty} G(\omega_2)P_e(\omega_2-\omega)e^{i\omega_2 t}\, d\omega_2 \right) P_n(\omega)\, \frac{d\omega}{2\pi} \tag{32}$$

Noting that the two expressions inside the integrand of Equation (32) are complex

conjugates of one another when $\omega_1 = \omega_2$, we can then write

$$E[r^2(t)] = \int_{-\infty}^{\infty} P_n(\omega) \left| \int_{-\infty}^{\infty} G(\omega_2) P_e(\omega_2-\omega) e^{i\omega_2 t} \, d\omega_2 \right|^2 \frac{d\omega}{2\pi} \tag{33}$$

Equation (33) is the mean square formulation of a sample response function r(t) for inputs of amplitude modulated stationary noise.

REFERENCES

1. H. Tuqal and M. Yildiz, "Mean-Square Response of a Viscoelastic Medium to Stationary Random Excitation," UNH-Sea Grant Report, April 1974.

2. M. C. Wang and G. E. Uhlenbeck, "On the Theory of the Brownian Motion II," Revs. Modern Phys., 17, Nos. 2,3, pp. 323-342, April-July 1954.

3. H. M. James, N. B. Nichols, and R. S. Phillips, "Theory of Servomechanisms," M.I.T. Radiation Laboratory Series, Vol. 25, pp. 333-369, McGraw-Hill, N.Y., 1947.

4. S. O. Rice, "Mathematical Analysis of Random Noise," Bell System Technical Journal, Vol. 23, 24, Selected Papers on Noise and Stochastic Processes, edited by Nelson Wax, Dover Publications, N.Y., 1954.

5. J. H. Laning and R. H. Battin, "Random Processes in Automatic Control," McGraw-Hill Book Co., N.Y., 1956.

6. W. B. Davenport and W. L. Root, "Random Signals and Noise," McGraw-Hill Book Co., N.Y. 1956.

7. D. Middleton, "An Introduction to Statistical Communication Theory," pp. 172, Sect. 3.2-3.3(3), McGraw-Hill, New York, 1960.

8. A. J. Curtis and T. R. Boykin, Jr., "Response of Two Degree Freedom Systems to White Noise Base Excitation," J. of Acoustical Society of America, Vol. 33, pp. 655-663, 1961.

9. C. J. Morrow, B. A. Troesch, and H. R. Spence, "Random Response of Two Coupled Resonators without Loading," J. of Acoustical Society of America, Vol. 33, pp. 46-55, 1961.

10. S. H. Crandall and A. Yildiz, "Random Vibration of Beams," ASME Journal of Applied Mechanics, pp. 267-275, 1962.

11. T. K. Caughney and H. J. Stumpf, "Transient Response of a Dynamic System Under Random Excitation," Journal of Applied Mechanics, Vol. 28, No. 4, Trans. ASME, Vol. 83, Series E, pp. 563-566, December 1961.

12. W. C. Hurty and M. F. Rubenstein, Dynamics of Structures, Prentice-Hall, Inc., New Jersey, 1965.